Tuning the Enzymatic Degradability of Polyhydroxybutyrate

by

Preetam Anbukarasu

A thesis submitted in partial fulfillment of the requirements for the degree of

Doctor of Philosophy

in

Materials Engineering

Department of Chemical and Materials Engineering

University of Alberta

Abstract

Enzyme-responsive degradable polymers are of great interest both from fundamental science and real-world application perspectives. Enzyme-responsive polymers, because of their ability to interface with and sense biological processes, can have many applications in systems that operate at the edge of biology and materials science. In this thesis, the methods and physical processes to control and characterize the enzyme response of a biodegradable polymer film – Polyhydroxybutyrate (PHB) – have been explored. The properties of PHB were controlled by altering the processing and physical parameters to yield PHB films that have a range of degradation characteristics, with the aim of integrating this material in food quality sensing and biological applications.

A simple, solvent casting process was used to prepare PHB films with acetic acid as a food-safe solvent. The use of acetic acid allowed for more flexible processing conditions and a more extensive range of final properties. The acetic acid based solvent casting process was used to prepare flexible PHB films with thickness ranging from 50 μm to 40 nm, which is challenging to obtain using existing solvents for PHB.

Since the degradation characteristics of thin films can vary substantially from their thicker counterparts, the effect of reducing the polymer film thickness on their degradation characteristics was studied. A diffraction-based degradation sensor was developed and validated to determine the change in the degradation of polymer thin films. It was found that the enzymatic degradation rate increases substantially with a decrease in thickness of the PHB film. However, constraining the film thickness down to the nanoscale was

found to impede enzymatic degradation, which could be attributed to the lack of ordered, crystalline structures in the constrained film.

The knowledge acquired from these degradation studies was utilized to create a time-temperature indicator (TTI) that works based on the temperature dependent degradation behavior of a dye-loaded PHB film. With elapsing time, the degradation of the dye-loaded PHB film was found to result in a gradual change in color of the enzyme solution, which correlated with the integrated time and temperature history to which it was exposed.

Preface

Parts of this work has been previously published in the literature.

Chapter 3 uses contents published in "**Tuning the properties of polyhydroxybutyrate films using acetic acid via solvent casting**," P. Anbukarasu, D. Sauvageau, A. Elias, Sci. Rep. 5 (2015) 17884. doi:10.1038/srep17884. Creative Commons License Nature Publication Group. P.A performed all experiments and wrote the manuscript. A.L.E. and D.S. supervised the work and contributed to designing the research and to writing the manuscripts.

Chapter 4 contains materials published in "**A diffraction-based degradation sensor for polymer thin films**," P. Anbukarasu, D.I. Martínez-Tobón, D. Sauvageau, A.L. Elias, Polym. Degrad. Stab. (2017). doi:10.1016/j.polymdegradstab.2017.05.020. Copyright © 2017 Elsevier. P.A performed the experiments and wrote the manuscript, D.M.T produced and characterized enzymes, A.L.E. and D.S. supervised the work and contributed to designing the research and to writing the manuscripts.

The results published in **"Enzymatic degradation of dimensionally constrained polyhydroxybutyrate films,"** P. Anbukarasu, D. Sauvageau, A.L. Elias, Physical Chemistry Chemical Physics, 30021-30030 (2017). doi: 10.1039/C7CP05133F. Copyright, © Royal Society of Chemistry, is used in Chapter 5. In this work, P.A performed the experiments and wrote the manuscript. A.L.E. and D.S. supervised the work and contributed to designing the research and to writing the manuscripts.

The contents published in "**Time-Temperature Indicator Based on Enzymatic Degradation of Dye-Loaded Polyhydroxybutyrate**," P. Anbukarasu, D. Sauvageau, A.L. Elias, Biotechnol. J. 1700050 (2017) 1700050. doi:10.1002/biot.201700050. Copyright © 2017 WILEY-VCH Verlag GmbH & Co. KGaA is used in Chapter 6. In this work, P.A performed the experiments and wrote the manuscript. A.L.E. and D.S. supervised the work and contributed to designing the research and to writing the manuscripts.

Dedication

This thesis is dedicated to infinite energy and intelligence which keeps this ever-expanding universe from falling apart.

Acknowledgments

Although this document claims that I am the sole author of this thesis, it would never have come to fruition without the expertise, knowledge, help, and guidance of a long list of people who have shaped this thesis as much as I have.

Firstly, I would like to thank my supervisors and mentors, Dr. Anastasia Elias and Dr. Dominic Sauvageau. I have always admired their diligence, focus, and enthusiasm for science and new ideas. Thank you for giving me the freedom and encouragement to try new ideas and experiments, even if most of them failed or went nowhere. I have become a better scientist and a better person over these past five years because of your guidance and mentorship, for which I will forever be grateful.

Over the course of my work, many people have helped me get from where I started to where I am now. I would like to thank the members of Elias Lab and Sauvageau (Scorpion) Lab, both past, and present, for all their assistance, ideas and help. Special thanks to Dr. Ben Nearingburg (for advise on a number of experiments), Dr. Zachary Storms (for advise on research and on the big picture), Dr. Chanchan Wang (for help with number of experiments), Diana Martinez Tobon (for providing me enzymes on a number of occasions, despite her busy schedules), Anthony Zebroff (for intellectually stimulating discussions), Andrea Jeffery (for her guidance, help and training when I was finding my foot in the lab), Sangita Sridar (for being an excellent friend and willing ear to listen to my ideas), Li Dan (for her help with a number of experiments), Adrian Lopera Valle (for excellent intellectual discussions), Joseph Caputo (for being a good confidant and for taking some of this work forward). I would like to thank my summer students over the years who have helped me with experiments and for carrying out some fascinating

research. There are many other members of the group who have helped me in ways that I cannot capture intangible words as I have done above. However, all of you have contributed equally to my work. Thank you all.

A number of experiments in this work would not have been possible without the expertise of many people throughout the campus. Thank you, George and Nathan, (EAS SEM Lab), Nancy, Shiau-Yin, Peng Li and Scott (Nanofab), for helping me make and characterize many of my samples. Thank you for maintaining such a vibrant community of researchers and scientists at the University.

Finally, I would like to thank my family and friends for their continued support and encouragement through these past five years. Thank you all.

TABLE OF CONTENTS

List of tables

List of figures

1. Responsive Biodegradable Polymers for Food Quality Sensing

1.1. Introduction

Prevention of pathogenic contamination and assurance of quality in fresh products is a massive challenge in the food processing industry. Lapses in food quality assurance have led to recalled products and financial losses, not to mention illness and even, in some cases, death. Many previous studies have implicated contamination in fresh meat and food products to be a leading cause of widespread foodborne illness outbreaks[1–5]. A 2011 report by the Center for Disease Control and Prevention (CDC) estimates that about 9.4 million people are affected each year by foodborne illnesses in the United States alone[6]. The food industry uses traditional pathogen detection techniques such as microbiological, immunological and nucleic acid assays to test food samples for contamination. These techniques are very accurate and sensitive, but require long analysis time and elaborate sample preparation[7,8]. In addition, these protocols are based on random sampling and discrete measurements, which leave open the possibility of untested contaminated samples proceeding through the supply chain and of contamination taking place during transportation or re-packaging further down the supply chain[9]. Therefore, complementary techniques that can be used for continuous, passive, real-time monitoring during packaging, transportation, and storage of food products are desirable. One potential approach to ensuring food safety in all packages, at all times is the use of an *in-situ* passive detector that continuously

monitors the package for the presence of a specific pathogen and the environmental conditions to which it is exposed.

Currently, there are very few cost-effective quality assurance platforms that can be integrated directly into food packaging and that are capable of continuous, passive monitoring[10]. Most existing and proposed systems require active electronic components and circuitry, which makes them prohibitively expensive and complicated to implement inside food packages. An ideal passive pathogen detector needs to be 1) inexpensive, 2) food safe when implemented inside the package, 3) capable of continuously tracking the parameters within the food package to ensure overall quality, and 4) able to produce an easily visualized response when the quality decreases.

Smart polymers are a class of materials that can interact with an external stimulus and undergo a concomitant change in properties[11]. This change can entail variations in mechanical properties, dimensional change[12] or a change in the visual appearance of the polymer. A sub-class of these materials based on degradable polymers undergo an irreversible change in properties in response to the relevant stimuli. In food safety applications, an irreversible response is desirable since it provides a permanent record of the cumulative impact of the stimuli of interest. Degradable polymers, with their ability to respond to a variety of stimuli including enzymes and other bio-markers, are important candidates for such applications. Since these systems work without the need for an external power source or complex electronics, they are ideal for deployment in constrained environments like food packages. In addition, these materials can be fabricated in large quantities inexpensively, and their processing parameters can be tuned to produce desired changes in physical properties[13] as a

response to individual or multiple stimuli. Furthermore, they can provide an irreversible response to cumulative exposure to environmental factors that influence the quality of food product such as storage time, temperature[14] and pathogenic bacteria. These advantages make degradable polymers ideal candidates for the intended application in food packaging.

1.2. Proposed Solution and Approach

The main goal of the work described in this thesis is to develop and characterize a polyhydroxybutyrate (PHB) based enzyme-responsive platform that can be deployed as a part of an *in-situ* pathogen detector (currently being developed by Dr. Elias and Dr. Sauvageau group)[15] and can be used for overall quality assessment of fresh food products through time-temperature monitoring.

This work specifically focuses on methods to fabricate and study PHB with a range of physical properties and surface features which influence its enzymatic degradation. Further emphasis has been placed on transducing the enzymatic stimulus into an irreversible visual change in the polymer, which is conducive to both rapid, qualitative observation by eye as well as to quantitative measurement using automated readers. The processability, patternability and the response behavior of PHB were studied from the perspective of incorporating it into a pathogen detection system and deploying it for the evaluation of the quality and freshness of food products as a time-temperature indicator (TTI). Figure 1 shows the general progression and objectives of this thesis.

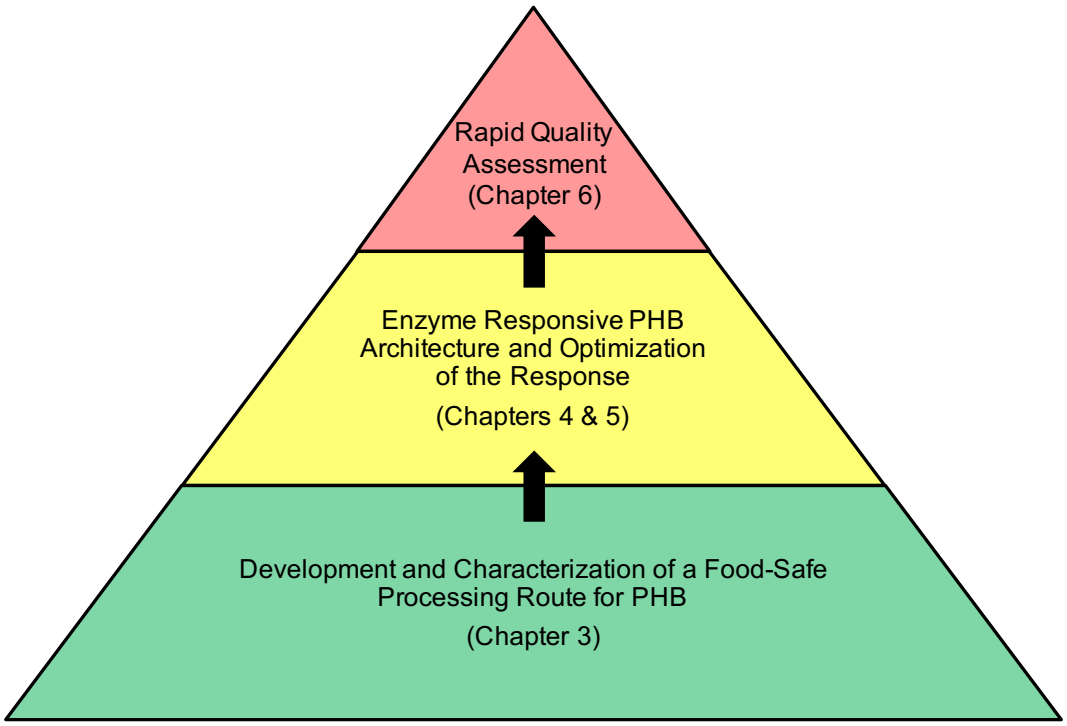

Figure 1.1 Schematic showing the principal objectives, progression and contributions made in this thesis.

1.3. Organization of Thesis

Chapter 2 presents a broad overview of the literature pertaining to biodegradable responsive polymers and provides the requisite background to develop and characterize enzyme-responsive polymer. The chapter starts with the review of degradable polymers (historical origins and their fundamental response behavior) and then focuses on degradable responsive polymers in the context of enzymatic stimulus. The chapter concludes by providing state of the art in *in situ* bacterial detection and the relevant context for the current research.

The potential application of enzyme-responsive PHB in food packaging makes it desirable to develop a food safe fabrication route. Chapter 3 presents a solvent casting process to fabricate PHB films with tunable properties using acetic acid as solvent. The effects of solvent casting temperature on the surface morphology, optical, mechanical and thermal properties of PHB films are characterized. In addition to thin films with varying thicknesses and properties, the versatility of the method is demonstrated by fabricating PHB films with high porosity, high optical clarity and flexibility. Before this work, the most common solvent for PHB used in the literature was chloroform, which, in addition to having a number of negative implications for the environment and human health, does not provide the level of tunability afforded by acetic acid. This work is the first instance in literature where acetic acid is demonstrated as a suitable solvent for processing PHB.

One of the principal objectives of this thesis is to characterize, in real time, the enzymatic response of the PHB films prepared under different processing conditions. In this work, the enzymatic response is manifested as an irreversible degradation of the PHB surface. The existing techniques to study this behavior (such as gravimetry and spectroscopy) have many limitations and complexities which make them unsuitable for real-time measurements. Chapter 4 presents a diffraction-based method for the evaluation of enzymatic degradation of PHB using a non-contact, real-time and automated system. This diffraction-based method is used to successfully characterize the degradation behavior of PHB thin films fabricated at different solvent casting temperatures and aged for various times. As further validation of the method, the dissolution stability of silk films is also determined. Further, a probabilistic model is

established to semi-quantitatively determine the degradation rate of the PHB film being characterized.

Chapter 5 explores further the effect of dimensional constraints on the degradation behavior of PHB. The relationship between the crystalline state of PHB and the enzymatic response under different dimensional constraints is determined using the diffraction metrology established in Chapter 4. The degradation is found to accelerate as the dimensional constraint increases, which presents the opportunity to engineer PHB films with different kinetics of enzymatic degradation by a simple reduction in film thickness. In addition, a PHB specimen constrained down to the nanoscale is fabricated using a μ-transfer molding process and its degradation behavior is also studied.

In the later parts of this thesis, the acetic acid based processing technique and the enzymatic degradation of PHB are utilized to develop materials and architectures that can provide useful information about the overall quality and freshness of food products in the form of an optical response. In Chapter 6 the concept for a TTI, based on the enzymatic degradation of a dye-loaded PHB film, is detailed. The chapter presents the characterization of the dye-loaded PHB and its enzymatic degradation, to ascertain its suitability as a TTI for fresh meat and dairy products. The kinetics of the degradation process is systematically studied to narrow down the parameters and processing conditions suitable for a TTI.

Chapter 7 provides a summary of the findings, contributions and conclusions made in this thesis. The future directions and potential applications of the enzymatically-responsive PHB are briefly presented.

1.4. Reference

1. Mead, P. S. *et al.* Nationwide outbreak of listeriosis due to contaminated meat. *Epidemiol. Infect.* **134,** 744 (2006).
2. Angelo, K. M. *et al.* Multistate outbreak of Listeria monocytogenes infections linked to whole apples used in commercially produced, prepackaged caramel apples: United States, 2014–2015. *Epidemiol. Infect.* **145,** 848–856 (2017).
3. Manning, L., Wallace, C. & Soon, J. in *Foodborne Diseases* 287–312 (CRC Press, 2016). doi:10.1201/b19463-14
4. Raheem, D. Outbreaks of listeriosis associated with deli meats and cheese: an overview. *AIMS Microbiol.* **2,** 230–250 (2016).
5. Currie, A. *et al.* Multi-Province Listeriosis Outbreak Linked to Contaminated Deli Meat Consumed Primarily in Institutional Settings, Canada, 2008. *Foodborne Pathog. Dis.* **12,** 645–652 (2015).
6. Scallan, E. *et al.* Foodborne Illness Acquired in the United States—Major Pathogens. *Emerg. Infect. Dis.* **17,** 7–15 (2011).
7. Singh, A., Poshtiban, S. & Evoy, S. Recent Advances in Bacteriophage Based Biosensors for Food-Borne Pathogen Detection. *Sensors* **13,** 1763–1786 (2013).
8. Baeumner, A. J. Biosensors for environmental pollutants and food contaminants. *Anal. Bioanal. Chem.* **377,** 434–445 (2003).
9. Lianou, A. & Sofos, J. N. A Review of the Incidence and Transmission of Listeria monocytogenes in Ready-to-Eat Products in Retail and Food Service Environments. *J. Food Prot.* **70,** 2172–2198 (2007).
10. Law, J. W.-F., Ab Mutalib, N.-S., Chan, K.-G. & Lee, L.-H. Rapid methods for the

detection of foodborne bacterial pathogens: principles, applications, advantages and limitations. *Front. Microbiol.* **5,** 770 (2015).

11. Aguilar, M. R. & San Román, J. Introduction to smart polymers and their applications. *Smart Polym. their Appl.* 1–11 (2014). doi:10.1533/9780857097026.1

12. Zhou, J. & Sheiko, S. S. Reversible shape-shifting in polymeric materials. *J. Polym. Sci. Part B Polym. Phys.* **1,** 1365–1380 (2016).

13. Samal, S. K., Dash, M., Dubruel, P. & Van Vlierberghe, S. Smart polymer hydrogels: properties, synthesis and applications. *Smart Polymers and their Applications* (Woodhead Publishing Limited, 2014). doi:10.1533/9780857097026.1.237

14. Taoukis, P. S, L. T. P. in *Novel Food Packaging Techniques* 104–125 (2003).

15. Elias, A. *et al.* Bacteriophage-based biosensor for microbial detection. US Patent No. 20160061830A1 (2015).

2. Background and Review of the Literature

This chapter provides an overview of biodegradable polymers, including their historical progression, uses, degradation mechanisms and parameters affecting the degradation behavior. The various parameters that influence degradation, including crystallinity, surface properties and thermal characteristics, are discussed. Further, this section also provides a brief overview of enzyme-responsive polymers in the context of biosensing and biomedical applications. The chapter ends by providing a short review of the techniques in literature for *in situ* detection of bacterial contamination and of the overall quality of food products, which is one of the ultimate intended purpose of the materials developed in this thesis. More detailed description and literature relevant to the work described are provided as separate introductions in each of the chapters.

2.1. Biodegradable Polymers: History, Motivation and Applications

Biodegradable polymers are materials that can be broken down by agents such as bacteria, fungi or other biological means under suitable environmental conditions[1]. Biodegradable polymers have been an integral part of nature since the dawn of life on earth. The natural world is filled with biodegradable polymers that are essential for the origin, sustenance and propagation of life. The three most important building blocks of life — namely, polynucleotides, polypeptides and polysaccharides — are all degradable polymers of biological origin. The ability of these degradable polymers to break down into smaller constituents at the end of their life cycle has been an enabler for the constant churning and evolution of new functions and diversification of living organisms[2]. Because of their ubiquity, we can observe the prevalence of biodegradable

polymers all around us. For example, cellulose (a polysaccharide) constitutes 33% of all plant matter[3,4] and polysaccharides (sugars and starch) constitute almost 70% of the total biomass consumed by many animals, including humans[5]. In addition to being an essential part of life, biodegradable polymers have found many everyday applications. Since antiquity to the present day, we have used a wide range of natural materials made of biodegradable polymers such as wood (polysaccharides), cotton (polysaccharides), rubber, silk (polypeptides) and leather (polypeptides) for functional and structural applications. The utility and desirability of materials made from natural degradable polymers made them expensive and objects of high value throughout history.

However, with the advent of low-cost synthetic polymers — bakelite (1907)[6,7], polyethylene (1933)[8,9], polyamide (1938) — in the early part of the 1900s, the dependence on biopolymers for functional applications decreased considerably. The low-cost, favorable physical properties and environmental stability of synthetic plastics made them ideal for functional applications where degradation at the end of life was not critical. Thus, an era of synthetic plastics ensued, which also brought along a glut of problems related to the environmental impact of plastic waste[10–12]. As the environmental impact of synthetic plastics became apparent, research interest in the development and discovery of a new class of polymers that can degrade in specific environmental conditions at the end of life increased[13,14]. Initial researches focused on degradation-inducing additives and on the chemical modification of common synthetic polyolefin[15–17] and polyesters to impart favorable degradation behavior to existing synthetic polymers[18–20]. Most of these additives/chemical modifications altered the polymer

backbones structure/chemistry and reduced their overall environmental stability. This approach has been successfully used to synthesize polymers that can be broken down by the action of environmental factors such as, pH, temperature and high energy radiation. The chemistry of the polymer chains was modified such that even a relatively small amount of external energy would cause the bonds to destabilize and break down into smaller chains[21–23]. Despite the induced degradability, these polymers did not find large-scale applications, since the low molecular weight species produced due to the degradation process were found to be harmful to the environment[24,25].

Another research approach carried out in the same period involves the polymerization of monomeric moieties that are degradable and safe in the environment. The resulting polymer was found to have chemical bonds that are susceptible to degradation either due to hydrolytic or catalytic attack by reactive species present in the environment, typically mild acids and bases. Using this approach, many synthetic degradable polymers not found in nature were synthesized; poly(lactic acid) (PLA)[26], poly(lactic-co-glycolic acid) (PLGA)[27] and polycaprolactone (PCL)[28] being the most widely used polymers synthesized by direct polymerization route. Further, the advances in polymerization techniques (such as the lactide ring opening reaction) has enabled commercially viable production of degradable polymers in the recent decades, making them suitable for low-cost applications such as films, coatings[29,30] and a number of biomedical devices[31,32]. However, the synthetic polymers produced by polymerization reactions have limitations related to their slow degradation rate and the inability to readily degrade at the end of life, since they lack biological agents that can readily break down the polymer chains with high specificity.

An alternative route for the large-scale production and extraction of degradable polymers is the utilization of bioengineering to leverage the tendency of certain microorganisms and plants to produce and accumulate biopolymers as a store of energy or structural material[33–35]. The biological origin of these polymers makes them susceptible to rapid degradation under suitable environmental conditions while being extremely stable and recalcitrant during normal use. The most common instances of such polymers produced by plants are cellulose and starch, which have favorable properties, including good degradability and environmentally friendly degradation products. Apart from plants, some bacterial species and fungi have also been identified to accumulate polymeric materials within their cell wall under specific resource-limited conditions[36–39]. While most microorganisms tend to store small quantities of oligosaccharides, polysaccharides and polypeptides required for the cell functions, production and accumulation of large amounts of polymers are not typically observed. Polyhydroxyalkanoates (PHA) – a family of bio-polyesters of which polyhydroxybutrate (PHB) is the most important and commonly encountered polymer – are prominent exceptions to this rule for bacterial origin polymers[36,37,40,41]. PHA is produced by some strains of bacteria as an energy reserve under resource limited conditions and in the presence of excess carbon[42]. Under suitable conditions, some strains of bacteria have been shown to accumulate as much as 75% PHB relative to the total dry weight of the cell[43]. PHA has many attractive properties such as excellent chemical stability, biocompatibility and degradability[44]. The degradation products of PHA (alkanoic acids) are benign and are in fact essential constituents of all living organisms. PHA, by having an unstable ester bond in its backbone. tends to undergo slow hydrolytic degradation

under mildly acidic condition[45]. In addition, the prevalence of PHA as an energy storage molecule in bacteria has led to the evolution of a range of depolymerase enzymes that can catalyze the hydrolysis of the ester bonds at much higher rates than possible in normal hydrolytic conditions[46–48]. Among PHAs, polyhydroxybutyrate (PHB), polyhydroxyvalerate (PHV) and poly(3-hydroxybutyrate-co-3-hydroxyvalerate) (PHBV) have attracted the most attention in the literature, because of their ease of production and mechanical properties similar to commercial thermoplastic polymers such as polypropylene. However, PHB suffers from some drawbacks such as lack of suitable versatile solvents, poor mechanical flexibility, poor processibility and a narrow thermal processing window. This thesis contributes towards remediating some of the issues and drawbacks of using PHB.

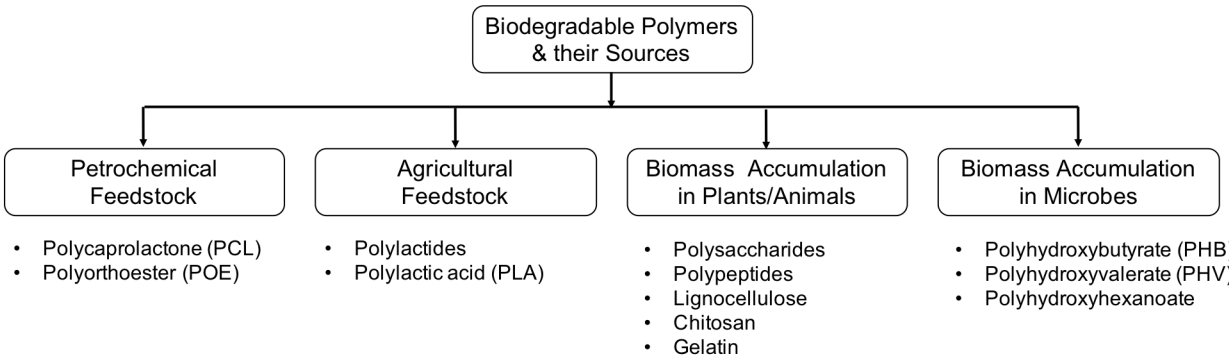

Figure 2.1 Schematic showing the diversity of degradable polymers based on their origin and source.

Figure 2.1 shows a classification of degradable polymers based on their origin and source. The physical properties and degradation behavior of these polymers are influenced by factors such as the chemistry of the polymer backbone, synthesis route, processing parameters and degradation processes involved. The interplay between the

different fabrication routes and processing parameters have led to a rich variety of both natural and synthetic degradable polymers with a range of degradation behaviors. As a result, the interest in biodegradable polymers and their applications has increased dramatically in the past few decades.

Figure 2.2 shows a plot of the number of publications on biodegradable polymers in the last four decades. Degradable polymers have found applications in many diverse fields starting from advanced biological implants to eco-friendly food packages. Because of their ability to interact with biological molecules, resorption characteristics and assimilation in physiological conditions, degradable polymers have evoked substantial interest for applications in biological and medical devices[49–53]. Most of the early applications for degradable polymers proposed in the literature revolve around bio-implants[50], drug delivery systems[51,52], resorbable sutures and tissue regeneration[53]. However, the use of biodegradable polymers was not viable for low-cost packaging applications due to the higher cost and inferior properties when compared to commodity polymers. With the advent of commercial-scale ring-opening polymerization for production of PLA[54] and fermentation processes for the production of PHB and its copolymers[55], degradable polymers have become more attractive for low-cost applications such as eco-friendly food packaging[56,57], and degradable and transient electronics[58,59]. All applications that necessitate the degradation of a polymer depend on the physio-chemical processes that pertain to chain scission. Therefore, the nature and mechanism of degradation are important factors that determine the suitability of these polymers in various environmental conditions and applications.

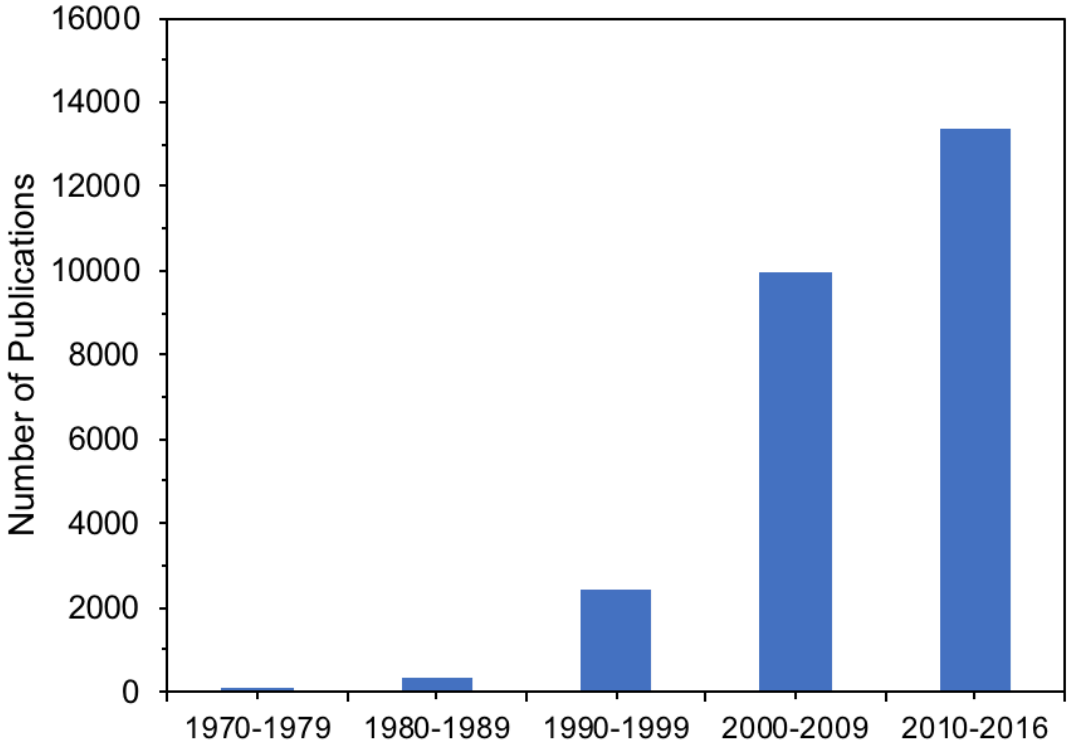

Figure 2.2 Number of publications with keyword degradation of polymers in the last few decades (Scopus database search as of October 2017).

2.2. Mechanism of Biodegradation in Polymers

Polymers are a class of macromolecular materials that are characterized by covalently bound, continuous chain-like molecules, resulting in very high molecular weights (ranging from 10^2 to 10^7 g/mol) and complex molecular configurations. Many of the unique properties of polymers can be directly correlated to their large size[60]. The interactions and intermolecular forces between the polymeric chains dictate their bulk mechanical, chemical and physical properties[61]. This strong dependence of properties on intermolecular interactions makes it critical to understand the mechanism by which the polymer chains degrade since it directly impacts their microstructure and properties.

Degradation is a process by which polymer chains are broken down into smaller chains, resulting in marked variations in the physical characteristics of the polymer. From a reaction standpoint, degradation essentially entails a mechanism for the repeated breaking of the bonds that form the polymeric backbone until the chains are reduced to their oligomeric form and further down to the monomeric building blocks.

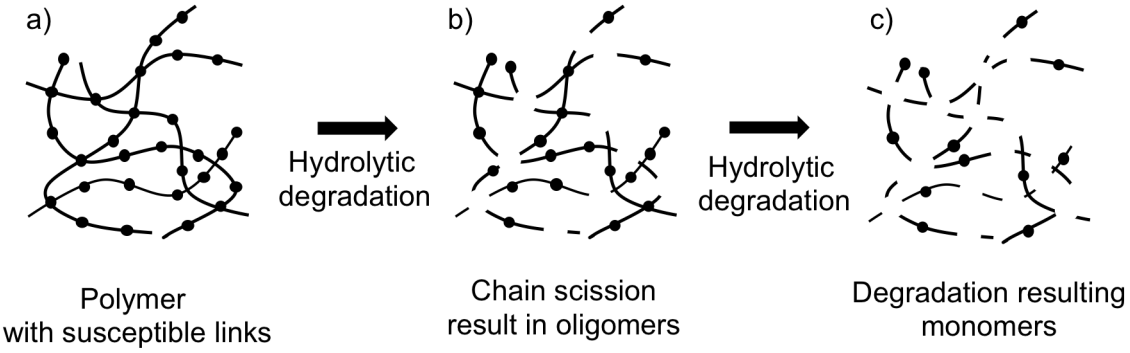

Figure 2.3 Schematic showing the degradation of polymer chains due to hydrolysis. The solid circles represent hydrolytically susceptible bonds in the polymer backbone. a) High molecular weight polymer chains before degradation, b) formation of lower molecular weight oligomers after chain scission, c) further degradation resulting in the formation of constituent monomers.

Figure 2.3 shows a schematic of the degradation process in polymer chains. This process can be achieved by the input of external energy that exceeds the bond strength of the polymeric backbone. Based on the energy source involved, the degradation process can broadly be classified into thermal[62], photolytic[63,64], mechanical[65,66] and chemolytic degradation. The first three mechanisms typically cause non-specific

degradation, irrespective of the polymer chemistry, wherein even polymers that are generally not classified as biodegradable, break down when sufficiently high thermal energy or high-energy radiation is applied. These physical degradation mechanisms are considered undesirable during the lifetime of the product and are typically not relevant for biodegradable polymers. On the other hand, enzyme-catalyzed chemolytic degradation can exhibit high specificity to the chemistry and the properties of the polymer. The high specificity can lead to relatively rapid degradation in the presence of suitable chemolytic and biochemical agents. Therefore, enzyme-mediated chemolytic mechanisms are the most relevant in view of biodegradable polymers[67–70]. The extent and susceptibility to degradation have a strong dependence on the type of biomolecule involved in the chain scission process. The enzymes that can degrade polymers such as PHB typically consist of two functional parts, namely: the substrate binding domain and the catalytic domain. The substrate binding domain is made of amino-acid configurations that enables reversible attachment to the polymer surface, whereas the catalytic domain consists of configurations that can breakdown hydrolytically unstable bonds in the polymer chain backbone. The susceptible bonds in the polymer chain are referred to as the active sites for enzyme attack. Figure 2.4 below shows a schematic of the process by which the enzymes attach to the polymer substrate and attack the active sites in the polymer backbone. This mechanism enables higher specificity and degradation rates at ambient temperatures when compared to other non-specific degradation processes.

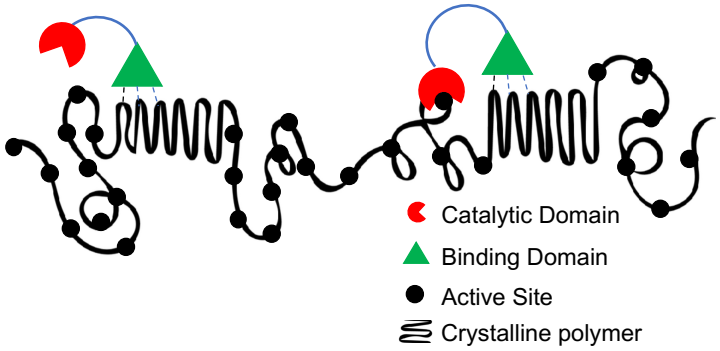

Figure 2.4 Schematic showing the process of enzymatic degradation of polymer.

Table 2.1 shows the chemical structure, relevant chemical processes and suitable enzyme catalyst for some common biodegradable polymers. The mechanism of biodegradation in all polymers involve the scission of the hydrolysable functional group in the backbone, with the assistance of a catalytic agent. Hydrolytic degradation is a process by which the polymer backbone is broken down in the presence of water molecules. The cleaving of hydrolytically unstable bonds in the polymer chain results in gradual erosion of the polymer surface and an overall reduction in molecular weight, which eventually lead to the loss of mechanical integrity of the bulk material[71,72]. In the context of polymer degradation, hydrolysis is a chemical process which can be influenced by the stability of polymer chain and the activity of the catalytic agent mediating the reaction. On the other hand, erosion is a physical process which depends on factors such as diffusion rates, dissolution stability and the kinetics of the hydrolysis itself. It is therefore important to understand the interactions between these physio-chemical processes to explain the macroscopic degradation behavior of polymers[73]. The main determinants of degradation behavior in polymers are discussed in the subsequent sections.

Table 2.1 Chemical structure, degradation mechanism and typical enzyme catalysts for some common biodegradable polymers.

Name	Chemical structure	Dominant degradation mechanism	Relevant Enzymes Catalyst
Starch	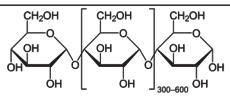	Photo & thermal degradation of C-O bonds	Amylase produced by digestive system in animals
Cellulose	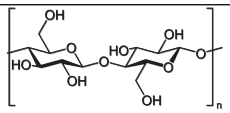	Hydrolysis into glucose or disaccharides	Cellulase[74] produced by bacteria and fungi
Polyanhydrides	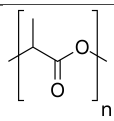	Rapid hydrolysis of anhydride bond	None; Rapid nonspecific hydrolysis in water
Poly-lactic acid	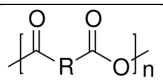	Hydrolysis of the backbone into lactide	Proteases produced by bacteria; Lipase and Esterase to limited extent[75,76]
Polyhydroxybutyrate	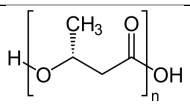	Enzymatic hydrolysis of ester bond	PHA Depolymerase[77,78]

2.3. Factors Affecting Hydrolytic Degradation of Polymers

2.3.1. Chemistry of the polymer

Two of the main factors that control the degradation of polymers are the structure and hydrolytic stability of bonds in the polymer backbone. For example, polyanhydrides are known to have some of the most hydrolytically unstable bonds among biodegradable polymers. As a result, polyanhydrides can degrade in as little as a few hours[73]. On the other hand, most polymers that fall under the class of polyamides and polyolefin are very stable and have degradation times in the range of hundreds of years under hydrolyzing environments[73]. Depending on the nature of chemical species/functional groups in the vicinity of the backbone, the degradation time can vary

widely even within materials belonging to the same class of polymers. Previous studies have shown that the variation in degradation rates with respect to polymer chemistry can be attributed to the fundamental effects of steric hindrance [79,80], electronic effects[81,82] and surface properties of the polymer.

In the literature, steric effects created by the introduction of a bulky functional group or a side chain in the polymer backbone have been shown to slow down degradation by blocking access to hydrolytically unstable bonds[79,80]. This mechanism is prominent in polyesters. Similarly, the conformation of the polymer in bulk can also result in steric effects that prevent access to the ester bonds. In contrast, the presence of an electronegative species at the alpha-position of the ester bond has been shown to assist degradation rates by reducing the bond energy[73]. Based on these fundamental inferences, a number of previous works have developed rational chemical modification approaches to control and tune polymers degradation behavior[82]. Since hydrolytic degradation is reliant on the ability of water molecules to come in contact with the polymer chains; the surface energy, hydrophobicity and the consequent water uptake can be altered through rational chemical modifications and polymer blending to influence degradation behavior. The literature shows instances where the introduction of hydrophilic monomers led to a positive impact on the degradation rate of a more hydrophobic polymer backbone[82]. Using this approach, new copolymers with tunable degradation properties have been developed. Similar results were realized by blending a hydrophilic polymer with a hydrophobic polymer that has limited degradability. For instance, previous work has shown that blends of polyglycolic acids and polylactic acid exhibit much higher degradation rates when compared to neat polyglycolic acid films[83].

Similar improvements in degradability have been found in a wide variety of polymeric systems including PHB due to the blending of hydrophilic and hygroscopic polymers[84–86]. These approaches are attractive, especially for biomedical applications, where tunability of degradation is an important consideration. Varying the chemistry of the polymer chains thus results in substantial variations in degradation behavior and properties. However, the process of blending, copolymerization and chemical modifications can give rise to undesirable changes in specificity of degradation, mechanical properties and processibility of the polymer necessitating alternative approaches for the control of degradation.

2.3.2 Environmental Factors and Catalysts

While the nature of chemical bonds in the polymer chain plays a pivotal role in determining the degradation behavior, the immediate environment can result in substantial variations in degradation. As discussed in the previous section, the presence of water in the immediate environment of most degradable polymers is a necessary (but not sufficient) condition for degradation to proceed. In addition to water molecules, external energy sufficient to overcome the activation energy of degradation is required to drive the reaction. In case of a purely hydrolytic degradation without the assistance of a catalyst, this energy has to be provided by the thermal vibrations of the surroundings[87]. However, most hydrolytic processes involve the influence of an additive or a catalyst, which can lower the activation energy and improve the kinetics of degradation by orders of magnitude.

The most common catalysts relevant for the hydrolytic degradation of polymers are acids, bases and enzymes. Both acids and bases influence the hydrolysis rate by altering the balance of hydronium ions and hydrogen ions. The equations below show the reaction of acid- and base-catalyzed hydrolysis of esters to carboxylic acid and alcohol. In this case, the presence of excess ionic species drives the reaction towards the formation of acids and alcohols by destabilizing the ester bonds. Reactions based on acids and bases as catalyst are the simplest and most common for hydrolysis of the polymer. However, these catalysts lack specificity and are effective only at elevated temperatures, which makes them unsuitable for rapid degradation of polymers[45].

$$CH_3COOCH_2CH_3 + H_2O \xrightarrow{H^+} CH_3COOH + CH_3CH_2OH$$

Ethyl Ethanoate — Ethanoic Acid — Ethanol

$$CH_3COOCH_2CH_3 + NaOH \longrightarrow CH_3COOH + CH_3CH_2OH$$

Ethyl Ethanoate — Ethanoic Acid — Ethanol

Since most biopolymers are based on chemistry intrinsic to living organisms, alternative catalysis routes exist based on enzymes. Enzymes are biomacromolecules that catalyze critical biological reactions such as the conversion of carbohydrates into simple sugars (glucosidase, amylase)[88,89] and the hydrolysis of triglycerides (lipases)[90]. Unlike acids and bases, enzymes exhibit very high specificity and activity at room temperature, which makes them suitable candidates for controlled degradation of specific polymers. Further, enzymatic degradation can be controlled and modulated by environmental co-factors — such as pH and temperature — and by the addition of chemical constituents that can act as promoters or inhibitors. Previous studies on the

enzymatic degradation of polymers showed that the degradation rate depends heavily on the enzyme concentration, reaction temperature and pH of the solution[81,91,92]. An increase in enzyme concentration has been shown to increase degradation rate, as long as the concentration is not so high as to cause saturation of the polymer substrate. Similarly, reaction temperature and pH can be modulated to reach optimal degradation conditions for the enzyme[93,94]. Many previous studies in the literature have shown similar behavior for a wide variety of enzymes and polymeric substrates[95,96].

2.3.3. Physical Properties of the Polymer

The pervious sections described the critical roles played by chemistry and environmental factors in controlling the degradation behavior of polymers. Both these parameters provide the possibility of tailoring degradable polymers with properties specific to given applications. However, altering the chemistry and the degradation environment may not be feasible in specific biomedical and food packaging applications, such as smart food packaging systems. It is therefore desirable to have the ability to control and alter the degradation of polymers by modifying their physical properties. The literature shows a direct correlation between physical properties such as crystallinity, glass transition temperature and molecular weight, and the final degradation rate. For instance, previous studies have demonstrated the preferential erosion of the amorphous phase (over the crystalline phase) in many semi-crystalline polymeric systems, including polylactic acid[97] and PHB[98,99]. The crystalline regions have a higher packing density and lower free volume than amorphous regions, which has been shown to impede the diffusion rate and the access to the active sites in the polymer chain[100,101].

In addition to the physical access to the active sites, the polymer chains have to be arranged in a suitable conformational state for the degradation process to proceed[102]. Depending on the kinetic energy available, the conformation of the polymer chains can either be frozen or be in a dynamic state, where the chain conformations change rapidly in a probabilistic manner as a function of temperature[61]. The state of the polymer chains at a given condition is dependent on its glass transition temperature (T_g). The glass transition temperature is a second-order transition where the polymer chains transform from a glassy state with limited mobility to a rubbery state where the conformations can change freely[61]. Therefore, the degradation process can be affected by the glass transition temperature, with lower T_g typically resulting in more degradation at a given temperature[103]. Even when the degradation is carried out above the T_g of the polymer, the crystalline regions do not degrade at a substantially faster rate since their close-packed structure reduces the ability of enzymes to access the active sites which are available only in specific crystal orientations[42]. These constraints greatly limit the ability of enzymes to catalyze the hydrolysis of the polymer backbone in crystalline regions. In addition, the mobility of amorphous regions in the immediate vicinity of the crystallites is limited due to the pinning effect caused by the crystals. Previous studies have shown that there are three distinct fractions for semi-crystalline polymers above their T_g, namely, crystalline regions, rubbery amorphous regions and glassy amorphous regions at the interface between the crystalline and rubbery regions[104]. The relative abundance of these different regions can have a strong influence on the degradation characteristics of the polymeric materials[104].

In addition to the conformational state of the polymer chains, the surface energy of the polymer has been demonstrated to play a pivotal role in the interaction between the domains of the enzyme and the surface of the polymer[78]. This interaction is of importance since the catalytic activity of the enzymes is a surface dependent process involving highly specific inter-molecular forces[78,105]. A change in surface energy can significantly influence the attachment kinetics and consequently the catalytic activity of enzymes. Previous studies have shown that an increase in the hydrophobicity of the interacting surfaces can alter the binding kinetics of the enzymes, which can manifest as a deviation in the degradation characteristics[106].

One of the most important parameters that can have a substantial indirect influence on the degradation behavior is the molecular weight of the polymer species. Generally, higher molecular weight results in slower degradation since more of the bonds in the polymer chain backbone must be cleaved for a measurable mass loss from the sample[73]. However, the most significant impact of molecular weight comes from its indirect influence on many of the physical properties including crystallinity, glass transition temperature and the surface hydrophobicity. Previous studies have demonstrated that an increase in molecular weight can lead to lower crystallinity[107,108], more conformational complexity[109] and substantial variations in surface tension[110,111]. As described in the previous sections, the changes in these physical properties can have a strong influence on the enzymatic degradation process. The interactions and interdependence between these factors have to be taken in consort to fully elucidate the role they play in the degradation of polymers.

Despite the complexity of the interactions between these parameters, it is possible to idealize their effects on degradation behavior based on the amount of energy, diffusion properties and mobility of the polymer chains when they are processed. The final degradation characteristics can thus be tuned by varying the processing parameters and consequently the physical properties of the polymer. These parameters include thermal processing temperature, processing time, film thickness, degradation temperature, etc. The focus of this thesis is to alter and tune the physical properties of PHB to control degradation behavior using the processing parameters mentioned above.

With the ability to tune and control the enzyme response and behavior of the polymer, it is possible to develop smart systems that can be used to sense and respond to the changes in their surroundings. The subsequent sections will delve into the utilization of degradable polymers for application as stimulus-responsive smart materials for sensing applications, with particular emphasis on enzymatic and bacterial sensing systems.

2.4. Enzyme-Responsive Polymers

2.4.1 Principles and Motivation

Responsive polymers are a class of materials that can sense an external stimulus and respond to it with a concomitant change in physical property. The literature shows many instances of synthetic smart polymers that can respond to external stimuli such as temperature[112], pH[113], electromagnetic radiation[114] and molecular species[115–117]. In addition to these responsive polymers, the last decade has seen a sharp rise in the design and development of smart materials that respond to biomolecules produced

in nature and living organisms[118–122]. The complex sensing, feedback and regulation mechanisms found in natural molecules such as enzymes and have been utilized to produce smart polymeric systems that can respond in a controlled manner with respect to the concentration, environmental conditions and the chemical properties of an analyte. Biodegradable polymers, by their ability to respond to a wide variety of biomolecules, have formed an integral part of these stimulus responsive smart materials. The complex interaction dynamics between the smart polymer and biological systems have opened the potential for advanced applications in drug delivery systems, cell support media, and biosensors[123,124]. In such applications, enzyme-responsive polymers are of particular interest[125–127]. Many dynamic processes in nature are controlled and regulated by enzymes, which act as highly specific catalysts for biological processes. In addition to facilitating biological reactions, enzymes and their reaction products can also act as markers for specific bioprocesses[128,129]. This affords the flexibility for enzyme-responsive materials to sense and control bioprocesses ranging from wound healing[130–132] to spoilage of food products[133–135].

Zelzer *et al.* define enzyme-responsive materials (ERM) as follows: “ERMs encompasses materials whose structure or functionality changes after the direct action of the enzyme”[136,137]*.* Biodegradable polymers – such as polyhydroxyalkanoates (PHA) and polylactic acid (PLA) – that can be modified by the direct action of enzymes fall under different classifications of ERMs based on the mechanism of response. The enzyme response of these polymers can be classified into three categories namely: (1) disassociation and degradation of macromolecules into smaller species, (2) polymerization or self-assembly of macromolecular constructs and (3) physical and

chemical structural change such as swelling. Among these mechanisms, degradation provides the most flexible parameters for an enzyme-responsive polymer which produces an irreversible change. As shown in the previous section, the degradation behavior and response of biodegradable polymers can be tuned and controlled by several factors which can enable enzyme-responsive systems that can be closely controlled according to the desired application and environmental conditions.

In this thesis, enzyme-responsive polymeric architectures and materials have been developed and optimized to undergo a predictable, irreversible change in physical properties in response to the presence of specific enzymatic species relevant to a specific environment. The subsequent section describes TTIs and other smart systems based on enzyme-responsive polymers. The final section of this chapter (Section 2.5) presents some background and literature on *in situ* bacterial detectors for food packaging, and shows the potential application of an enzyme-responsive polymer in a bacteriophage-based biosensor for pathogen detection.

2.4.2 Enzyme-Responsive Polymers for Smart Systems

Enzyme-responsive polymers and aggregates have found a number of interesting applications for systems that sense and respond to biological molecules. Enzyme-responsive polymer systems that can mimic complex biological regulations and response behaviors have been reported in the literatures[138]. For instance, Ulijn *et al.* has reviewed a wide range of polymeric hydrogels that can respond to enzymes for applications ranging from drug delivery to smart sensing systems[129,137,138]. In these instances, the smart polymer senses a biomolecule and responds to it by changing its visual appearance, dimensions or optical properties. Similarly, Hu *et. al* has reviewed

different enzyme-responsive polymers, arrays and constructs for smart devices that can mimic and interface with biological systems[139]. In these cases, the smart polymers have been shown to exhibit a range of self-assembly, degradation and release behavior that are typically associated with biological agents.

In this thesis, the enzyme response characteristics of PHB films have been used to fabricate a TTI. TTIs are class of passive smart devices that can be used to determine food quality and temperature abuse. TTIs produce a detectable response to the combined effects of time and temperature to which a food product is exposed [140]. Many food products lose quality when exposed to elevated temperature during transportation and storage. Also, the quality of food degrades substantially with longer storage time, due partially to bacterial and enzymatic activity. The literature describes a number of enzymatic TTIs that worked based on the variation in enzymatic activity at given storage conditions. However, existing systems either do not have the response accuracy for relevant food products or are prohibitively expensive for deployment in a food packages. Chapter 5 describes a PHB film based enzymatic TTI that overcomes most of the drawbacks of existing enzymatic TTIs. An in-depth review of the TTI landscape is provided in the introduction of Chapter 5.

2.5. *In situ* Bacterial Detection with Enzyme-Responsive Polymers

Pathogen contamination of food is a significant problem for the food industry. To minimize its impact, the food industry uses traditional pathogen detection techniques such as microbiological, immunological and nucleic acid assays to test food samples for contamination. These techniques are very accurate and sensitive, but require long analysis time and elaborate sample preparation[141,142]. Complementary methods that can be used for both on-site inspection and real-time monitoring during packaging, transportation, storage and sale of the product are therefore desirable. An enzyme-responsive smart label incorporated directly inside the food package, which can respond to specific marker enzyme produced by the pathogen in the food can prove to be a potential solution to this problem.

There are two main components in a pathogen-detecting label: the sensing unit and the response unit. The sensing unit recognizes the analyte of interest while the response unit gives a change that could be detected by an observer or by an instrument. The sensing and response mechanisms of the detector depend on the nature of the analyte used to identify the pathogen. The analyte for pathogen detection can be broadly classified as indirect or direct.

2.5.1 Indirect Analyte

Indirect analytes include any generic chemical compound produced as a result of bacterial activity. When growing on food products bacteria can produce metabolites such as CO_2, NH_3, acetic acid, lactic acid, etc. These metabolites can be used as indirect analytes for the detection of contaminants. Previous works have explored the possibility of using CO_2[143], H_2S[144] and volatile amine compounds[145] for detection of

bacterial growth in food packages. However, this indirect analyte approach suffers from a lack of sensitivity and poor selectivity. Therefore, it has been used mainly to indicate food spoilage rather than for early detection of pathogens.

2.5.2 Direct Analyte

Direct analyte approaches involve using a pathogen of interest or one of its specific components as an analyte. The most common recognition mechanisms that can be utilized for direct pathogen detection are antibodies and bacteriophages. Antibodies are proteins produced by the immune system to mark pathogenic bacteria and viruses for destruction. Antibodies can bind to specific sites, known as antigens, present on bacterial surfaces. Some antibodies can also bind and inactivate toxins produced by pathogens. Bacteriophages, on the other hand, are obligate parasites that can infect and replicate inside specific strains of bacteria. Both sensing methods lend high selectivity and sensitivity, which enables them to be used for early detection of pathogens. Antibody based recognition units have been demonstrated in the literature for proof of concept point of care devices. For instance, Goldsmith *et al.* have developed a system in which a barcode is printed using labeled antibody[146,147]. In the presence of a specific antigen, the antibody binds to them, causing the barcode to become inactivated. Bodenhamer *et al.* have proposed a system where an antibody is immobilized on a substrate in a specific pattern[148,149]. Another batch of labeled antibody is suspended in a gel and coated on this substrate. In the presence of the specific antigen, the suspended antibody binds to it, and this antibody-antigen pair binds to the immobilized antibody, causing a color change[148,149]. Charych *et al.* have demonstrated a bacterial toxin detection system that consists of a poly-diacetylene layer conjugated with

the antibody. The polymer changes color from red to blue when the antibody binds to a toxin[150]. The main challenge of antibody based systems is the limited number of antibodies suitable for binding to the pathogen of interest and the tendency of bacterial to evolve such that a certain antibody is no longer effective. Antibody systems have certain drawbacks such as high cost of synthesis, instability at high temperature, and susceptibility to damage by chemical and enzymatic reactions[141].

Lakshmanan *et al.* have developed a bacteriophage-based pathogen sensor, in which the phage is immobilized on a magneto-elastic material[151]. The adsorption of pathogens by the phage leads to a change in the resonance frequency of the magnetoelastic material, which could be detected by vibrating the material over a range of frequencies. Schofield *et al.* proposed a pathogen detection system in which a recombinant phage was engineered to induce expression of a bio-luminescent gene in the infected pathogen[152]. The luminescence can be observed using a compact, light intensity measurement device. Bacteriophages (commonly referred to as phages) can help mitigate some of the problems encountered in antibody-based systems, since phages are resistant to a variety of chemicals and enzymes. Some phages can withstand relatively high temperatures and can remain infectious even after long periods of inactivity. Also, phages infect specific strains of pathogens and can be genetically engineered to express certain marker proteins.

The present work is part of a larger project aiming to develop a polymer based smart material for the detection of pathogenic bacteria. The overall technology uses a genetically engineered bacteriophage as the sensing unit and an enzyme-responsive biopolymer film as the response unit[153]. The reporter phage is designed to induce the

expression of a specific enzyme able to degrade the biopolymer once it infects the pathogen. Once the phage replication process is completed, the phage lyses the pathogen which releases the enzyme. The enzyme degrades the polymer leading to a visual change, which can be used to visualize the presence of the pathogen without the need for sampling or external testing.

This thesis focuses on new methods to produce films and structures of the enzyme-responsive polymer PHB with a broad range of physical properties. In addition, the work aims to develop visualization techniques for the suitable integration of PHB film in the smart material platform.

2.6. References

1. Karlsson, S. & Albertsson, A. Biodegradable polymers and environmental interaction. *Polym. Eng. Sci.* **38,** 1251–1253 (1998).
2. Maurizi, M. R. Proteases and protein degradation inEscherichia coli. *Experientia* **48,** 178–201 (1992).
3. Lynd, L. R., Weimer, P. J., van Zyl, W. H. & Pretorius, I. S. Microbial cellulose utilization: fundamentals and biotechnology. *Microbiol. Mol. Biol. Rev.* **66,** 506–77, table of contents (2002).
4. O'Sullivan, A. C. Cellulose: the structure slowly unravels. *Cellulose* **4,** 173–207 (1997).
5. Muñoz, K. A., Krebs-Smith, S. M., Ballard-Barbash, R. & Cleveland, L. E. Food intakes of US children and adolescents compared with recommendations. *Pediatrics* **100,** 323–329 (1997).
6. Baekeland, L. H. Original papers: The synthesis, constitution, and uses of bakelite. *Ind. Eng. Chem.* **1,** 149–161 (1909).
7. Baekeland, L. H. Bakelite, a condensation product of phenols and formaldehyde, and its uses. *J. Franklin Inst.* **169,** (1910).
8. Clarke, W. J. V. Properties of Different Polyethylenes. *Trans. Am. Inst. Electr. Eng.* **64,** 919–922 (1945).
9. Shackleton, J. W. II. General Characteristics of Polyethylene. *Trans. Am. Inst. Electr. Eng.* **64,** 912–916 (1945).
10. Rochman, C. M. *et al.* Policy: Classify plastic waste as hazardous. *Nature* **494,** 169–171 (2013).

11. Barnes, D. K. A., Galgani, F., Thompson, R. C. & Barlaz, M. Accumulation and fragmentation of plastic debris in global environments. *Philos. Trans. R. Soc. B Biol. Sci.* **364,** 1985–1998 (2009).
12. Jambeck, J. R. *et al.* Marine pollution. Plastic waste inputs from land into the ocean. *Science* **347,** 768–71 (2015).
13. Rodrigues, F. Prospects for biodegradable plastics. *Chem. Tech.* 409–415 (1971).
14. Rodrigues, F. Prospects for biodegradable plastics. *Mod. Plast.* **48,** 92–94 (1971).
15. Zuchowska, D., Steller, R. & Meissner, W. Structure and properties of degradable polyolefin - Starch blends. *Polym. Degrad. Stab.* **60,** 173–187 (1998).
16. Landuzzi, A. & Ghosh, J. Improving Functionality of Polyolefin Films Through the Use of Additives. *J. Plast. Film & Sheeting* **19,** (2003).
17. Le Brasseur, G. Degradable polyethylenes for agricultural use. *INFORM. CHIM.* **No. 149,** 231–235 (1975).
18. Potts, J. E., Clendinning, R. A. & Ackart, W. B. The effect of chemical structure on the biodegradability of plastics. *The plastics inst. Conference on the degradability of polymers and plastics* (1973).
19. Griffin, G. J. L. Biodegradable Fillers In Thermoplastics. *Am Chem Soc Div Org Coatings Plast Chem Prepr* **33,** 88–96 (1973).
20. Worne, H. Modify plastics for degradability. *Plast. Technol* **17,** 23–28 (1971).
21. Liu, X., Gao, C., Sangwan, P., Yu, L. & Tong, Z. Accelerating the degradation of polyolefins through additives and blending. *J. Appl. Polym. Sci.* **131,** 9001–9015 (2014).
22. Abd El-Rehim, H. A., Hegazy, E.-S. A., Ali, A. M. & Rabie, A. M. Synergistic effect

of combining UV-sunlight-soil burial treatment on the biodegradation rate of LDPE/starch blends. *J. Photochem. Photobiol. A Chem.* **163,** 547–556 (2004).

23. Cichy, B. *et al.* Polyolefin oxo-degradation accelerators - A new trend to promote environmental protection. *Polish J. Chem. Technol.* **12,** 44–52 (2010).
24. Wagner, M. *et al.* Microplastics in freshwater ecosystems: what we know and what we need to know. *Environ. Sci. Eur.* **26,** 12 (2014).
25. Matthew Cole, Pennie Lindeque, Claudia Halsband, T. S. G. Microplastics as contaminants in the marine environment: A review. *Mar. Pollut. Bull.* **62,** 2588–2597 (2011).
26. Dorgan, J. R., Braun, B., Wegner, J. R. & Knauss, D. M. in *Degradable Polymers and Materials Principles and Practice* 102–125 (2006). doi:10.1021/bk-2006-0939.ch007
27. Gentile, P., Chiono, V., Carmagnola, I. & Hatton, P. V. An overview of poly(lactic-co-glycolic) acid (PLGA)-based biomaterials for bone tissue engineering. *Int. J. Mol. Sci.* **15,** 3640–59 (2014).
28. Labet, M. & Thielemans, W. Synthesis of polycaprolactone: A review. *Chem. Soc. Rev.* **38,** 3484–3504 (2009).
29. Drumright, R. E., Gruber, P. R. & Henton, D. E. Polylactic acid technology. *Adv. Mater.* **12,** 1841–1846 (2000).
30. Madhavan Nampoothiri, K., Nair, N. R. & John, R. P. An overview of the recent developments in polylactide (PLA) research. *Bioresour. Technol.* **101,** 8493–8501 (2010).
31. Tyler, B., Gullotti, D., Mangraviti, A., Utsuki, T. & Brem, H. Polylactic acid (PLA)

controlled delivery carriers for biomedical applications. *Adv. Drug Deliv. Rev.* **107,** 163–175 (2016).

32. Chen, Y. *et al.* Review of Multifarious Applications of Poly (Lactic Acid). *Polym. - Plast. Technol. Eng.* **55,** 1057–1075 (2016).
33. Brodin, M., Vallejos, M., Opedal, M. T., Area, M. C. & Chinga-Carrasco, G. Lignocellulosics as sustainable resources for production of bioplastics – A review. *J. Clean. Prod.* **162,** 646–664 (2017).
34. Mohnen, D. Pectin structure and biosynthesis. *Curr. Opin. Plant Biol.* **11,** 266–277 (2008).
35. Tharanathan, R. N. & Kittur, F. S. Chitin - The Undisputed Biomolecule of Great Potential. *Crit. Rev. Food Sci. Nutr.* **43,** 61–87 (2003).
36. Lee, S. Y. Bacterial polyhydroxyalkanoates. *Biotechnol. Bioeng.* **49,** 1–14 (1996).
37. Lee, S. Y. Plastic bacteria? Progress and prospects for polyhydroxyalkanoate production in bacteria. *Trends Biotechnol.* **14,** 431–438 (1996).
38. Rinaudo, M. Chitin and chitosan: Properties and applications. *Prog. Polym. Sci.* **31,** 603–632 (2006).
39. Ghormade, V., Pathan, E. K. & Deshpande, M. V. Can fungi compete with marine sources for chitosan production? *Int. J. Biol. Macromol.* **104,** 1415–1421 (2017).
40. Vert, M. Aliphatic polyesters: Great degradable polymers that cannot do everything. *Biomacromolecules* **6,** 538–546 (2005).
41. Zinn, M., Witholt, B. & Egli, T. Occurrence, synthesis and medical application of bacterial polyhydroxyalkanoate. *Adv. Drug Deliv. Rev.* **53,** 5–21 (2001).
42. Orts, W. & Nobes, G. Poly (hydroxyalkanoates): biorefinery polymers with a whole

range of applications. The work of Robert H. Marchessault. *Can. J.* **86,** 628–640 (2008).

43. Madison, L. L. & Huisman, G. W. Metabolic engineering of poly(3-hydroxyalkanoates): From DNA to plastic. *Microbiol. Mol. Biol. Rev.* **63,** 21–53 (1999).

44. Vert, M., Li, S. M., Spenlehauer, G. & Guerin, P. Bioresorbability and biocompatibility of aliphatic polyesters. *J. Mater. Sci. Mater. Med.* **3,** 432–446 (1992).

45. Yu, J., Plackett, D. & Chen, L. X. L. Kinetics and mechanism of the monomeric products from abiotic hydrolysis of poly[(R)-3-hydroxybutyrate] under acidic and alkaline conditions. *Polym. Degrad. Stab.* **89,** 289–299 (2005).

46. Steinbüchel, A. & Valentin, H. E. Diversity of bacterial polyhydroxyalkanoic acids. *FEMS Microbiol. Lett.* **128,** 219–228 (1995).

47. Jendrossek, D. & Handrick, R. *Microbial degradation of polyhydroxyalkanoates*. *Annual Review of Microbiology* **56,** (2002).

48. Tokiwa, Y. & Ugwu, C. U. Biotechnological production of (R)-3-hydroxybutyric acid monomer. *J. Biotechnol.* **132,** 264–272 (2007).

49. Lendlein, A. & Langer, R. Biodegradable, elastic shape-memory polymers for potential biomedical applications. *Science (80-.).* **296,** 1673–1676 (2002).

50. Middleton, J. C. & Tipton, A. J. Synthetic biodegradable polymers as orthopedic devices. *Biomaterials* **21,** 2335–2346 (2000).

51. Jeong, B., Bae, Y. H., Lee, D. S. & Kim, S. W. Biodegradable block copolymers as injectable drug-delivery systems. *Nature* **388,** 860–862 (1997).

52. Panyam, J. & Labhasetwar, V. Biodegradable nanoparticles for drug and gene delivery to cells and tissue. *Adv. Drug Deliv. Rev.* **55,** 329–347 (2003).

53. Hutmacher, D. W. Scaffolds in tissue engineering bone and cartilage. *Biomaterials* **21,** 2529–2543 (2000).

54. Odile Dechy-Cabaret, Blanca Martin-Vaca, A. & Bourissou*, D. Controlled Ring-Opening Polymerization of Lactide and Glycolide. *Chem. Rev.* **104,** 6147–6176 (2004).

55. Marchessault, R. H. *et al.* Poly(β-hydroxyalkanoates): Biorefinery polymers in search of applications. *Makromol. Chemie. Macromol. Symp.* **19,** 235–254 (1988).

56. Siracusa, V., Rocculi, P., Romani, S. & Rosa, M. D. Biodegradable polymers for food packaging: a review. *Trends Food Sci. Technol.* **19,** 634–643 (2008).

57. Bucci, D. Z., Tavares, L. B. B. & Sell, I. PHB packaging for the storage of food products. *Polym. Test.* **24,** 564–571 (2005).

58. Acar, H. *et al.* Study of Physically Transient Insulating Materials as a Potential Platform for Transient Electronics and Bioelectronics. *Adv. Funct. Mater.* **24,** 4135–4143 (2014).

59. Dagdeviren, C. *et al.* Transient, biocompatible electronics and energy harvesters based on ZnO. *Small* **9,** 3398–404 (2013).

60. Sperling, L. H. *Introduction to Physical Polymer Science: Fourth Edition*. *Introduction to Physical Polymer Science: Fourth Edition* (CRC Press, 2005). doi:10.1002/0471757128

61. Painter, P. C. & Coleman, M. M. *Essentials of polymer science and engineering*. (DEStech Publications, Inc, 2009).

62. Sánchez-Jiménez, P. E., Pérez-Maqueda, L. A., Perejón, A. & Criado, J. M. A new model for the kinetic analysis of thermal degradation of polymers driven by random scission. *Polym. Degrad. Stab.* **95,** 733–739 (2010).

63. Davidson, R. S. The photodegradation of some naturally occurring polymers. *J. Photochem. Photobiol. B Biol.* **33,** 3–25 (1996).

64. Andrady, A. L. *Wavelength Sensitivity in Polymer Photodegradation*. *Advances in Polymer Science* **128,** (1997).

65. Capone, C., Di Landro, L., Inzoli, F., Penco, M. & Sartore, L. Thermal and mechanical degradation during polymer extrusion processing. *Polym. Eng. Sci.* **47,** (2007).

66. Norris, J. O. W., Norman, S. A. & Tribble, M. J. Mechanical degradation of polymer coated glass optical fibers under γ irradiation. in *Proceedings of SPIE - The International Society for Optical Engineering* **1314,** (1990).

67. Nduko, J. M., Sun, J. & Taguchi, S. *Biosynthesis, Properties, and Biodegradation of Lactate-Based Polymers*. *ACS Symposium Series* **1192,** (2015).

68. Mizuno, W. *et al.* Degradation behavior of injection molded biodegradable polymers in soil, aqueous environments, and an activated sludge. *Kobunshi Ronbunshu* **58,** 59–65 (2001).

69. Eubeler, J. P., Bernhard, M. & Knepper, T. P. Environmental biodegradation of synthetic polymers II. Biodegradation of different polymer groups. *TrAC - Trends Anal. Chem.* **29,** 84–100 (2010).

70. Mayer, J. M. *et al. Biodegradation of Polymer Films in Marine and Soil Environments*. *ACS Symposium Series* **627,** (1996).

71. Wang, Y., Han, X., Pan, J. & Sinka, C. An entropy spring model for the Young's modulus change of biodegradable polymers during biodegradation. *J. Mech. Behav. Biomed. Mater.* **3,** 14–21 (2010).

72. Iordanskii, A. L., Zaikov, G. E. & Berlin, A. A. Diffusion kinetics of hydrolysis of biodegradable polymers. Weight loss and control of the release of low molecular weight substances. *Polym. Sci. - Ser. D* **8,** 211–218 (2015).

73. Gopferich, A. Mechanism of Polymer Degradation and Erosion. *Biomaterials* **17,** 103–114 (1996).

74. Berghem, L. E. R. & Pettersson, L. G. The Mechanism of Enzymatic Cellulose Degradation. Isolation and Some Properties of a beta-Glucosidase from Trichoderma viride. *Eur. J. Biochem.* **46,** 295–305 (1974).

75. Lee, S. H., Kim, I. Y. & Song, W. S. Biodegradation of polylactic acid (PLA) fibers using different enzymes. *Macromol. Res.* **22,** 657–663 (2014).

76. Lee, S. H. & Yeo, S. Y. Improvement of hydrophilicity of polylactic acid (PLA) fabrics by means of a proteolytic enzyme from Bacillus licheniformis. *Fibers Polym.* **17,** 1154–1161 (2016).

77. Jendrossek, D. & Handrick, R. Microbial Degradation of Polyhydroxyalkanoates*. *Annu. Rev. Microbiol.* **56,** 403–432 (2002).

78. Mukai, K., Yamada, K. & Doi, Y. Kinetics and mechanism of heterogeneous hydrolysis of poly[(R)-3-hydroxybutyrate] film by PHA depolymerases. *Int. J. Biol. Macromol.* **15,** 361–366 (1993).

79. D'Souza, A. J. M. & Topp, E. M. Release from polymeric prodrugs: Linkages and their degradation. *J. Pharm. Sci.* **93,** 1962–1979 (2004).

80. Chu, C. C. The effect of pH on thein vitro degradation of poly(glycolide lactide) copolymer absorbable sutures. *J. Biomed. Mater. Res.* **16,** 117–124 (1982).

81. Pitt, C. G., Hendren, R. W., Schindler, A. & Woodward, S. C. The enzymatic surface erosion of aliphatic polyesters. *J. Control. Release* **1,** 3–14 (1984).

82. Hofmann, D., Entrialgo-Castaño, M., Kratz, K. & Lendlein, A. Knowledge-Based Approach towards Hydrolytic Degradation of Polymer-Based Biomaterials. *Adv. Mater.* **21,** 3237–3245 (2009).

83. Middleton, J. C. & Tipton, A. J. Synthetic biodegradable polymers as orthopedic devices. *Biomaterials* **21,** 2335–2346 (2000).

84. Characterization of polyhydroxybutyrate-hydroxyvalerate (PHB-HV)/maize starch blend films. *J. Food Eng.* **89,** 361–369 (2008).

85. Crystallization behavior and environmental biodegradability of the blend films of poly(3-hydroxybutyric acid) with chitin and chitosan. *Carbohydr. Polym.* **41,** 351–356 (2000).

86. Lai, S.-M., Don, T.-M. & Huang, Y.-C. Preparation and properties of biodegradable thermoplastic starch/poly(hydroxy butyrate) blends. *J. Appl. Polym. Sci.* **100,** 2371–2379 (2006).

87. Yu, J., Plackett, D. & Chen, L. X. L. Kinetics and mechanism of the monomeric products from abiotic hydrolysis of poly [(R) -3-hydroxybutyrate] under acidic and alkaline conditions. **89,** (2005).

88. Michlmayr, H. & Kneifel, W. β-Glucosidase activities of lactic acid bacteria: Mechanisms, impact on fermented food and human health. *FEMS Microbiol. Lett.* **352,** 1–10 (2014).

89. Pandey, A. *et al.* Advances in microbial amylases. *Biotechnol. Appl. Biochem.* **31,** 135–152 (2000).

90. Mrozik, A., Hupert-Kocurek, K., Nowak, B. & Łabuzek, S. Microbial lipases and their significance in the protection of the environment. *Postep. Mikrobiol.* **47,** 43–50 (2008).

91. Leu, S.-Y. & Zhu, J. Y. Substrate-Related Factors Affecting Enzymatic Saccharification of Lignocelluloses: Our Recent Understanding. *BioEnergy Res.* **6,** 405–415 (2013).

92. Alexis, F. Factors affecting the degradation and drug-release mechanism of poly(lactic acid) and poly[(lactic acid)-co-(glycolic acid)]. *Polym. Int.* **54,** 36–46 (2005).

93. Holum, J. R. *Elements of general and biological chemistry*. (Wiley, 1987).

94. Bennett, T. P. *Modern topics in biochemistry; structure and function of biological molecules*. (Macmillan, 1966).

95. Iwata, T., Abe, H. & Kikkawa, Y. *Enzymatic Degradation*. *Poly(Lactic Acid): Synthesis, Structures, Properties, Processing, and Applications* (2010). doi:10.1002/9780470649848.ch22

96. Madras, G. *Enzymatic degradation of polymers*. *Biodegradable Polymers for Industrial Applications* (2005). doi:10.1533/9781845690762.3.411

97. Giuliana, G. & Roberto, P. Effect of PLA grades and morphologies on hydrolytic degradation at composting temperature: Assessment of structural modification and kinetic parameters. *Polym. Degrad. Stab.* **98,** 1006–1014 (2013).

98. Abe, H., Matsubara, I., Doi, Y. & Matsubara, I. Physical Properties and Enzymatic

Degradability of Polymer Blends of Bacterial Poly[(R)-3-hydroxybutyrate] and Poly[(R,S)-3-hydroxybutyrate] Stereoisomers. *Macromolecules* **28,** 844–853 (1995).

99. Spyros, A., Kimmich, R., Briese, B. H. & Jendrossek, D. 1H NMR Imaging Study of Enzymatic Degradation in Poly(3-hydroxybutyrate) and Poly(3-hydroxybutyrate-co-3-hydroxyvalerate). Evidence for Preferential Degradation of the Amorphous Phase by PHB Depolymerase B from Pseudomonas lemoignei. *Macromolecules* **30,** 8218–8225 (1997).
100. Water absorption and states of water in semicrystalline poly(vinyl alcohol) films. *Polymer (Guildf).* **37,** 1371–1376 (1996).
101. Tsuji, H. & Ikada, Y. Blends of crystalline and amorphous poly(lactide). III. Hydrolysis of solution-cast blend films. *J. Appl. Polym. Sci.* **63,** 855–863 (1997).
102. Hiraishi, T., Komiya, N. & Maeda, M. Y443F mutation in the substrate-binding domain of extracellular PHB depolymerase enhances its PHB adsorption and disruption abilities. *Polym. Degrad. Stab.* **95,** 1370–1374 (2010).
103. He, Y., Shuai, X., Kasuya, K. I., Doi, Y. & Inoue, Y. Enzymatic degradation of atactic poly(R,S-3-hydroxybutyrate) induced by amorphous polymers and the enzymatic degradation temperature window of an amorphous polymer system. *Biomacromolecules* **2,** 1045–1051 (2001).
104. Hancock, B. C. & Zografi, G. Characteristics and Significance of the Amorphous State in Pharmaceutical Systems. *J. Pharm. Sci.* **86,** 1–12 (1997).
105. Reis, P., Holmberg, K., Watzke, H., Leser, M. E. & Miller, R. Lipases at interfaces: A review. *Adv. Colloid Interface Sci.* **147–148,** 237–250 (2009).

106. Hiraishi, T., Hirahara, Y., Doi, Y., Maeda, M. & Taguchi, S. Effects of mutations in the substrate-binding domain of poly[(R)-3-hydroxybutyrate] (PHB) depolymerase from Ralstonia pickettii T1 on PHB degradation. *Appl. Environ. Microbiol.* **72,** 7331–7338 (2006).

107. Tung, L. J. & Buckser, S. The Effects of Molecular Weight on the Crystallinity of Polyethylene. *J. Phys. Chem.* **62,** 1530–1534 (1958).

108. Zen, A. *et al.* Effect of Molecular Weight on the Structure and Crystallinity of Poly(3-hexylthiophene). *Macromolecules* **39,** 2162–2171 (2006).

109. Hariharan, A., Kumar, S. K. & Russell, T. P. A lattice model for the surface segregation of polymer chains due to molecular weight effects. *Macromolecules* **23,** 3584–3592 (1990).

110. Sauer, B. B. & Dee, G. T. Molecular weight and temperature dependence of polymer surface tension: comparison of experiment with theory. *Macromolecules* **24,** 2124–2126 (1991).

111. Moreira, J. C. & Demarquette, N. R. Influence of temperature, molecular weight, and molecular weight dispersity on the surface tension of PS, PP, and PE. I. Experimental. *J. Appl. Polym. Sci.* **82,** 1907–1920 (2001).

112. Schmaljohann, D. Thermo- and pH-responsive polymers in drug delivery. *Adv. Drug Deliv. Rev.* **58,** 1655–1670 (2006).

113. Schmaljohann, D. Thermo- and pH-responsive polymers in drug delivery. *Adv. Drug Deliv. Rev.* **58,** 1655–1670 (2006).

114. Roy, D., Cambre, J. N. & Sumerlin, B. S. Future perspectives and recent advances in stimuli-responsive materials. *Prog. Polym. Sci.* **35,** 278–301 (2010).

115. Gil, E. S. & Hudson, S. M. Stimuli-reponsive polymers and their bioconjugates. *Prog. Polym. Sci.* **29,** 1173–1222 (2004).

116. Qiu, Y. & Park, K. Environment-sensitive hydrogels for drug delivery. *Adv. Drug Deliv. Rev.* **53,** 321–339 (2001).

117. Stuart, M. A. C. *et al.* Emerging applications of stimuli-responsive polymer materials. *Nat. Mater.* **9,** 101–113 (2010).

118. Lin, Z.-T. *et al.* A Nanoparticle-Decorated Biomolecule-Responsive Polymer Enables Robust Signaling Cascade for Biosensing. *Adv. Mater.* **29,** (2017).

119. Hoffman, A. S. *et al.* Conjugates of Stimuli-Responsive Polymers and Biomolecules: Random and Site-Specific Conjugates of Temperature-Sensitive Polymers and Proteins. *Macromol. Symp.* **118,** 553–563 (1997).

120. Mendes, P. M. Stimuli-responsive surfaces for bio-applications. *Chem. Soc. Rev.* **37,** 2512–2529 (2008).

121. Cole, M. A., Voelcker, N. H., Thissen, H. & Griesser, H. J. Stimuli-responsive interfaces and systems for the control of protein-surface and cell-surface interactions. *Biomaterials* **30,** 1827–1850 (2009).

122. de la Rica, R., Aili, D. & Stevens, M. M. Enzyme-responsive nanoparticles for drug release and diagnostics. *Adv. Drug Deliv. Rev.* **64,** 967–978 (2012).

123. Islam, M. R. *et al.* Responsive polymers for analytical applications: A review. *Anal. Chim. Acta* **789,** 17–32 (2013).

124. Islam, M. R., Gao, Y., Li, X. & Serpe, M. J. Responsive polymers for biosensing and protein delivery. *J. Mater. Chem. B* **2,** 2444–2451 (2014).

125. Hu, J., Zhang, G. & Liu, S. Enzyme-responsive polymeric assemblies,

nanoparticles and hydrogels. *Chem. Soc. Rev.* **41,** 5933–5949 (2012).

126. Chandrawati, R. Enzyme-responsive polymer hydrogels for therapeutic delivery. *Exp. Biol. Med.* **241,** 972–979 (2016).

127. Ma, C. D. *et al.* Liquid Crystal Interfaces Programmed with Enzyme-Responsive Polymers and Surfactants. *Small* **11,** 5747–5751 (2015).

128. Schiffer, D. *et al.* Enzyme-responsive polymers for microbial infection detection. *Expert Rev. Mol. Diagn.* **15,** 1125–1131 (2015).

129. Zelzer, M. & Ulijn, R. V. *Enzyme-responsive polymers: Properties, synthesis and applications*. *Smart Polymers and their Applications* (2014). doi:10.1533/9780857097026.1.166

130. Said, S. S. *et al.* Bioburden-responsive antimicrobial PLGA ultrafine fibers for wound healing. *Eur. J. Pharm. Biopharm.* **80,** (2012).

131. Schiffer, D. *et al.* Lysozyme-responsive polymer systems for detection of infection. *Eng. Life Sci.* **15,** (2015).

132. Griffin, M., Casadio, R. & Bergamini, C. M. Transglutaminases: Nature's biological glues. *Biochem. J.* **368,** (2002).

133. Yada, R. Y. *Improving and tailoring enzymes for food quality and functionality*. *Improving and Tailoring Enzymes for Food Quality and Functionality* (2015). doi:10.1016/C2013-0-16520-8

134. Terefe, N. S., Buckow, R. & Versteeg, C. Quality-Related Enzymes in Fruit and Vegetable Products: Effects of Novel Food Processing Technologies, Part 1: High-Pressure Processing. *Crit. Rev. Food Sci. Nutr.* **54,** 24–63 (2014).

135. Whitaker, J. R. Enzymes: monitors of food stability and quality. *Trends Food Sci.*

Technol. **2,** 94–97 (1991).

136. Zelzer, M. & Ulijn, R. V. *Enzyme-responsive polymers: properties, synthesis and applications*. *Smart Polymers and their Applications* (Woodhead Publishing Limited, 2014). doi:10.1533/9780857097026.1.166
137. Zelzer, M., Todd, S. J., Hirst, A. R., McDonald, T. O. & Ulijn, R. V. Enzyme responsive materials: design strategies and future developments. *Biomater. Sci.* **1,** 11–39 (2013).
138. Ulijn, R. V *et al.* Bioresponsive hydrogels. *Mater. Today* **10,** 40–48 (2007).
139. Hu, J., Zhang, G. & Liu, S. Enzyme-responsive polymeric assemblies, nanoparticles and hydrogels. *Chem. Soc. Rev.* **41,** 5933 (2012).
140. Robertson, G. L. *Food Packaging: Principles and Practice*. (CRC Press, 1998).
141. Singh, A., Poshtiban, S. & Evoy, S. Recent Advances in Bacteriophage Based Biosensors for Food-Borne Pathogen Detection. *Sensors* **13,** 1763–1786 (2013).
142. Baeumner, A. J. Biosensors for environmental pollutants and food contaminants. *Anal. Bioanal. Chem.* **377,** 434–445 (2003).
143. Puligundla, P., Jung, J. & Ko, S. Carbon dioxide sensors for intelligent food packaging applications. *Food Control* **25,** 328–333 (2012).
144. Smolander, M. *et al.* Myoglobin-based indicators for the evaluation of freshness of unmarinated broiler cuts. *Innov. Food Sci. Emerg. Technol.* **3,** 279–288 (2002).
145. Pacquit, A. *et al.* Development of a smart packaging for the monitoring of fish spoilage. *Food Chem.* **102,** 466–470 (2007).
146. Goldsmith, R. M. Detection of contaminants in food. (1994).
147. Goldsmith, R. M., Goldsmith, C. H. & Woodaman, J. G. Dual bar code for food

contamination detection. (2002).

148. Bodenhamer, W. T. Method and apparatus for selective biological material detection. (2000).

149. Lander, T. & Bodenhamer, W. T. Biological material detecting articles of manufacture. (2005).

150. Charych, D. *et al.* A 'litmus test' for molecular recognition using artificial membranes. *Chem. Biol.* **3,** 113–120 (1996).

151. Lakshmanan, R. S. *et al.* Detection of Salmonella typhimurium in fat free milk using a phage immobilized magnetoelastic sensor. *Sensors Actuators B Chem.* **126,** 544–550 (2007).

152. Schofield, D. A., Molineux, I. J. & Westwater, C. 'Bioluminescent' Reporter Phage for the Detection of Category A Bacterial Pathogens. *J. Vis. Exp.* (2011). doi:10.3791/2740

153. Elias, A. *et al.* Bacteriophage-based biosensor for microbial detection. US Patent No. 20160061830A1 (2015).

3. Polyhydroxybutyrate films using acetic acid as solvent

In the following manuscript, a method for fabrication of PHB film with tunable mechanical, optical and thermal properties using acetic acid as solvent has been proposed. The most common solvent for processing PHB used in literature is chloroform (a well-documented health and environmental hazard), making it undesirable for fabricating PHB films that form a part of food packages. Therefore, acetic acid was explored in this article as a greener solvent for processing of PHB thin films. This article demonstrates the versatility of the acetic acid solvent casting process by fabrication flexible PHB films of different thicknesses, porous structures and sheets. The results presented in this work could thus form the basis for deploying PHB thin films for smart packaging, porous media for biomedical applications and optically clear films for degradable optoelectronics.

The manuscript was published in *Scientific Reports*, under the title **"Tuning the properties of polyhydroxybutyrate films using acetic acid via solvent casting".** The contents are reproduced with some edits here in accordance with the author's rights and copyright policies of the publisher, Nature and Scientific Reports.

Tuning the properties of polyhydroxybutyrate films using acetic acid via solvent casting

Preetam Anbukarasu, Dominic Sauvageau, Anastasia Elias

Department of Chemical and Materials Engineering, University of Alberta, T6G 1H9, Edmonton, Canada

3.1. Abstract

Biodegradable Polyhydroxybutyrate (PHB) films were fabricated using acetic acid as an alternative to common solvents such as chloroform. The PHB films were prepared using a solvent casting process at temperatures ranging from 80ºC to 160ºC. The crystallinity, mechanical properties and surface morphology of the films cast at different temperatures were characterized and compared to PHB films cast using chloroform as a solvent. Results revealed that the properties of the PHB film varied considerably with solvent casting temperature. In general, samples processed with acetic acid at low temperatures had comparable mechanical properties to PHB cast using chloroform. This acetic acid based method is environmentally friendly, cost efficient and allows more flexible processing conditions and broader ranges of polymer properties than traditional methods.

3.2. Introduction

Polyhydroxybutyrate (PHB) is a polymer of bacterial origin that can be broken down by enzymes known as PHB depolymerases[1–3]. PHB, in its natural state as produced from bacterial fernmentation, is very sterioregular and isotactic. This regularity of the polymer chains enables PHB to crystallize readily into an orthorhombinc crystal structure. The high sterioregularity plays an important role in the crystallization during extraction and cold-crystallization during storage at room temperature, and dictates the final properties of the polymer. Pure PHB can be degraded by a variety of enzymes over a broad range of temperatures, resulting in non-toxic degradation products[4]. It is a truly biodegradable and food-safe alternative to petroleum-based polymers. PHB has the potential for use in medical applications[5,6] and food packaging materials[7]. Also, PHB can be functionalized and chemically modified[6,8] to form self-assembled micelles[9] and gels that have good biocompatibility and biodegradability.

Despite these advantages, the challenges in processing PHB into flexible, thin films is one of the main factors that prevent its widespread application[10]. Its high melting point (~ 175ºC to 180ºC) and low degradation temperature (~ 220ºC) limit the possibility of thermal processing to prepare PHB films. Approaches such as heat treatment, co-polymerization[11–13], blending[14,15] and the addition of plasticizers[16] have been used to improve the thermal processability. By using a combination of approaches mentioned above, PHB can be extruded, rolled or pressed into films having good mechanical properties.

Thermal processing assisted by additives is the most cost effective and industrially relevant approach for large-scale production of PHB films. However, most of the additives that improve thermal processing can also reduce biodegradation rates, increase cost, generate toxic degradation products[17,18] or cause health hazards related to leaching of plasticizers[13-21]. Recent works are exploring eco-friendly plasticizers[22,23], green polymer blend, composites[24,25] and additives[26] to overcome these drawbacks, but some of the issues with using additives still exists. Films produced by thermal processing can also have limited flexibility and optical clarity, even in the presence of plasticizers and additives. Such limitations are acceptable in applications, such as compostable bags and disposable containers. However, for other specialized applications – such as bio-medical implants and optical films, which require PHB with properties including high porosity, low thickness and optical clarity – alternative processing routes that offer more flexibility in processing conditions and PHB properties are necessary.

One such approach for fabricating PHB films is to use a solvent casting process[27], which involves dissolving the polymer in a suitable solvent and evaporating the solvent to obtain a high-quality film. Solvent casting enables tunability of mechanical and optical properties of the film through the variation of processing parameters such as solvent casting time and temperature. The solvent casting process is capable of producing ultra-thin films that have high optical clarity and porous films that can degrade rapidly in physiological conditions. Despite these advantages, the added cost and hazards that come with solvents has limited solvent casting to niche applications such

as cellulose triacetate films for photographic sheets[28] and polyvinyl alcohol films for polarizers in liquid crystal displays[29]. A relatively safe and cost-effective solvent can bring down the cost of solvent casting and enable the production of high-quality PHB films through this route.

To produce continuous films that have good mechanical properties, a compatible solvent that has a similar solubility parameter to PHB is necessary. A previous study revealed that only a few solvents are suitable candidates for PHB, of which chloroform is one of the most compatible and most commonly used[30,31]. However, previous reports have rated chloroform as one of the most damaging chemicals to the environment and human health[32–34]. In addition, the high affinity of PHB to chloroform can cause traces of chloroform to remain in the polymer even after long aging time, which could prove to be a health risk in medical implants and food packages. The potential for PHB to be used in food packaging and for medical applications makes it even more desirable to find food-safe and risk-free solvents. The Hansen solubility parameter of PHB is δ_d = 16.5, δ_h = 8.6. δ_p = 9.0, which results in an overall solubility parameter of 19.1 – 19.8 when the influence of all interactions is considered[30]. Most common solvents (apart from chlorinated organic solvents) do not have interaction values that are compatible with PHB, which makes it challenging to prepare PHB by solvent casting. However, with an increase in dissolution temperature, the interaction parameters change, which typically makes the polymer more soluble in a suitable solvent[30].

The present work explores acetic acid as a solvent to dissolve and process PHB through solvent casting. Acetic acid is cost effective, safe to handle and easy to recover, as demonstrated by its extensive use in the synthesis of polymers such as cellulose acetate and polyvinyl acetate[35]. Although acetic acid is not the most compatible solvent for PHB, its high boiling point (118ºC) enables dissolution and processing of PHB at elevated temperatures. The incompatibility of acetic acid also allows us to control both the microstructure and properties of the films by taking advantage of the phase separation and crystallization behavior exhibited by the PHB/acetic acid system.

Some previous works have used a mixture of dilute acetic acid and an organic solvent to blend PHB and polymers such as chitosan[36]. Other works have used a combination of acetic acid and organic solvents (typically dimethyl sulfoxide) to conjugate polymeric side chains to PHB[37,38]. However, in all these instances, the dilute acetic acid was used to dissolve the combining polymer (chitosan, cellulose) and to assist blending or conjugation, while organic solvents such as chloroform or hexafluoro-2-propanol were used to dissolve the PHB prior to blending. To our knowledge, glacial acetic acid by itself has never been used to dissolve and produce PHB films.

In this work, we present the impact of the solvent casting processing conditions on the thermal behavior, crystallinity, mechanical properties and surface roughness of PHB films.

3.3. Materials and Method

Polymer and Chemicals

The PHB (98%) used in the work was obtained as thermally processed pellets (BRS Bulk Bio-pellets, Bulk Reef Supply, Golden Valley, USA). The PHB pellets were washed with isopropyl alcohol to prevent microbial contamination and otherwise used as received. Acetic acid (99%) and chloroform (99%) were obtained from Sigma-Aldrich, Canada and used as received.

PHB film preparation

The PHB pellets were mixed with acetic acid and heated to boiling in a covered beaker under constant stirring until the sample was completely dissolved (typically ~ 40 to 60 minutes) (Figure 3.1.a). A polymer solution with a concentration of 0.05 g/ml of PHB in acetic acid was used to prepare all test films.

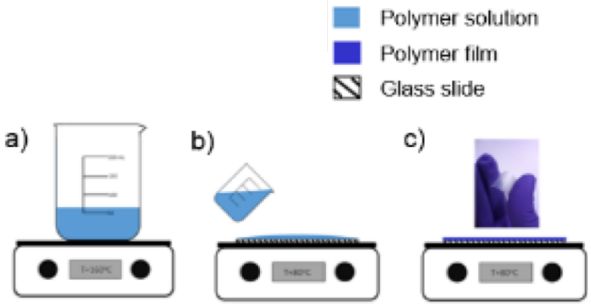

Figure 3.1 Schematic of PHB film preparation by solvent casting. a) The PHB is dissolved in acetic acid at 160ºC, b) the solution is poured onto a glass slide held at the casting temperature, c) samples are baked for 3 or 6 minutes (depending on the casting temperature).

Approximately 4.5-5 ml of polymer solution – previously brought to the required casting temperature – was poured on a pre-heated glass slide (70 mm X 35 mm) maintained at the required casting temperature (80ºC, 100ºC, 120ºC, 140ºC or 160ºC) (Figure 3.1.b). Films were obtained after complete evaporation of the solvent (Figure 3.1.c). The solvent casting time was varied based on the boiling point of acetic acid (118ºC): samples cast at temperatures above 118ºC were dried for 3 minutes, whereas the samples cast at temperatures below 118ºC were dried for 6 minutes to ensure complete removal of solvent. The prepared film samples were stored at room temperature for 24 hours prior to characterization.

As a comparative sample, PHB was solvent cast using chloroform. PHB was dissolved in chloroform at 70ºC for 1 hour and then poured onto glass slides at room temperature; the solution was dried at 25ºC for 24 hours to prepare film samples. The samples were aged for five days at atmospheric pressure and room temperature, and then vacuum dried for 3 hours to remove most of the residual chloroform.

Elemental analysis

The chemical composition of the as-received PHB material was characterized using an Axis Ultra (Kratos Analytical) X-ray photoelectron spectrometer (XPS) and a Carlo Erba EA1108 Elemental Analyzer for CHNS and oxygen detection. XPS was carried out over binding energy values ranging from 0 eV to 1500 eV, at a scan rate and energy step of 2 eV/second and 400 meV, respectively. The areas of peaks corresponding to given elemental bonds were used to determine the chemical

composition of the sample. CHNS analysis was carried out following a modified form of the Pregl-Dumas technique[53]. The C:O and C:H ratios were used to confirm the purity of the as-received material.

Optical transmittance

The optical transmittance of the PHB samples was characterized using a Perkin-Elmer Lambda 900 NIR-UV-Vis spectrometer with an integrating sphere and optical bench attachment. The PHB samples were mounted in front of the integrating sphere perpendicular to the path of the incident light beam so that all the light transmitted through the sample was captured by the detector. The transmittance was determined for wavelengths ranging from 300 nm to 800 nm.

X-ray diffraction (XRD)

The crystallinity was determined using a Rigaku X-ray diffraction (XRD) system in glancing incidence angle mode. The scan was carried out between 5º and 60º at a rate of 2º/min using Cu Kα X-rays at 44 kV. An Ultima VI goniometer fitted with a thin film attachment was used to characterize the samples. An X-ray beam spot of 5 mm diameter was used for all scans. The samples were attached to a glass slide and kept as flat as possible. Baseline correction and de-convolution of the amorphous halo from the actual XRD pattern were carried out using Igor Pro 6.35A5. The area under the crystalline peak was used as a measure of overall crystallinity of samples cast at different temperatures. The crystallinity percentage with respect to solvent casting temperature was plotted and compared with results obtained using chloroform.

Thermogravimetric analysis (TGA)

The extent of thermal degradation due to dissolution and processing of PHB in acetic acid was determined using a Mettler Toledo TGA/DSC 1 system. TGA scans were carried out from 25ºC to 380ºC, at a heating rate of 10ºC/minute. The temperature of complete degradation and the range of temperatures over which the degradation occurred were used to determine the extent of degradation.

Differential scanning calorimetry (DSC)

The melting temperature and the shape of the melting endotherm of the base material and processed samples were determined using a differential scanning calorimeter (DSC). The DSC was calibrated using indium and zinc standards. At least 5 mg of sample were used for each run, and closed aluminum pans were used for the samples. DSC analysis was carried out from 25ºC to 195ºC at a heating rate of 10ºC/min for the as-received material. While, the heating rate was maintained at 20ºC/min for the DSC runs of all solvent cast films. This was done to limit the extent of recrystallization and thermal effects during the heating cycle.

Tensile testing

The PHB films were sectioned into rectangular samples of dimensions 25 mm × 5 ± 0.5 mm × 55 ± 8 μm (length x width x thickness). An Instron 5943 tensile tester with a 1kN load cell was used to carry out all tests. Data was collected at a strain rate of 0.5 mm/min. For each casting temperature, at least four samples were tested, and the average (with standard error) was plotted with respect to the processing temperature.

The elastic modulus was obtained by measuring the slope over the linear region of the stress-strain curve.

Atomic force microscopy (AFM)

The surface morphology and the root mean square roughness (RMS) of solvent cast PHB surfaces were determined using a Bruker Nano Dimension Edge atomic force microscope (AFM). The AFM was operated in tapping mode using a tip with a spring constant of 40 N/m. Characterization of each sample was carried out on the smooth, cast surface obtained when the sample was peeled away from the glass slide. The RMS roughness over an area of 3 μm^2 was obtained at five relatively flat regions free from any visible voids.

3.4. Results and Discussion

Purity and composition of as-received PHB

We determined the chemical composition and melting point of as-received PHB using X-ray photoelectron spectrometer (XPS), CHNS analysis, and differential scanning calorimetry (DSC). The XPS results showed that the as-received material contained ~ 1 wt. % Si, which likely remained in the sample as impurity after the pelletization of PHB. We found that the C:O ratio of the as-received polymer was within 1% from the theoretical ratio (C:O ratio of 1.5) of pure PHB. These numbers are consistent with a PHB purity of 98-99%. The melting point of the as-received PHB at a heating rate of 10ºC/min was found to be ~ 180ºC, which agrees well with the values reported for PHB in the literature[22,23].

Appearance of PHB films

PHB films prepared at different temperatures using acetic acid as a solvent were translucent. Figure 3.2 show images of PHB films – prepared at various temperatures – placed on a printed pattern. The samples processed at 80ºC, 140ºC and 160ºC were more transparent than the ones processed at 100ºC and 120ºC. The samples prepared using chloroform were found to have similar optical transmittance to samples prepared at 100ºC and 120ºC.

Figure 3.2 Images of PHB films processed at different temperatures overlaid on the right side (separated by red lines) of a printed pattern, demonstrating the translucency of PHB films. Results from a film processed using chloroform (CF) are shown for comparison. The film thickness of each sample was 40 ± 10 μm

Figure 3.3 shows a plot of optical transmittance of the film at different incident light wavelengths vs. solvent casting temperature. All films had relatively high optical transmittance (>82%) in the visible portion of the spectrum. The optical transmittance at all wavelengths was found to follow a parabolic trend, with lowest (80ºC) and higher processing temperatures (140ºC and 160ºC) resulting in films with higher optical transmittance. The films processed at intermediate temperatures had the lowest

transmittance, indicating that they scatter, absorb and reflect the most light. As these films were observed to have the most uneven surfaces, this reduced transmittance can be attributed mainly to light scattering from the surface. The inlay in Figure 3.3 shows images of a transmitted laser beam (λ = 532 nm) after it passed through the PHB films, cast at different temperatures. These images show that the samples prepared at 100ºC and 120ºC had a relatively small specular beam and substantial scattering. This behavior corresponds well with our observations of the uneven and cloudy appearance of these films.

The cloudy appearance can be attributed to scattering of light at the interface of crystalline-amorphous regions, and the presence of residual solvent – which can remain in samples even after long aging periods. The concentration of residual solvent is expected to be higher in samples processed from chloroform than acetic acid since chloroform interacts more strongly with PHB than acetic acid[30].

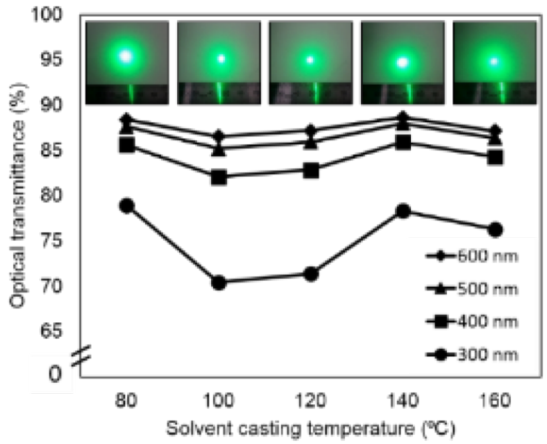

Figure 3.3 Optical transmittance vs. solvent casting temperature. The transmittance values were obtained at wavelengths of 600 nm, 500 nm, 400 nm and 300 nm. The inlay shows the images of transmitted laser beam after passing through the PHB films, arranged from lowest processing temperature (left) to highest processing temperature (right).

We also found that the samples prepared at high temperatures were homogenous while samples prepared at lower temperatures had a patchy appearance. Figure 3.4 shows stereomicroscope images of samples prepared using acetic acid. False-colored images are also shown to emphasize the undulations and features on the surface. The images indicate the presence of two distinct regions in the films, which were more apparent in the samples prepared at lower temperatures. Increasing the processing temperature resulted in more homogenous surfaces. Samples prepared at 160˚C were very smooth and had no undulation on the surface.

In contrast, the chloroform samples, which were cast at room temperature, had a much smoother appearance, owing to the fact that the solvent evaporation rate was much slower. The higher chemical compatibility of PHB and chloroform can also limit the extent of phase separation and the consequent roughening of the film surface.

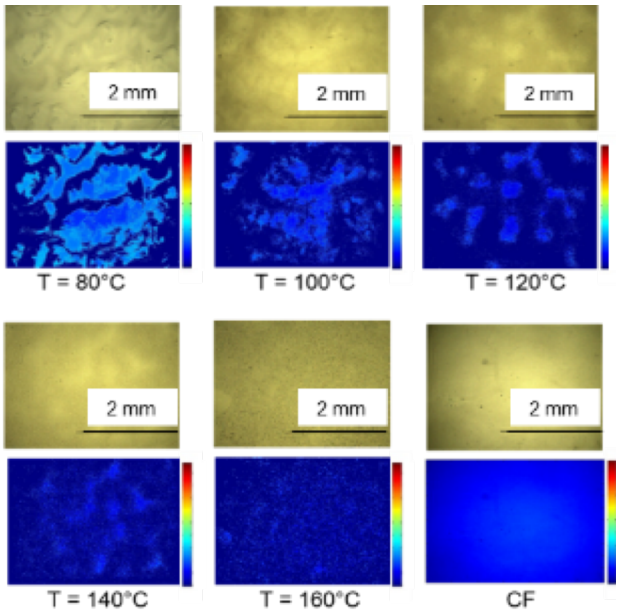

Figure 3.4 Stereomicroscope images of the PHB films solvent cast at different temperatures using acetic acid (AA) as a solvent. False-colored images (in blue) show the undulations and macroscopic features on the surface, which indicate the presence of two distinct regions in the samples. A sample processed with chloroform (CF) as the solvent is shown for comparison.

Crystallinity

Figure 3.5 shows a plot of crystallinity percentage (estimated from X-ray diffraction (XRD)) as a function of processing temperature and compared to a control sample prepared at room temperature using chloroform as a solvent. The analysis of XRD diffraction peaks revealed that the crystallinity of PHB prepared using acetic acid ranged from 64% at 80ºC to 78% at 160ºC; whereas, the crystallinity of PHB processed with chloroform was approximately 60.5%. The use of glancing incidence angle and deconvolution function to calculate the contribution of amorphous regions in the polymer introduces peak broadening, and systematic instrumental error in the crystallinity values

obtained using this method. Therefore, the crystallinity values are suitable only for comparison with other samples studied in this work and could deviate from absolute crystallinity values. Nonetheless, a clear trend is seen: all samples prepared using acetic acid have a higher crystallinity than the sample prepared with chloroform. This trend can be attributed to two main factors: (1) acetic acid-processed samples were cast at higher temperatures than the chloroform samples. Therefore, more thermal energy was available for the formation and growth of crystalline structures. (2) Chloroform is a “better” and more compatible solvent for PHB; residual solvent in the sample can increase polymer chain mobility and suppress crystal growth. The PHB samples also exhibited increased crystallinity with increased processing temperature, reflecting that more thermal energy resulted in a more ordered structure. The high driving force available for these samples could enable the formation of films with larger crystallite sizes and more stable crystallites that do not undergo transformations during storage at ambient temperature conditions.

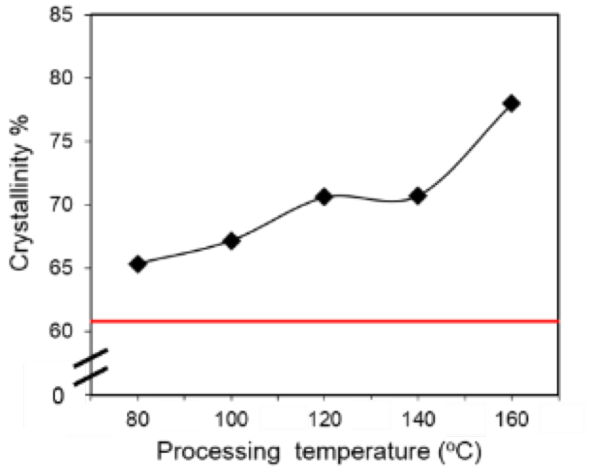

Figure 3.5 Percent crystallinity with respect to the processing temperature. The straight red line indicates the crystallinity of PHB prepared using chloroform at room temperature. The crystallinity for film cast from chloroform at room temperature is represented as a line to enable easier comparison with samples cast using acetic acid at different temperatures.

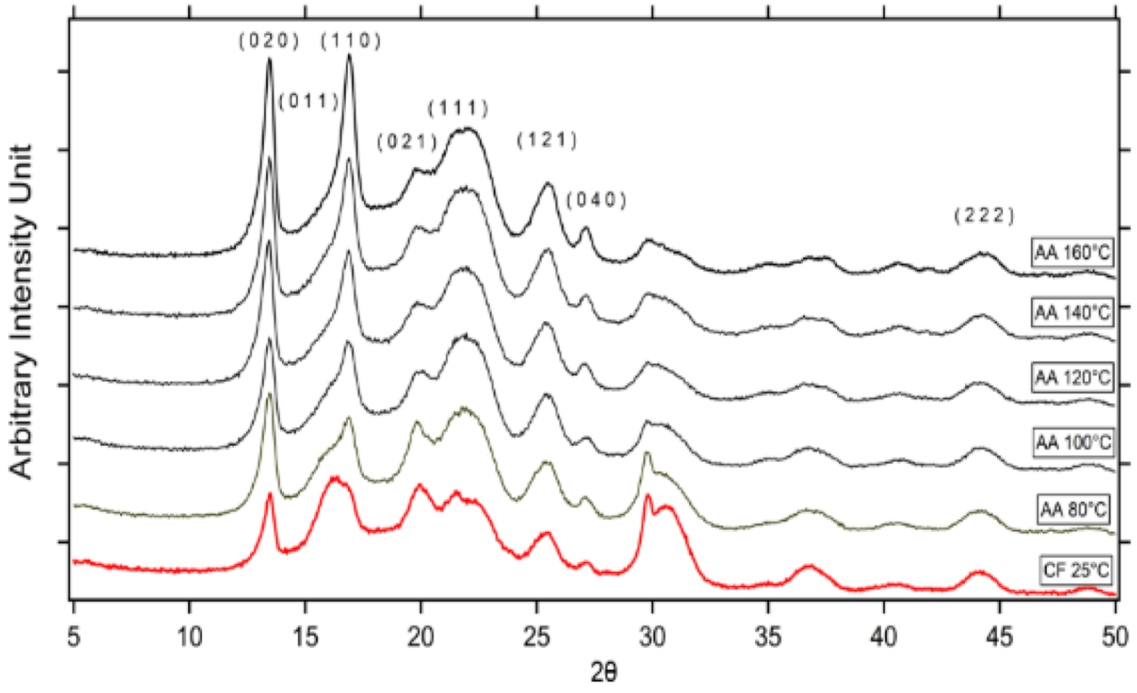

Figure 3.6 Combined XRD plot of PHB processed in acetic acid (AA) at different temperatures. The pattern obtained from PHB prepared with chloroform (CF) is shown in red for comparison.

Further examination of the structure of the films by XRD revealed that not only the percent crystallinity varied as a function of temperature, the type of crystals formed varied as well. A combined plot of XRD pattern of PHB films prepared at different solvent casting temperatures using acetic acid and chloroform as a solvent is shown in Figure 3.6. A general increase in intensity is seen as a function of processing temperature, reflecting the previous results. This increase can be attributed to an increase in ordering and higher overall crystallinity of the samples.

Peaks corresponding to orthorhombic crystal planes (020), (110), (021), (111), (121), (040) and (222) at 2θ values of 13.5º, 16.85º, 19.8º, 21.4º, 25.5º, 27.2º and 44º, respectively, were found to be similar for all samples. However, the peaks corresponding to (011) at 2θ = 16.2º had much lower intensity in all acetic acid-processed samples than in chloroform-processed PHB. This indicates that the (011) plane orientation is suppressed when PHB is processed using acetic acid at higher temperatures, suggesting the presence of a preferred orientation of crystals within the samples. The lattice parameters and the peak locations for all the samples were found to be similar, indicating that the orthorhombic PHB crystals (Figure 3.7) did not change substantially with increasing processing temperature. These outcomes agree well with the results previously reported in the literature[40,41].

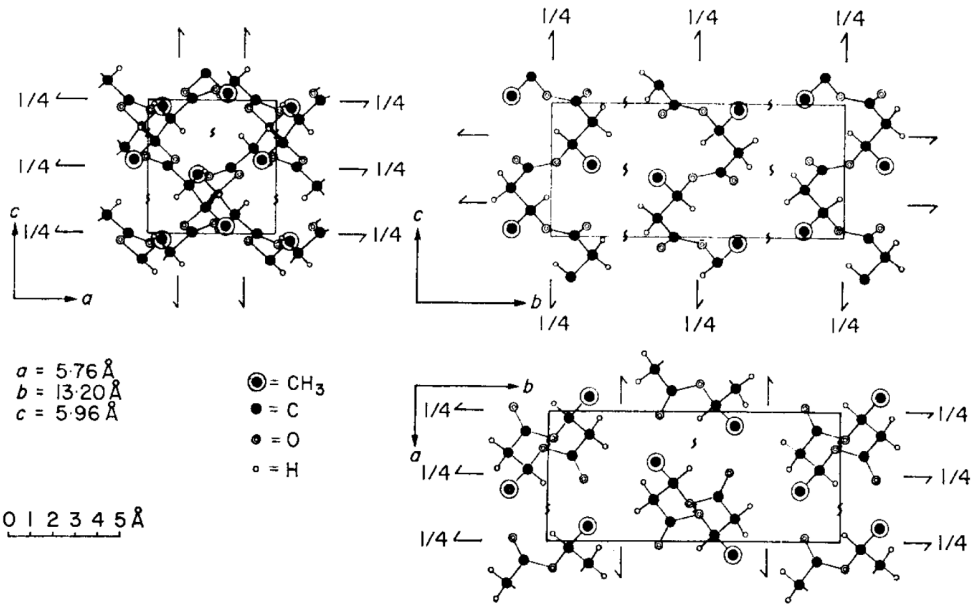

Figure 3.7 Schematic showing the crystal structure of PHB and the orientation of polymer chains in the three axes of the orthorhombic structure[43] (Reproduced with permission from Elsevier B.V.)

Thermal degradation

One important consideration while choosing acetic acid as a solvent for PHB is the possibility of polymer degradation through acid hydrolysis during processing. PHB is known to degrade into smaller units by random scission of ester bonds when exposed to acidic solutions[42]. Moreover, the use of high processing temperatures can accelerate this reaction and decrease the thermal stability of the sample. Therefore, we analyzed the extent of PHB degradation caused by acetic acid using thermogravimetric analysis (TGA).

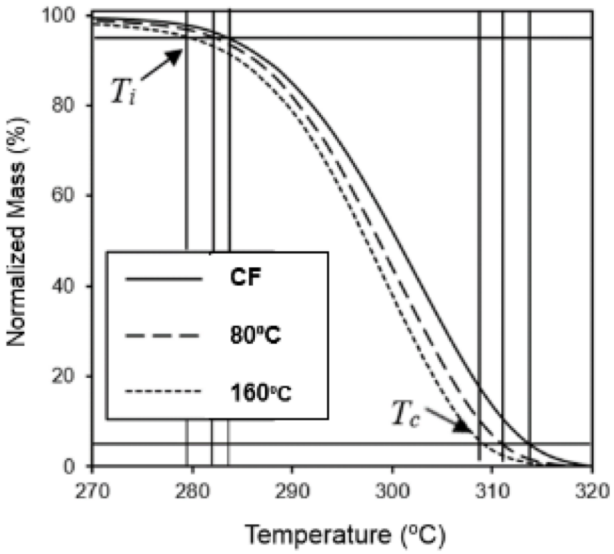

Figure 3.8 TGA plot of PHB films prepared under different conditions: solvent cast in chloroform (CF), solvent cast in acetic acid at 80ºC, and solvent cast in acetic acid at 160ºC. The upper and lower horizontal lines correspond to 95% normalized mass and 5% normalized mass respectively, while the vertical lines indicate the thermal degradation onset temperature (Ti) and the complete degradation temperature (Tc) of each sample. The data points were collected every second for all samples.

Figure 3.8 shows a combined plot of TGA carried out on samples solvent cast using acetic acid at two different temperatures compared with samples cast using chloroform. Figure 3.8 also indicates the temperature at which the samples lost 5% of their mass (thermal degradation onset temperature (T_i)) and the temperature when samples lost 95% of their mass (complete degradation temperature (T_c)). We used T_i and T_c of the samples to determine the effect of acetic acid processing on PHB. We also obtained the TGA profile of PHB prepared with chloroform for comparison with acetic acid-processed samples. The samples cast from acetic acid had lower T_i and T_c than the sample cast from chloroform. These results indicate that the use of acetic acid

as a solvent and higher casting temperatures can cause mild hydrolysis and degradation of PHB. We found that the T_i and T_c were marginally lower for the 160ºC sample (279°C and 308°C, respectively) compared to the 80ºC sample (283°C and 312 °C, respectively). The slope of the weight loss curves with respect to temperature was found to be very similar (the difference in slope is close to the instrumental limit) for samples prepared at 80°C and 160°C. The samples prepared using acetic acid were dissolved at elevated temperature for ~ 1 hour, while the solvent casting process itself lasted only a few minutes, which explains why both the slopes and the temperature at which the degradation is complete (100% mass loss) are similar for these samples. In contrast, the sample cast from chloroform had a lower slope and reached 100% mass loss at a slightly higher temperature. These factors also indicate that the samples prepared using acetic acid as solvent underwent slight degradation (and likely experienced a small decrease in molecular weight mainly during the dissolution process), while the solvent casting step did not cause much change because of the short thermal exposure time. However, the average molecular weight of the PHB films after solvent casting measured using gel permeation chromatography showed only a small variations between as-received and solvent cast PHB (MW of as-received PHB: 79,000 ± 2130; MW of PHB film: 81,200 ± 2300). Overall, the acetic acid processing route used in this work did not cause substantial degradation and more importantly allowed for the production of free-standing thin films that have good thermal stability.

Melting behavior

The melting behavior of the PHB films was determined using DSC. The melting curves of the films prepared at different temperatures are shown in Figure 3.9. The melting endotherm consisted of two distinct peaks for all PHB samples while the as-received material exhibited a large peak with a small shoulder at a lower temperature. The double melting behavior is quite common in polymeric materials and has been explained based on two theories: namely, the melting and recrystallization model[43] and the double lamellar thickness population model[44,45]. Previous works have reported the double-melting behavior for PHB and have shown that it occurs according to the melting and recrystallization model as observed by the change in the shape of the endotherms at different heating rates[46,47].

The magnitude of the low-temperature endotherm is directly related to the amount of as-formed metastable crystals while the high-temperature endotherm corresponds to the melting of ordered crystals. From the DSC curves, we observed that the magnitude of the first endotherm followed a parabolic trend (the magnitude of the endotherm increased from 80°C to 140°C but decreased for sample prepared at 160°C) with increasing processing temperature. The presence of such metastable as-formed crystals can be attributed to the phase-separation behavior and instability exhibited by the PHB/acetic acid system. The mechanism of phase separation can also influence the ordering of the crystals, with nucleation and growth at appropriate temperature allowing for the formation of highly ordered crystals and low temperatures resulting in relatively disordered metastable crystals. The samples prepared at lower temperatures (80°C and

100°C) were more likely to phase separate, since the rate of change of polymer solution concentration is much lower and the chemical compatibility decreases with decrease in temperature. Therefore, a smaller fraction of metastable crystals was present, as shown by the relatively small amplitude of the first melting endotherm. As the temperature increased (e.g. to 120°C and 140°C), the rapid solvent removal could result in the formation of more metastable crystals (and a relative increase in the magnitude of the first peak with respect to the second). With further increase in temperature (160°C), the phase separation effect could become less important and the availability of large amounts of thermal energy enables the formation of highly ordered crystals at the expense of metastable crystallites (resulting in a larger second peak and a smaller first peak).

We also observe that the DSC heating curve for the sample prepared using chloroform consists of two melting peaks at approximately the same location as the other samples. However, an additional endotherm at ~ 60ºC was apparent for the sample processed with chloroform. This peak matches with the evaporation temperature of chloroform, indicating that a small quantity of chloroform remained in the sample even after long aging time. This could limit the applicability of chloroform-cast PHB films for use in packaging and other applications that involve direct contact with food or the body. The strong interaction between PHB and chloroform can also affect crystal formation. Therefore, the underlying crystallization conditions and structure of the sample solvent cast using chloroform would be much different from the samples

cast using acetic acid. Nonetheless, as for the samples cast from acetic acid, a large metastable peak is seen for these samples as well.

These results suggest that all the samples (including those cast from chloroform) contain a mixture of stable and metastable crystallites, with intermediate processing temperatures resulting in more metastable crystals. Despite the fact that the samples cast from chloroform contained a significant fraction of both types of crystals, these samples were much smoother and uniform in appearance than the samples cast from acetic acid at low temperatures. The large fraction of metastable crystals in chloroform-processed samples can be explained by the low processing temperature, which limits the amount of thermal energy available for the formation of ordered crystals. The uniform surface, on the other hand, can be attributed to slow solvent evaporation rate and higher compatibility of PHB and chloroform. We expect that the proportion, quantity, and relative size of the different crystal types can influence the mechanical properties of the samples since stable, and metastable crystals are expected to have different mechanical properties. These properties are characterized in the next section.

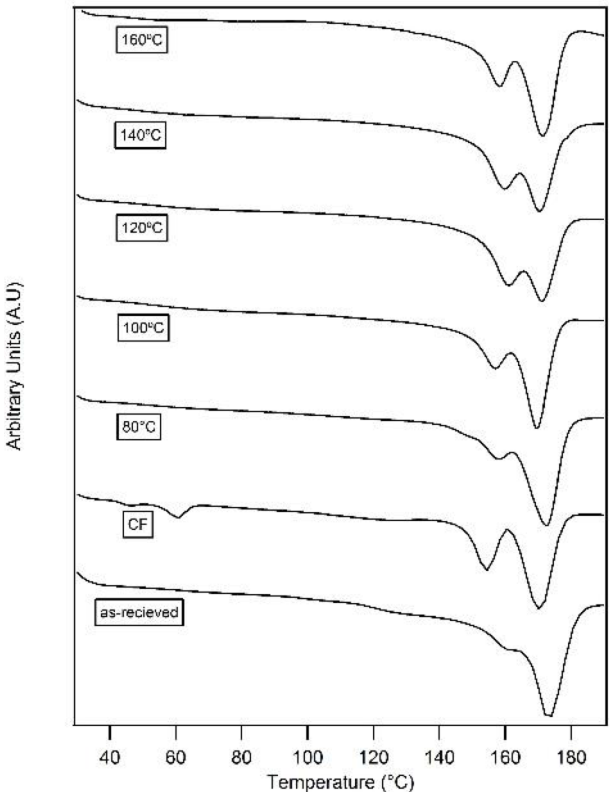

Figure 3.9 Combined plot of the DSC melting curves for PHB samples prepared at different temperatures in acetic acid (AA). The as-received sample and sample solvent using chloroform (CF) are also shown for comparison. All samples were run at a scan rate of 20°C /min.

Mechanical properties

Figure 3.10 shows plots of mechanical properties of PHB films solvent cast in acetic acid at different temperatures. Results from samples cast with chloroform are also shown for comparison. In general, both the strain to failure and peak tensile stress was much higher for the films cast at 80°C than at the higher processing temperatures. In contrast, the elastic modulus did not change substantially as a function of temperature, except at a processing temperature of 140ºC. The decrease in strain to failure correlates well with the increase in crystallinity with processing temperature. The

presence of amorphous regions (above the glass transition temperature) lends flexibility to the polymer. With increasing processing temperature, more crystallites are formed at the expense of amorphous regions, which results in increased brittleness of the polymer[48]. The presence of a large number of crystallites has been shown to vitrify amorphous polymer chains. This vitrification further embrittles PHB and lowers the strain to failure and ultimate tensile stress[49–51]. We attribute an almost constant elastic modulus to the low strain (0.5 mm/min) rate used for the tensile test. Low strain rates can have an effect analogous to deforming a polymer at elevated temperatures, where the elastic modulus decreases and converges to a minimum for a given strain rate[52]. Low strain rates can also accommodate changes in the orientation of crystallites, which enables amorphous chains to elongate reversibly, especially at small strains (~ 1%).

Interestingly, the samples prepared at 160ºC deviated from the general trend, exhibiting a higher strain at failure than samples cast at 120ºC and 140ºC. This behavior could be attributed to partial melting and the consequent stress relaxation of PHB at 160ºC. Although this processing temperature was lower than the melting point of PHB (~180ºC), the melting process can begin at temperatures as low as 150ºC, enabling a small proportion of the sample to melt and accommodate the stresses generated at the crystalline-amorphous interfaces. The stress relaxation effect can explain the increase in strain to failure for the samples prepared at 160ºC, despite it exhibiting much higher overall crystallinity than the rest of the samples. The relatively high strain to failure and ultimate tensile stress of samples processed at 80ºC can be explained by the low crystallinity and the possible presence of trace quantities of acetic acid (although we did

not observe any evidence of residual solvent from the TGA heating curves). In the latter case, acetic acid could have a plasticizing effect on PHB, causing an increase in strain to failure. Overall, the properties of the samples processed at all temperatures were comparable with those of the chloroform-cast films.

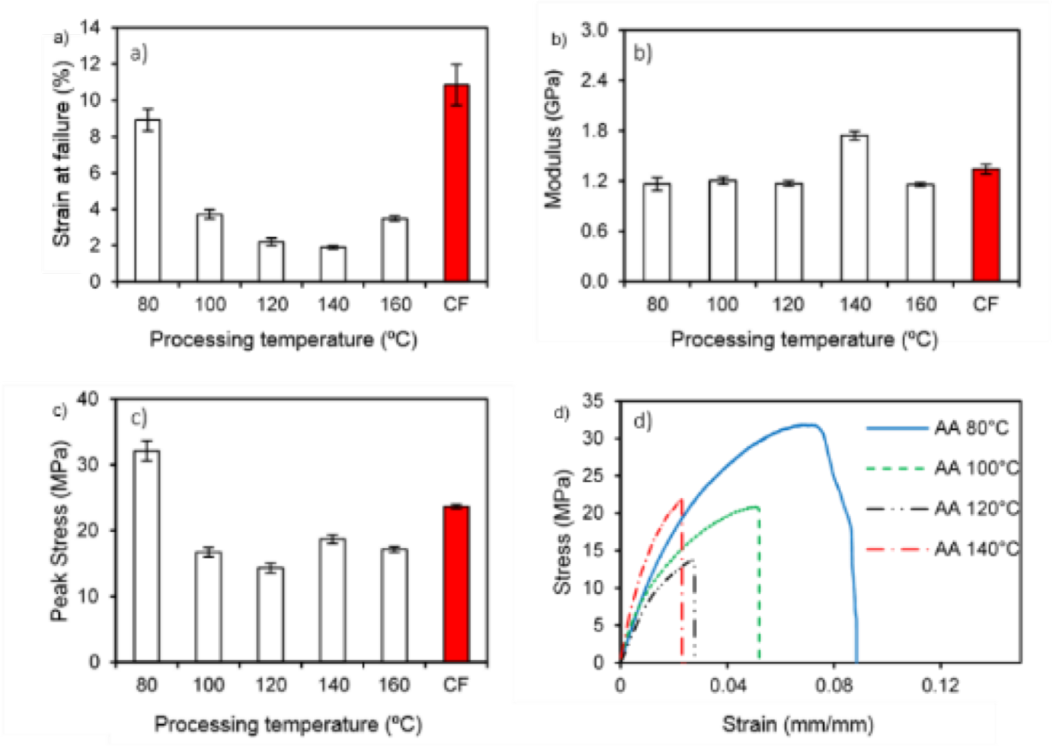

Figure 3.10 Mechanical characterization of PHB films prepared in acetic acid (AA) at different casting temperatures. a) Strain to failure vs. casting temperature, b) Elastic modulus vs. temperature, c) Ultimate tensile stress vs. temperature, d) Representative stress-strain curves. Average values and standard error are shown in (a-c) and are based on at least 4 measurements. Results from samples cast with chloroform (CF) are also shown for comparison.

Surface morphology and roughness

The surface morphology of the PHB films prepared at different temperatures is shown in Figure 3.11; characterization was performed on the surfaces that were cast against the glass slide. The atomic force microscopy (AFM) images show a trend of decreasing roughness with increasing processing temperature. In addition to this, the samples processed with acetic acid have contrasting surface morphology from those processed with chloroform. We found that the PHB films prepared with chloroform had rough and globular structures on their surface. The samples processed with acetic acid at low temperatures had a fibrous, needle-like structures and roughness in the range of 20 nm, whereas the samples processed at high temperatures had smooth, uniform surfaces. The needle-like structures were likely caused by small crystallites and impurities on the surface. The RMS surface roughness with respect to solvent casting temperature is shown in Figure 3.12 and was found to decrease progressively with increasing processing temperature. The RMS roughness of PHB prepared with chloroform was found to be in the range of 1 μm, which is over an order of magnitude higher than the samples prepared using acetic acid.

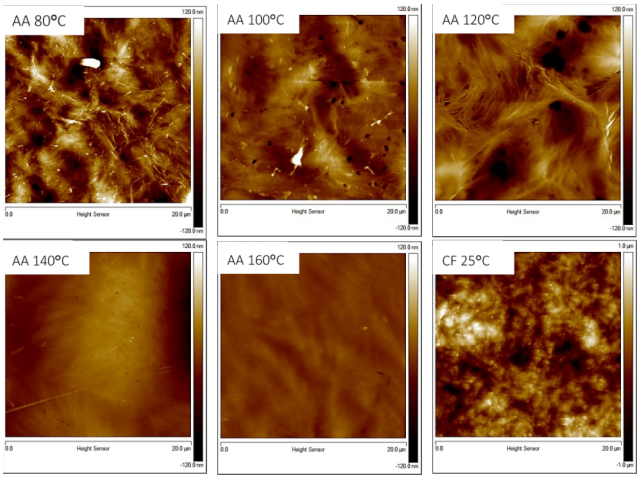

Figure 3.11 AFM scans of PHB samples processed at different temperatures in acetic acid (AA) or chloroform (CF). Scan area: 20 μm2. The topography scale is ±120 nm for all acetic acid-processed samples, and ±1000 nm for the chloroform-processed sample.

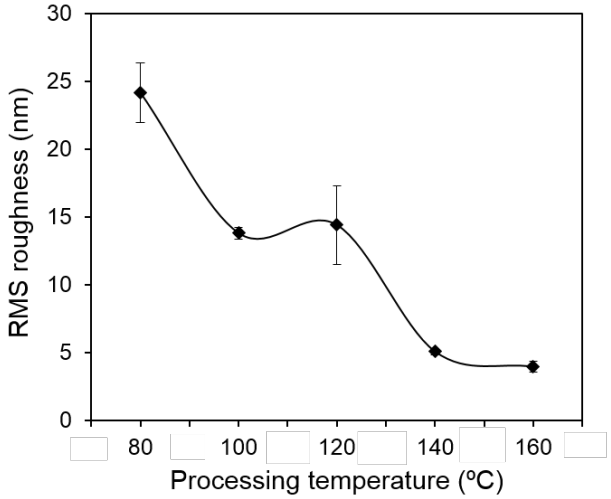

Figure 3.12 RMS roughness of PHB films solvent cast with acetic acid with respect to the processing temperature.

The increase in roughness with decreasing temperature can be explained by the fact that the polymer chains have less energy available to form ordered structures throughout the surface when processed at low temperatures. Therefore, more amorphous regions are present on the surface, along with the highly ordered crystallites. A large number of crystalline-amorphous interfaces can explain the increased roughness seen in PHB surface processed at room temperature using chloroform. In this case, small crystals and amorphous zones populated the surface.

The high surface roughness of chloroform-processed samples could also contribute to the cloudy appearance seen in Figure 3.2 since a surface with roughness comparable to the wavelength spectrum of visible light would result in more scattering. The acetic acid-processed samples, on the other hand, are expected to have much lower scattering since the surface features are much smaller than the wavelength spectrum of visible light.

3.5. Discussion

In summary, we have shown that PHB can be solvent cast into films using acetic acid as a solvent, with only a marginal decrease in thermal stability. The different solvent casting temperatures employed in this work enabled us to control the solvent evaporation rate and cooling rate. These factors affect microscopic features namely: 1) crystallinity 2) nature and orderliness of the crystals, and 3) fraction of stable/metastable crystals. These microscopic features lead to differences in properties.

In general, at low casting temperatures, the solvent evaporates slowly, and there is limited thermal energy available for crystallization. Films, therefore, have low crystallinity, have good mechanical properties (in terms of tensile strength and strain to failure), and reasonable optical transmittance. However, films processed at lower temperatures have rougher surfaces both at the macroscopic and microscopic scale – due to variations in thickness resulting from phase separation, and due to inhomogeneities caused by the limited thermal energy available for crystallization. On the other hand, higher solvent casting temperatures yield films that are more crystalline, more transparent, and have higher surface uniformity. However, these films have relatively low tensile strength and strain. These results show that the proper selection of casting temperature and solvent evaporation rate can be used to achieve films with the desired set of properties.

These results establish that acetic acid is a viable solvent to process PHB films. This method can easily be adapted and altered to produce PHB that has a much wider set of properties than what is possible with other processing routes. Figure 3.13 shows an ensemble of different forms in which PHB can be processed using acetic acid. In addition to films and sheets that have varying optical transmittance (Figure 3.13.c & 13.d), we have been able to produce PHB films that have high porosity (Figure 3.13.a) by rapid phase separation of PHB and acetic acid by introduction of non-solvent (water in this case). Porous PHB could be useful in bio-implant and biomedical applications, because of its rapid and controllable degradation behavior. We have also been able to spray coat a thin layer of PHB (with acetic acid as solvent) on glass, paper and on other

plastic surfaces using a simple airbrush. Such varied forms of PHB can find potential applications as biological scaffolds, packaging materials, sensing devices and as enzyme activity screening assays.

While all these forms of PHB can be prepared using chloroform as a solvent or using thermal processing, acetic acid as solvent provides the greatest versatility in processing conditions and PHB properties.

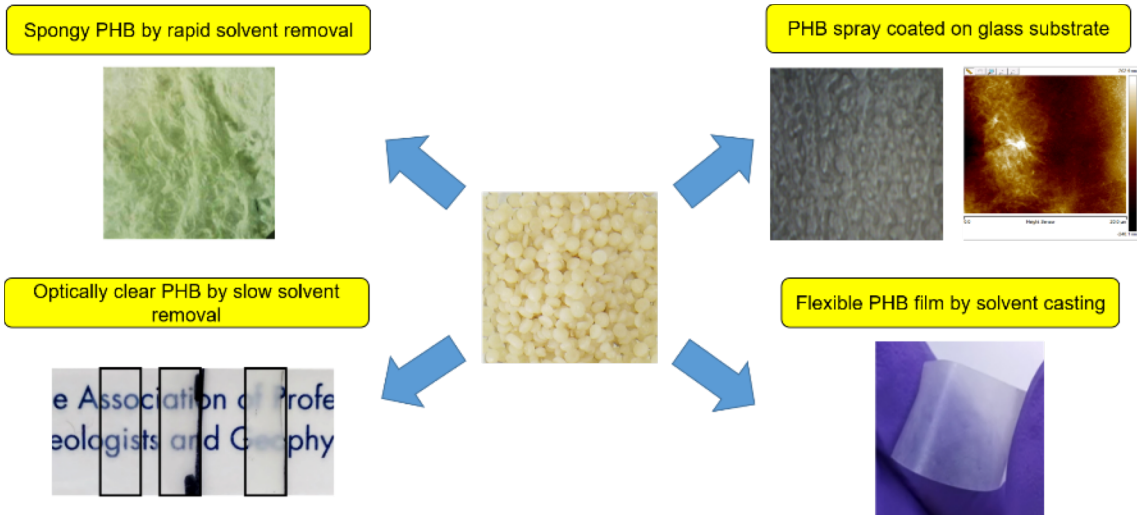

Figure 3.13 Ensemble of different forms of PHB produced using acetic acid as a solvent. a) Porous PHB by rapid removal of solvent, b) spray coated PHB layer on a glass substrate, c) PHB thin films that have different optical transmittance. Films prepared at different acetic acid concentrations at 80ºC. Optical transmittance decreases from left to right, d) Flexible PHB films prepared by solvent casting from acetic acid.

3.6. Conclusion

We have demonstrated the possibility of using acetic acid as a cost-effective solvent to prepare flexible PHB films. These films exhibited optical, mechanical and surface properties similar to or better than those of films produced using chloroform, the typical solvent for PHB. The films prepared with acetic acid in 6 minutes had comparable properties to films prepared using chloroform in 24 hours. The relatively high dissolution and solvent casting temperature while requiring more thermal energy, afford the advantage of short processing times and the ability to tune the properties of the film. The crystallinity of the films can be varied through the selection of a suitable casting temperature, allowing the mechanical and optical properties of the films to be altered based on the requirement. The proposed method offers a simple route to make high quality, flexible PHB films for applications ranging from surgical films to biodegradable implants.

Acknowledgements

The authors would like to thank the Alberta Livestock and Meat Agency for providing funding for this research. The tensile tester and DSC used in this work were purchased with funding from the Canada Foundation for Innovation.

Author Contributions

P.A perfromed all experiments and wrote the manuscript. A.L.E. and D.S. supervised the work, and contributed to designing the research and to writing the manuscripts.

3.7. References

1. Kumagai, Y., Kanesawa, Y. & Doi, Y. Enzymatic degradation of microbial poly(3-hydroxybutyrate) films. *Die Makromol. Chemie* **193,** 53–57 (1992).
2. Yoshie, N., Oike, Y., Kasuya, K., Doi, Y. & Inoue, Y. Change of Surface Structure of Poly(3-hydroxybutyrate) Film upon Enzymatic Hydrolysis by PHB Depolymerase. *Biomacromolecules* **3,** 1320–1326 (2002).
3. Orts, W. J. *et al.* Poly(hydroxyalkanoates): Biorefinery polymers with a whole range of applications. The work of Robert H. Marchessault. *Can. J. Chem.* **86,** 628–640 (2008).
4. Philip, S., Keshavarz, T. & Roy, I. Polyhydroxyalkanoates: biodegradable polymers with a range of applications. *J. Chem. Technol. Biotechnol.* **82,** 233–247 (2007).
5. Zinn, M., Witholt, B. & Egli, T. Occurrence , synthesis and medical application of bacterial polyhydroxyalkanoate. **53,** 5–21 (2001).
6. Kai, D. & Loh, X. J. Polyhydroxyalkanoates: Chemical Modifications Toward Biomedical Applications. *ACS Sustain. Chem. Eng.* **2,** 106–119 (2014).
7. Bucci, D. Z., Tavares, L. B. B. & Sell, I. PHB packaging for the storage of food products. *Polym. Test.* **24,** 564–571 (2005).
8. Loh, X. J., Goh, S. H. & Li, J. Hydrolytic degradation and protein release studies of thermogelling polyurethane copolymers consisting of poly[(R)-3-hydroxybutyrate], poly(ethylene glycol), and poly(propylene glycol). *Biomaterials* **28,** 4113–4123 (2007).
9. Loh, X. J., Zhang, Z.-X., Wu, Y.-L., Lee, T. S. & Li, J. Synthesis of Novel

Biodegradable Thermoresponsive Triblock Copolymers Based on Poly[(R)-3-hydroxybutyrate] and Poly(N-isopropylacrylamide) and Their Formation of Thermoresponsive Micelles. *Macromolecules* **42,** 194–202 (2009).

10. Wang, L. *et al.* Processability modifications of poly(3-hydroxybutyrate) by plasticizing, blending, and stabilizing. *J. Appl. Polym. Sci.* **107,** 166–173 (2008).
11. Miller, N. D. & Williams, D. F. On the biodegradation of poly-β-hydroxybutyrate (PHB) homopolymer and poly-β-hydroxybutyrate-hydroxyvalerate copolymers. *Biomaterials* **8,** 129–137 (1987).
12. Barham, P. J., Barker, P. & Organ, S. J. Physical properties of poly(hydroxybutyrate) and copolymers of hydroxybutyrate and hydroxyvalerate. *FEMS Microbiol. Lett.* **103,** 280–298 (1992).
13. Bauer, H. & Owen, A. J. Some structural and mechanical properties of bacterially produced poly-β-hydroxybutyrate-co-β-hydroxyvalerate. *Colloid Polym. Sci.* **266,** 241–247 (1988).
14. Koyama, N. & Doi, Y. Morphology and biodegradability of a binary blend of poly((R)-3-hydroxybutyric acid) and poly((R,S)-lactic acid). *Can. J. Microbiol.* **41,** 316–322 (1995).
15. Zhang, M. & Thomas, N. L. Blending polylactic acid with polyhydroxybutyrate: The effect on thermal, mechanical, and biodegradation properties. *Adv. Polym. Technol.* **30,** 67–79 (2011).
16. Savenkova, L. *et al.* Mechanical properties and biodegradation characteristics of PHB-based films. *Process Biochem.* **35,** 573–579 (2000).
17. Sauvageau, D., Cooper, D. G. & Nicell, J. A. Relative rates and mechanisms of

biodegradation of diester plasticizers mediated by Rhodococcus rhodochrous. *Can. J. Chem. Eng.* **87,** 499–506 (2009).

18. Nalli, S., Cooper, D. G. & Nicell, J. a. Metabolites from the biodegradation of di-ester plasticizers by Rhodococcus rhodochrous. *Sci. Total Environ.* **366,** 286–94 (2006).
19. Yang, C. Z., Yaniger, S. I., Jordan, V. C., Klein, D. J. & Bittner, G. D. Most Plastic Products Release Estrogenic Chemicals : A Potential Health Problem that Can Be Solved. **119,** 989–996 (2011).
20. Fasano, E., Bono-Blay, F., Cirillo, T., Montuori, P. & Lacorte, S. Migration of phthalates, alkylphenols, bisphenol A and di(2-ethylhexyl)adipate from food packaging. *Food Control* **27,** 132–138 (2012).
21. Erythropel, H. C., Maric, M., Nicell, J. A., Leask, R. L. & Yargeau, V. Leaching of the plasticizer di(2-ethylhexyl)phthalate (DEHP) from plastic containers and the question of human exposure. *Appl. Microbiol. Biotechnol.* **98,** 9967–9981 (2014).
22. Janigová, I., Lacík, I. & Chodák, I. Thermal degradation of plasticized poly(3-hydroxybutyrate) investigated by DSC. *Polym. Degrad. Stab.* **77,** 35–41 (2002).
23. Erceg, M., Kovačić, T. & Klarić, I. Thermal degradation of poly(3-hydroxybutyrate) plasticized with acetyl tributyl citrate. *Polym. Degrad. Stab.* **90,** 313–318 (2005).
24. Cyras, V. P., Commisso, M. S., Mauri, A. N. & Vázquez, A. Biodegradable double-layer films based on biological resources: Polyhydroxybutyrate and cellulose. *J. Appl. Polym. Sci.* **106,** 749–756 (2007).
25. Seoane, I. T., Manfredi, L. B. & Cyras, V. P. Properties and Processing Relationship of Polyhydroxybutyrate and Cellulose Biocomposites. *Procedia*

Mater. Sci. **8,** 807–813 (2015).

26. Díez-Pascual, A. M. & Díez-Vicente, A. L. Poly(3-hydroxybutyrate)/ZnO Bionanocomposites with Improved Mechanical, Barrier and Antibacterial Properties. *Int. J. Mol. Sci.* **15,** 10950–10973 (2014).
27. Siemann, U. Solvent cast technology – a versatile tool for thin film production. 1–14 (2005). doi:10.1007/b107336
28. Takeda, R. & Shiraishi, H. Process for producing cellulose triacetate film. (1992).
29. Bermel, M. S. Polyvinyl alcohol films prepared by coating methods. (2007).
30. Terada, M. & Marchessault, R. H. Determination of solubility parameters for poly(3-hydroxyalkanoates). *Int. J. Biol. Macromol.* **25,** 207–215 (1999).
31. Jacquel, N., Lo, C.-W., Wu, H.-S., Wei, Y.-H. & Wang, S. S. Solubility of polyhydroxyalkanoates by experiment and thermodynamic correlations. *AIChE J.* **53,** 2704–2714 (2007).
32. Tardiff, R. G. Health Effects of Organics: Risk and Hazard Assessment of Ingested Chloroform. *J. Am. Water Works Assoc.* **69,** 658–661 (1977).
33. Weisel, C. P. & Jo, W. K. Ingestion, inhalation, and dermal exposures to chloroform and trichloroethene from tap water. *Environ. Health Perspect.* **104,** 48 (1996).
34. Prat, D., Hayler, J. & Wells, A. A Survey of Solvent Selection Guides. *Green Chem.* (2014). doi:10.1039/C4GC01149J
35. Le Berre, C., Serp, P., Kalck, P. & Torrence, G. P. in *Ullmann's Encyclopedia of Industrial Chemistry* (Wiley-VCH Verlag GmbH & Co. KGaA, 2000).
36. Kim Meera. Antimicrobial Activity of PHB/Chitosan Films and Quality of White

Bread Packaged with the Films. *Korean J. Hum. Ecol.* **14,** 321–330 (2005).

37. Yalpani, M., Marchessault, R. H., Morin, F. G. & Monasterios, C. J. Synthesis of poly(3-hydroxyalkanoate) (PHA) conjugates: PHA-carbohydrate and PHA-synthetic polymer conjugates. *Macromolecules* **24,** 6046–6049 (1991).

38. Yalpani, M. Functionalized poly(hydroxyalkanoates) and method of manufacturing same. (1993).

39. Mester, Z. & Sturgeon, R. E. *Sample Preparation for Trace Element Analysis*. (Elsevier, 2003).

40. Van De Witte, P., Dijkstra, P. J., Van Den Berg, J. W. A. & Feijen, J. Phase separation processes in polymer solutions in relation to membrane formation. *ELSEVIER J. Membr. Sci.* **117,** 1–31 (1996).

41. Gazzano, M., Tomasi, G. & Scandola, M. X-ray investigation on melt-crystallized bacterial poly(3-hydroxybutyrate). *Macromol. Chem. Phys.* **198,** 71–80 (1997).

42. Hurrell, B. L. & Cameron, R. E. A wide-angle X-ray scattering study of the ageing of poly(hydroxybutyrate). *J. Mater. Sci.* **33,** 1709–1713 (1998).

43. Cobntbekt, J. & Marchessault, R. H. Physical properties of poly-β-hydroxybutyrate. IV. Conformational analysis and crystalline structure. *J. Mol. Biol.* **71,** 735–756 (1972).

44. Holmes, P. A. Applications of PHB - a microbially produced biodegradable thermoplastic. *Phys. Technol.* **16,** 32–36 (1985).

45. Sauer, B. B., Kampert, W. G., Neal Blanchard, E., Threefoot, S. a. & Hsiao, B. S. Temperature modulated DSC studies of melting and recrystallization in polymers exhibiting multiple endotherms. *Polymer (Guildf).* **41,** 1099–1108 (2000).

46. Hsiao, B. S., Zuo, F., Mao, Y. & Schick, C. in *Handbook of Polymer Crystallization* (eds. Piorkowska, E. & Rutledge, G. C.) 1–30 (John Wiley & Sons, Inc., 2013).

47. Menczel, J. D. & Prime, R. B. *Thermal Analysis of Polymers: Fundamentals and Applications*. (John Wiley & Sons, 2014).

48. Gunaratne, L. M. W. K., Shanks, R. a. & Amarasinghe, G. Thermal history effects on crystallisation and melting of poly(3-hydroxybutyrate). *Thermochim. Acta* **423,** 127–135 (2004).

49. Gunaratne, L. M. W. K. & Shanks, R. A. Multiple melting behaviour of poly(3-hydroxybutyrate-co-hydroxyvalerate) using step-scan DSC. *Eur. Polym. J.* **41,** 2980–2988 (2005).

50. El-Hadi, A., Schnabel, R., Straube, E., Müller, G. & Henning, S. Correlation between degree of crystallinity, morphology, glass temperature, mechanical properties and biodegradation of poly (3-hydroxyalkanoate) PHAs and their blends. *Polym. Test.* **21,** 665–674 (2002).

51. Barham, P. J. & Keller, A. The Relationship between Microstructure and Mode of Fracture in Polyhydroxybutyrate. **24,** 69–77 (1986).

52. de Koning, G. J. M., Lemstra, P. J., Hill, D. J. T., Carswell, T. G. & O'Donnell, J. H. Ageing phenomena in bacterial poly[(R)-3-hydroxybutyrate]: 1. A study on the mobility in poly[(R)-3-hydroxybutyrate] powders by monitoring the radical decay with temperature after γ-radiolysis at 77 K. *Polymer (Guildf).* **33,** 3295–3297 (1992).

53. de Koning, G. J. M. & Lemstra, P. J. Crystallization phenomena in bacterial poly[(R)-3-hydroxybutyrate]: 2. Embrittlement and rejuvenation. *Polymer (Guildf).*

34, 4089–4094 (1993).

54. Schultz, J. M. Microstructural aspects of failure in semicrystalline polymers. *Polym. Eng. Sci.* **24,** 770–785 (1984).

4. A Diffraction-Based Degradation Sensor for Polymer Thin Films

This manuscript proposes a method to characterize the degradation of polymer thin films using a simple, non-contact optical method which entails patterning diffraction gratings on the polymer surface. This is the first instance in literature, wherein the degradation of the polymer can be detected in real-time with high accuracy using a non-contact method. This paper proposes and discusses the theoretical framework of using a diffraction grating to detect changes on the polymer surface due to degradation. As a proof of concept, the enzymatic degradation of the PHB thin films was characterized successfully using the diffraction sensor. Further, the versatility of the method was established by characterizing the variations in the degradation rate of PHB films cast at different temperatures. The result in this manuscript indicate that the diffraction-based degradation sensor has potential applications for rapid screening of the polymers for high throughput material selection.

The results presented in this manuscript has been published in *Polymer Degradation and Stability* entitled, **"A Diffraction-Based Degradation Sensor for Polymer Thin Films".** The contents are reproduced here in accordance with the author's rights and copyright policies of the publisher, Elsevier, and Polymer Degradation and Stability.

A Diffraction-Based Degradation Sensor for Polymer Thin Films

Preetam Anbukarasu, Diana Isabel Martínez-Tobón, Dominic Sauvageau, Anastasia Leila Elias

Department of Chemical and Materials Engineering, University of Alberta, T6G 1H9, Edmonton, Canada

4.1. Abstract

With the recent rise of organic electronics, bioelectronics, and transient devices, polymer thin films are finding prominence as substrates, functional layers and diffusion barriers. While some of these applications require degradable polymers, others necessitate materials with high stability and resistance to degradation during operation. Due to their minuscule thickness and mass, it is challenging to characterize the degradation and stability of thin films using existing techniques developed mainly for bulk materials. We introduce here a diffraction-based degradation sensor that can monitor the physical changes that take place as polymer chains are removed during the surface degradation of a polymer film without requiring expensive equipment and extensive sample preparation. To assess the degradation of a polymer film, the surface of the polymer is first patterned with a diffraction grating. This grating form the key component of the degradation sensor, which also includes a laser and a photodetector to monitor diffraction efficiency as a function of time. When the patterned polymer surface degrades, the diffraction efficiency decreases. As validation, we use this approach to observe both enzymatic degradation of polyhydroxybutyrate films, and dissolution stability of silk. We demonstrate that the degradation sensor can monitor,

with high reliability, the degradation of samples with minute mass changes, enabling qualitative and quantitative comparisons in different sample types and/or exposed to various degradation environments.

4.2. Introduction

Polymeric thin films form an essential part in a range of technological fields including micro-electronic devices, optical components, and functional coatings[1,2]. Recent advances in bioelectronics[3], wearable[4,5], implantable[6,7] and transient devices[8–11], have made polymer films even more indispensable. In addition to being light and flexible, polymer thin films can be designed to degrade in a predictable manner, making them suitable for applications such as transient and implantable devices[10,12] and controlled drug release systems[13]. While degradability is a desirable feature of the aforementioned applications, in other applications this property impedes the long-term function of the device; proper selection of the material for a given application and environment is therefore important. A wide range of polymers exhibit some degree of degradability, from biopolymers such as polylactic acid (PLA) and polyhdroxybutyrate (PHB) to petroleum-based polymers such as polycaprolactone (PCL) and poly(butylene) succinate (PBS)[14].

As the footprint of devices become smaller and smaller, the polymer films that form their functional layers are reduced in size. Due to dimensional constraints, high surface to volume ratio, and processing-dependent properties, polymer thin films can have different degradation behavior than their bulk counterparts[15]. The conditions under

which the materials are used (temperature, humidity, exposure to microorganisms, etc.) can also have a strong impact on their stability and degradation. Therefore, to create devices that can work reliably during their lifetime, we need to characterize and measure the degradation and stability of these thin films under relevant conditions.

Although knowledge of the stability, dissolution and degradation of polymer thin films is critical to many applications, currently, there are only a few methods available to evaluate these properties[16]. Gravimetric techniques, which are often used to characterize bulk materials, are slow and are not sensitive enough to measure the small changes in mass experienced by micro- and nano-scale polymer films during degradation. Advanced gravimetric techniques such as quartz crystal microbalance (QCM)[17,18] and resonant micro-cantilevers[19,20] can overcome the sensitivity limitations of traditional methods. However, these techniques require extensive sample preparation and sample-specific optimization. Researchers have also used chromatography[21,22] and spectroscopy[22–25] in studies where degradation products are analyzed with respect to time. While these approaches provide a method to determine degradation and dissolution kinetics, they require high precision instruments and samples devoid of impurities. Even with extensive sample preparation, it can be challenging to observe the degradation processes of thin films reliably. These issues with the current characterization techniques often result in long, cumbersome degradation studies which do not provide a complete portrait of the thin films stability. Therefore, it is desirable to have a simple, rapid and sensitive method to assess the stability and degradation behavior of polymer thin films.

To address these challenges, we propose a diffraction-based degradation sensor to characterize the surface degradation and stability of polymer thin films. Optical gratings cause a beam of normal, incident light to diffract at a particular angle, as expressed by

$$n\lambda = d\ sin\theta$$

Here, θ is the angle of the diffracted beam, λ is the wavelength of light, d is the distance between the centers of two adjacent grating peaks and n is the order of diffraction. In addition, the intensity of the diffracted beam and diffraction efficiency are also well defined for gratings with a given periodicity and peak height[26]. For example, the efficiency of the 1st order diffraction for square wave gratings is given by

$$\eta_{\pm 1} = \left(\frac{2}{\pi}\sin\Delta\phi\right)^2$$

where $\eta_{\pm 1}$ is the efficiency of 1st order diffraction and $\Delta\phi$ is the phase difference introduced by the difference in path length that results when light travels through the crest and trough of the diffraction grating. This equation shows that the diffraction efficiency varies with a sin^2 dependence, when the height of the grating (which controls the phase difference) is altered[26].

The unique and well-defined optical properties of gratings[27,28] (Figure 4.1.a & 1.b), are useful in high precision sensing applications[29]. Consequently, researchers have used diffraction gratings to fabricate a wide variety of biosensors[30–33] and environmental sensors[34,35]. The high surface sensitivity and the non-contact nature of

diffraction intensity measurements make them ideal for real-time monitoring of polymeric surfaces[36].

The degradation sensor described herein consists of a diffraction grating — patterned directly on the polymer of interest — coupled with a laser beam and an intensity measurement system. The intensity of the diffracted beam (diffraction efficiency) is measured using a custom-built data acquisition system while the polymer is exposed to a degrading or dissolving environment (such as an enzyme solution in contact with the polymer, Figure 4.1.c). As the polymer surface is modified due to degradation, the surface loses its periodic, repeating patterns in a probabilistic manner, and this process decreases the diffraction efficiency. Thus, monitoring the diffracted beam intensity over time provides us with a measure of the stability of the polymer surface.

In this work, we validate the efficacy of the sensor by observing the enzymatic degradation of polyhydroxybutyrate (PHB) (a biodegradable polymer with applications in biomedical implants[37,38]) and the dissolution stability of silk films exposed to water. PHB films of nano-scale thicknesses with diffraction gratings on their surface were prepared using a replica molding/solvent casting process[39] (Figure 4.1.d). The PHB films were then degraded with an enzyme and the changes in diffraction efficiency was recorded over time. Atomic force microscopy of the PHB surface at different times during the degradation process was used to determine the relationship between the changes on the surface and the variation in the diffraction efficiency. We demonstrate that the

technique is sensitive enough to resolve both the differences in degradation rates between samples that have different crystallinities and the effect of enzyme concentration on the degradation of PHB. In addition, the stability of silk films treated to have varying resistance to dissolution in water was characterized using the diffraction sensor. These experiments show how the degradation sensor can monitor the stability of polymer films, even at the micro- and nano-scale.

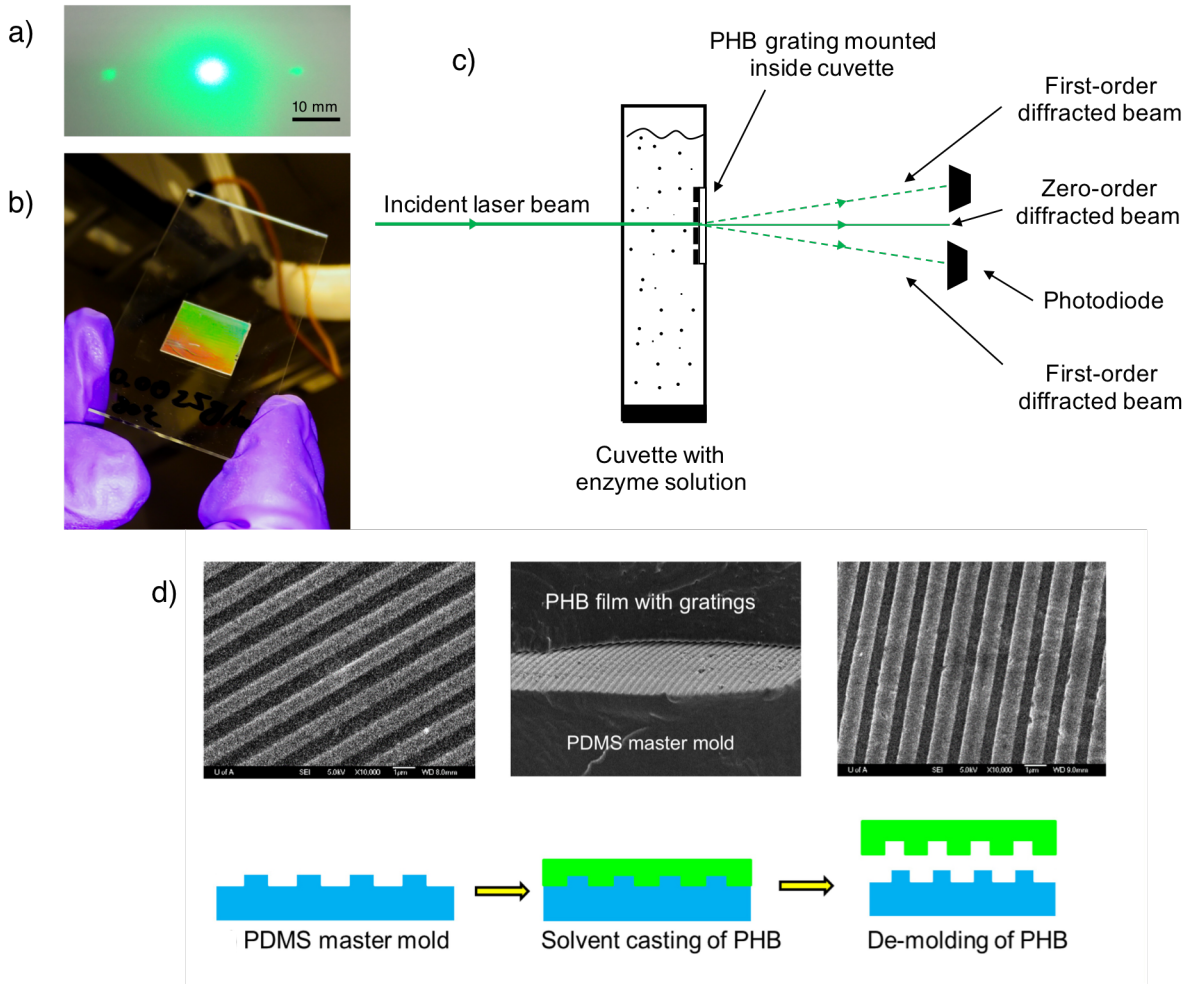

Figure 4.1 Experimental set-up, sample preparation and representative images illustrating the operation of the diffraction-based degradation sensor to study the degradability and stability of polymer films. (a) Diffraction pattern obtained by passing a beam of laser through the polymer thin film patterned with a grating. (b) The rainbow-like appearance, characteristic of a surface patterned with a diffraction grating, which can be used for qualitative observation of degradation. (c) Schematic of the small-angle diffraction efficiency measurement system (Not to scale). (d) Schematic of replica molding/solvent casting process used to pattern polymer surfaces with diffraction gratings. A PHB thin film is shown as an example.

4.3. Materials and Methods

Chemicals

The PHB (98 %) used in this work was obtained as thermally-processed pellets (BRS Bulk Bio-pellets, Bulk Reef Supply, Golden Valley, MN, USA). The chemical composition of as-received PHB determined using X-ray photoelectron spectrometer (XPS), and CHNS analysis showed the presence of ~ 1 wt.% Si as an impurity. The C:O ratio of the as-received PHB was within 1% from the theoretical ratio (C:O ratio of 1.5) of pure PHB. These numbers were consistent with a PHB purity of 98-99 %[39]. The PHB pellets were washed with isopropyl alcohol (Sigma Aldrich, Canada) to prevent microbial contamination and otherwise used as received. Acetic acid (99 %) was obtained from Sigma-Aldrich, Canada and used as received.

Extracellular enzyme preparation

Comamonas testosteroni, DSMZ 6781 was grown under the cultivation conditions recommended by the provider (Tryptic Soy Broth – TSB, Becton Dickinson, 30°C, 150 rpm) until it reached an approximate optical density at 600 nm (OD_{600}) of 4. The bacterial culture was added to 250-mL shake flasks containing mineral medium (medium 457 DSMZ – Brunner) at a concentration of 10 v/v%, for a total volume of 40 mL. PHB films were also placed in the flasks as the only carbon source for the bacteria (1 w/v%); these films were formed by solvent casting at 140°C (as described in previous work [39]). The cultures were incubated at 30°C and 150 rpm for 3 days until they reached an average OD_{600} value of 5.4. The cultures were centrifuged (Sorval RC 6 PLUS,

Thermo) at 10,000 rcf and 4°C for 30 minutes. The supernatants were pooled, filter sterilized (0.2 μm), diluted by a factor of 10 with mineral medium, and stored at 4°C before being used for the tests. The PHA deploymerase ($PhaZ_{Cte}$) concentration was ~ 0.17 μg/mL, based on semi-quantitative polyacrylamide gel electrophoresis analysis of the extracellular solution. Solutions with different enzyme concentrations were obtained by diluting the starting enzyme solution with the required quantity of mineral medium.

Patterning of PHB with diffraction gratings

PHB thin films patterned with diffraction gratings were fabricated using a solvent casting/replica molding process [40,41], as shown in Figure 4.1.c. A polydimethylsiloxane (PDMS) master mold patterned with a negative image of the microscopic grooves with a periodicity (center-to-center distance) of 1.64 μm and height of 125 nm was used to create the gratings on the PHB surface. The as-received PHB pellets were dissolved in acetic acid (0.005 g of PHB/mL of acetic acid) on a hot plate maintained at a temperature of 160ºC. The polymer solution was then poured on top of the PDMS master mold and allowed to dry at a constant temperature (80ºC or 110ºC or 140ºC). All samples were annealed at the respective temperature for 30 seconds after complete evaporation of the solvent as determined by visual observation. The resulting PHB films were transferred onto glass substrates, revealing the replicated optical gratings on the surface. The PHB films prepared at different temperatures were aged for 1 day at 22ºC and atmospheric pressure before being used. The PHB films were then exposed either to enzyme solution or to water to determine their degradation stability.

Preparation of silk film with diffraction gratings

Silk films were prepared using the established protocol detailed by *Rockwood et. al* [42]. Briefly, silk cocoons of *Bombyx Mori* (Lilysilk, Canada) were cut into small pieces and boiled in a 0.02 M Na_2CO_3 solution for 30 minutes. The silk fibroin was extracted from the solution, rinsed with water and dried overnight. The silk fibroin was then dissolved in a 9.3 M LiBr solution at 60˚C for 4 hours. The solution was dialyzed at room temperature against distilled water for 48 hours to obtain an aqueous solution of silk fibroin. The solution was centrifuged at 2,100 rcf for 15 minutes to remove any undissolved particles. The supernatant was extracted and stored at 4˚C until use. The solution was diluted to produce a solution concentration of 0.05 g/mL, which was then poured on the PDMS mold patterned with diffraction gratings. The silk films were heat-treated – at 60˚C or 100˚C for a 1 hour – or methanol-treated for 1 hour to make them more resistant to dissolution in water. The different silk films were then exposed to water to determine their stability to water dissolution.

Degradation Sensor

The schematic of the diffraction-based degradation sensor is shown in Figure 4.1.d. The sensor setup involves three main components: 1) the light source, 2) the polymer sample patterned with a diffraction grating (mounted in a plastic cuvette containing the desired solution), and 3) the photodiode to measure the beam intensity. A commercially available diode laser (λ = 650 ± 10 nm, power = 2.5-3 mW) was used as the light source. A pair of silicon photodiodes in reverse-biased configuration placed at a

distance of 10 ± 0.5 cm from the sample was used to measure the intensity of each of the diffracted beams. In this work, the transmitted beam was blocked by an opaque surface placed in the beam path to prevent it from interfering with the light intensity measurements of the photodiodes. The laser and the diffraction grating on the PHB surface were aligned so that the diffracted beams impinged directly on the photodiodes. The entire sensor setup was maintained in complete darkness at all times during the experiment.

The light source and the photodiode were controlled using a data acquisition system developed in-house based on the Arduino programming environment. The system was programmed to switch on the laser once every 15 minutes and to acquire 10 data points from each photodiode with a 1-second interval between each data point. An average of these data points at each time step was taken as the value of the diffracted beam intensity. At least 3 diffracted beam intensity measurements were used to construct the diffracted beam intensity curve. The intensity at each time point was normalized to the diffraction intensity at the beginning of the degradation reaction and plotted against degradation time.

X-ray diffraction (XRD)

The crystalline peaks of the various PHB thin films were determined using a Rigaku X-ray diffraction (XRD) system in glancing incidence angle mode. An Ultima VI goniometer fitted with a thin film attachment was used to characterize the samples.

Scans were carried out between 5º and 60º at a rate of 2º/min using Cu Kα X-rays. An X-ray beam spot of 5 mm diameter was used for all scans. The samples were mounted on a glass slide to keep them as flat as possible. Baseline correction from the actual XRD pattern was carried out using Igor Pro 6.35A5.

Atomic Force Microscope (AFM)

The surface morphology and the 2D cross-section of PHB thin film surfaces were determined using a Bruker Nano Dimension Edge atomic force microscope (AFM). The AFM was operated in tapping mode using a tip with a spring constant of 40 N/m. The images were obtained over 50 μm × 50 μm areas for all samples, and two-dimensional cross-sectional profiles of PHB gratings exposed to enzyme solutions for different times were obtained using the NanoScope Analysis software.

Macroscopic diffraction analysis

The diffraction pattern of PHB films (degraded for different times in the enzyme solution) illuminated by a commercially available laser pointer (λ = 532 ± 5 nm, maximum power ~ 25 mW) was photographed for analysis. The laser illuminated a PHB grating mounted on a glass slide, and the pattern was imaged on a flat surface, 9 cm from the grating. Photographs of the surface were taken with a digital camera maintained at a constant distance and angle (~ 12 cm away from the beam spots and ~ 15º between the normal and the camera) from the flat surface.

4.4. Results and Discussion

Diffraction-based Degradation Sensor

As a proof-of-concept, we first characterized a thin film of polyhydroxybutyrate. Polyhydroxybutyrate is a hydrophobic, surface-degradable polymer, which undergoes hydrolysis in the presence of a depolymerase enzyme. To monitor the degradation process, PHB was cast from solution against a patterned PDMS master to form a thin film (total thickness of 925 nm) with a grating on the surface (Figure 4.1.d). The properties of the grating (step height and periodicity) determine the charcteristics of the diffraction pattern. A higher step height generally results in a higher diffraction intensity, while the periodicity of the lines (i.e. the pitch) determines the spacing of the pattern, and should generally be on the order of the wavelength of light. In this work, the line height and periodicity were determined by the features of the PDMS master, and were 125 nm and 1.64 μm, respectively.

The PHB film with a grating on its surface (total mass, ~10^{-4}g) was mounted in a plastic cuvette containing a desired solution (the degradation environment). In our proof-of-concept experiments three different media were utilized: one comprising a low concentration solution of a depolymerase known to degrade PHB ($PhaZ_{Cte}$), one comprising a high concentration solution of $PhaZ_{Cte}$, and a control solution containing only water. When the sample was illuminated with a diode laser, the grating resulted in the diffraction of the laser beam, leading to the appearance of two (first-order) diffracted beam spots, one on either side of the (zero-order) transmitted beam (Figure 4.2, inset). The average normalized intensity of the diffracted beams was monitored as a function

of degradation time, and the resulting intensity vs time curves for each solution are plotted in Figure 4.2. For the control sample (exposed to water), the intensity of the diffracted beam did not change as a function of time, indicating the stability of PHB under these conditions. PHB — by virtue of its hydrophobicity[43] — is not affected by exposure to water for as long as hundreds of hours. Consequently, the PHB does not undergo any substantial moisture absorption (absorption < 1%) or surface changes/swelling on exposure to water[44]. On the other hand, the samples exposed to depolymerase enzyme showed a consistent, gradual decrease in the intensity of the diffracted beam. For both the high and low concentration solutions, the curve initially undergoes a gradual roll-off, followed by a region of exponential decay in which the intensity of the diffracted beam eventually decreases to 0. The intensity of the sample exposed to the high concentration solution undergoes a faster decay than the sample exposed to the low concentration solution.

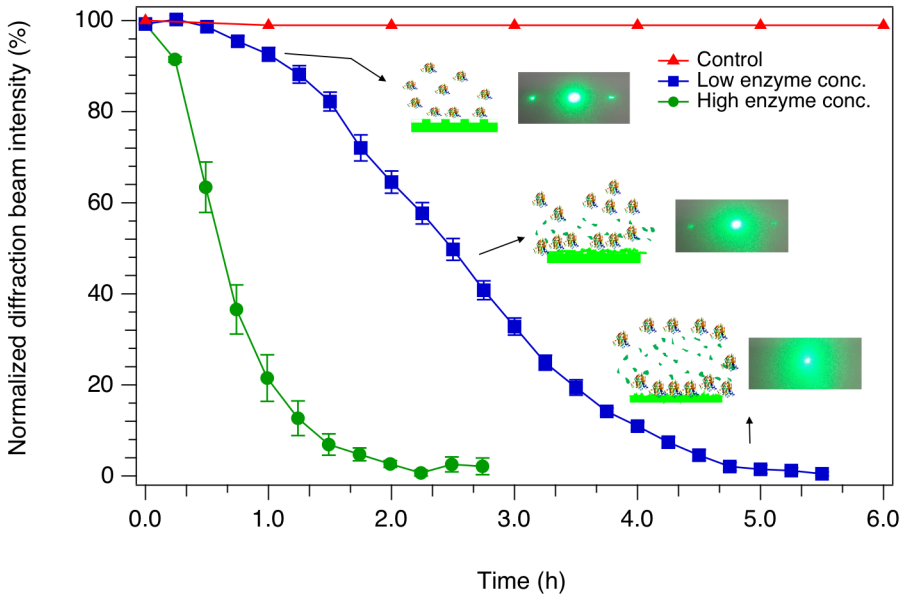

Figure 4.2 Plot of the diffracted beam intensity vs. degradation time for a sensor that includes a PHB thin film (solvent cast at at 80°C and aged for 1 day) exposed to a solution containing ~ 0.17 µg/mL (high enzyme concentration, green curve) and ~ 0.07 µg/ml (low enzyme concentration, blue curve) of the depolymerase enzyme PhaZCte.

Initially, the change in intensity of the normalized diffraction beam is low. There are two possible explanations for this observation: (1) The microsopic surface structure can be altered only when a sufficient number of polymer chains are released from the surface due to bond cleavage. At the start of the degradation, some polymer chains may be cleaved without significantly affecting the structure of the grating. (2) A non-linear relationship between the shape of the grating and the diffracted intensity may exist during the initial stage of degradation.

Subsequently, a more rapid decay in intensity as a function of time is observed. To relate the change in intensity to the change in mass, a simple probabilistic model was implemented. In this model (described in depth in subsequent section), each unit length of the grating is assumed to contribute equally to the overall initial intensity of the diffraction pattern. Discrete volume elements are randomly removed from the surface of the polymer, and the resulting intensity is calculated based on the fraction of grating remaining. A similar trend is observed as for the experimental data, where the intensity decays exponentially as a function of mass. This suggests that within this region, the rate of degradation ($\Delta m/\Delta t$) is linear, despite the exponential shape of the intensity vs. time curve, since even after complete degradation of the gratings on polymer surface, the degradation rate essentially remains constant, as do the surface area available for enzymatic attack. A linear rate is typical of surface-limited reactions [45]. Ultimately, the intensity of the diffracted beam tends towards zero. At this point, the thickness of the grating is insufficient to introduce the phase difference required for diffraction to occur.

Diffraction Efficiency and Surface Profile

The changes in the surface profile of PHB gratings at different stages of the degradation process, and their relationship to the diffraction intensity were determined using AFM and manual observations of the diffracted beams, respectively. Figure 4.3.a shows AFM images of a PHB grating imaged after different degradation times. For the control sample, and the sample incubated for 30 mins, the 125 nm high grooves with 1.64 μm pitch are clearly seen. With passing time, the grating surface was found to erode and become more randomized, which is concomitant with the observed decrease

in diffracted beam intensity (Figure 4.3.c). Figure 4.3.b shows a cross-section of the PHB surface at different degradation times measured by AFM, which illustrates that the grating periods were eroded within 120 minutes of exposure to the enzyme solution. We can also observe the increase in RMS roughness and appearance of deep pits and crevasses on the surface, indicative of polymer degradation and erosion.

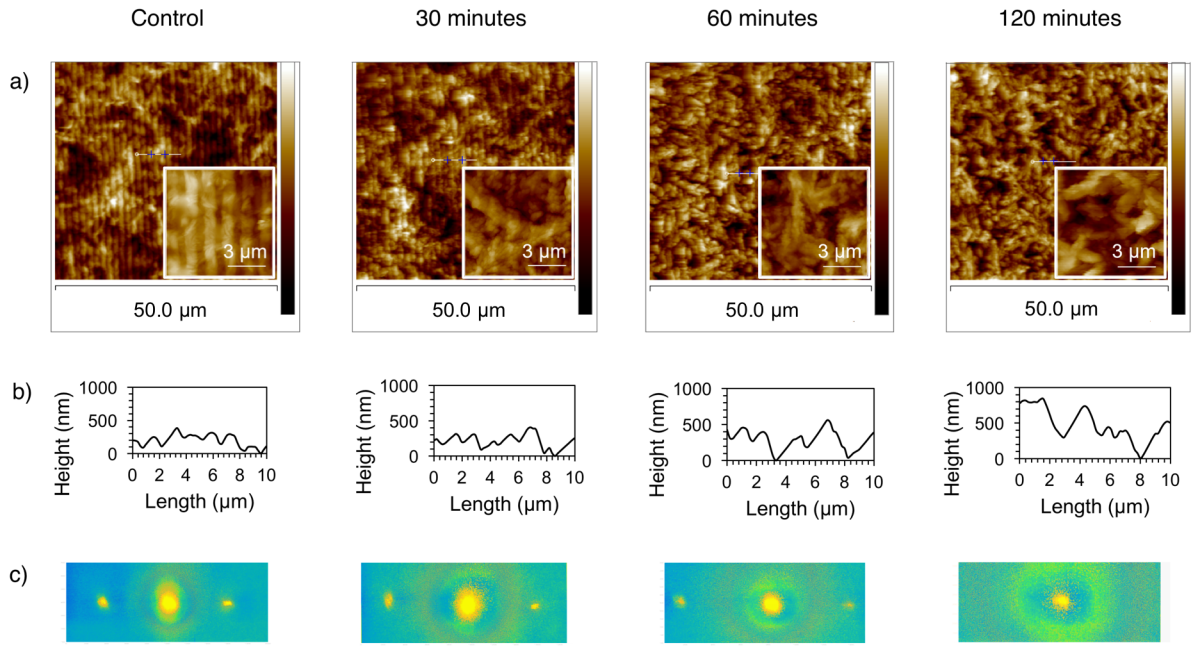

Figure 4.3 Surface profile and corresponding changes in diffraction efficiency at different degradation times. (a) Surface morphology of the PHB sample (processed at 80°C and aged for 1 day) after exposure to a solution containing ~ 0.17 µg/mL of the depolymerase enzyme PhaZCte (corresponding to high conc. in Figure 4.2), as measured by AFM. Samples exposed to water for 24 hours (Control), and to the enzyme solution for 30 minutes, 60 minutes, and 120 minutes are shown from left to right. Inset images are shown at higher magnification (3 µm scale bar). (b) 2D cross-sectional profiles for each sample. (c) Corresponding diffraction patterns expressed as colored intensity maps.

Diffraction Efficiency and Degradation Rate

These results clearly show that the diffraction-based degradation sensor can provide information about the degradation of polymeric thin films. The change in mass that leads to the observed change in diffraction efficiency can be estimated based on the geometry of the sample. A 1-cm^2 polymer film with a thickness of 1 μm weighs only about 10^{-4} g (assuming a density of 1.25 g/cm^3), and a substantial fraction of material has to be removed to result in a measurable change in weight. The grating over the same 1 cm^2 area (with height of 125 nm, where the peaks and valleys have equal width) has a mass of only ~ 8 x 10^{-6} g / cm^2, and, the removal of this small mass from the surface leads to a substantial change in optical properties. In fact, the entire mass of the grating does not need to be removed to produce a measurable change; the area of grating illuminated by the beam (< 2 mm^2) is much smaller than the total area of the sample (1 cm^2). The change in intensity from 100% to 0% in the illuminated region therefore corresponds to a decrease in mass of < 2 x 10^{-7} g (the total mass of the grating within the illuminated area). Furthermore, in Figure 4.2, five intermediate measurements can be seen during the switch from the diffracting to non-diffracting states, which, assuming a linear relationship, would correspond to steps of ~ 2 x 10^{-6} g/cm^2, or 3 x 10^{-8} g (for a spot size of 2 mm^2). Even smaller mass changes could be resolved using smaller beams (for example a focused 50 μm^2 beam spot could monitor a sample with a mass in the range of 10^{-12} g).

The mass changes of 3 x 10^{-8} g (for a spot size of 2 mm^2) that can be qualitatively observed using our sensor are considerably lower than the limit of detection of a traditional micro-balance (~ mg). On the other hand, the mass resolution of the diffraction sensor is slightly weaker than that which can be achieved by quartz crystal microbalance (QCM) under ideal, adsorption-only conditions (typically ng/cm^2, compared with μg/cm^2 here). However, the complex interplay between enzyme adsorption, desorption and polymer mass-loss kinetics occurring during a degradation process interferes with QCM measurements[46]. The diffraction approach affords the advantage of highly localized analysis of the polymer surface, where the minimum area of sample required is limited primarily by the size of the beam spot, the ability to align the beam with the sample area, and the sensitivity of the photodiode. Further theoretical analysis of the diffraction system would be required to relate the change in optical properties in our sensors directly to mass. As a starting point, the next section provides a probabilistic model that can be used to approximately estimate the mass loss for a given decrease in the diffraction intensity. Nonetheless, qualitative analysis of very small sample sizes is possible using our sensor in its current state, allowing the comparison of the stability and degradation of polymers with different properties and/or exposed to different degradation environments.

Probabilistic Model

In the experimental data showing the intenisty of a beam diffracted by a polymer grating as a function of degradation time, the change in diffraction intensity ($\Delta i/\Delta t$) does not provide a direct measure of the degradation rate, which is usually expressed as

mass loss per unit time ($\Delta m/\Delta t$). The change in diffraction intensity can be related to the mass loss rate in differential form as:

$$\frac{\Delta i}{\Delta t} = \frac{\Delta i}{\Delta m} \cdot \frac{\Delta m}{\Delta t}$$

In this equation, we can obtain $\Delta i/\Delta t$ from the experimental results. However, it is challenging to measure $\Delta i/\Delta m$, since the mass changes of the gratings are too small and subtle to be determined accurately using traditional methods.

To explore the relationship between diffracted light intensity and mass, a probabalistic model was implemented. In this model, the grating and substrate were divided into rectangular elements, and the grating is defined by lines of elements which are 125 nm taller than the substrate beneath. This simplified model assumed that each unit length along the edge of the constituent lines contributes equally to the overall intensity of the diffraction pattern. Elements (i.e. mass) were then randomly removed from either the grating or substrate, and the new diffraction intensity was calculated based on the new total length of edges present between the grating (crest) and adjacent substrate (trough). An edge was considered to be an interface (along the original edge of the line) where a step height difference of 125 nm or greater exists (the height may increase if a section of the substrate adjacent to the line is removed, although the probability of very large step heights is vanishingly small).

In the model, the polymer film (including the grating and the polymer layer beneath the grating) was assumed to be composed of unit elements of constant size (length $\times$ width $\times$ thickness = 800 nm $\times$ 800 nm $\times$ 125 nm). The width and height of the

unit element were chosen to correspond to the width and thickness of the grating, respectively, and the length was chosen to match the width. These unit elements were then removed from the polymer surface in a probabilistic manner. Consequently, the shape of the grating changes and more randomness was introduced on the surface. This is certainly an approximation of the physical process; in reality the size of a polymer unit would be smaller, and a more complex model would be required to describe the relationship between the surface profile variations in the nanoscopic scale of individual polymer chain and the intensity of the diffracted beam. Nonetheless, the described simplified system can lead to some useful insight, as described below.

Figure 4.4 shows a set of theoretical surfaces obtained by removing a certain number of elements in the probabilistic model. The mass loss at a given point was calculated based on the number of elements removed, the size of an element, and the density of the polymer. The corresponding intensity was determined by scaling the initial intensity by the fractional length of remaining edges between the gratings and substrate. The profiles obtained are similar to the AFM profiles of the polymer samples at different stages of degradation (Figure 4.3), indicating the ability of the model to approximate real world changes experienced by the polymer surface. Figure 4.4 also includes the diffraction intensity as a function of mass loss as predicted by the model. From these results, we found that the diffraction intensity follows an exponential decay trend versus changes in mass on the polymer surface as expressed by:

$$I = I_0 e^{-\alpha M}$$

Here, I is the intensity of the diffracted beam, I_o is the initial intensity of the diffracted beam, α is a dimensional constant which depends on the surface area being monitored, the density of the polymer and the dimensions of the volume element. For PHB with 1 cm^2 surface area and the volume element size selected for the current model (800 nm $\times$ 800 nm $\times$ 125 nm), the value of $\alpha \approx 1.6 \times 10^7$ $mm^2 \cdot hr/g$. M represents the mass change experienced by the modeled surface. Using this relation, the intensity change that corresponds to a given mass loss can be estimated ($\Delta i/\Delta m$). As for the calculations given in the previous section, the total change in mass corresponding to a 100% drop in intensity is 2 x 10^{-6} g/cm^2; intermediate mass loss values as small as (0.5 x 10^{-6} g/cm^2) can be easily read off of the x-axis for a given change in intensity on the y-axis.

The mass values depicted on the x-axis are calculated knowing the size of the volume elements considered in the model, and are valid for the specified grating geometry (125 lines with a width of 800 nm, spaced with a pitch of 1600 nm) and polymer density (1.25 g/cm^3). To translate these values to another polymer grating, precise knowledge of the grating geometry and polymer density would be required.

The theoretical curve also follows the latter part of the plot depicting the normalized beam intensity versus time (Figure 4.2). Importantly, this result suggests that within this region, a constant rate of mass loss – as expected for a surface-limited reaction – yields the resulting exponential change in diffraction intensity. Interestingly, the subtleties of the initial part of the curve are not captured by the model. In the

experimental results, there is a more gradual decrease in intensity as a function of time at the start of the results (Figure 4.2). This may indicate that the mass loss is initially limited, due to non-solubilizing chain scission. Alternatively, the differences observed here may stem from the fact that this model assumes a *linear* relationship between the number of edge units comprising the grating and diffraction intensity, whereas the actual physical relationship between these variables may be non-linear. An extensive physical model would be required to elucidate the relationship between the change in shape of the grating and the change in the diffraction intensity.

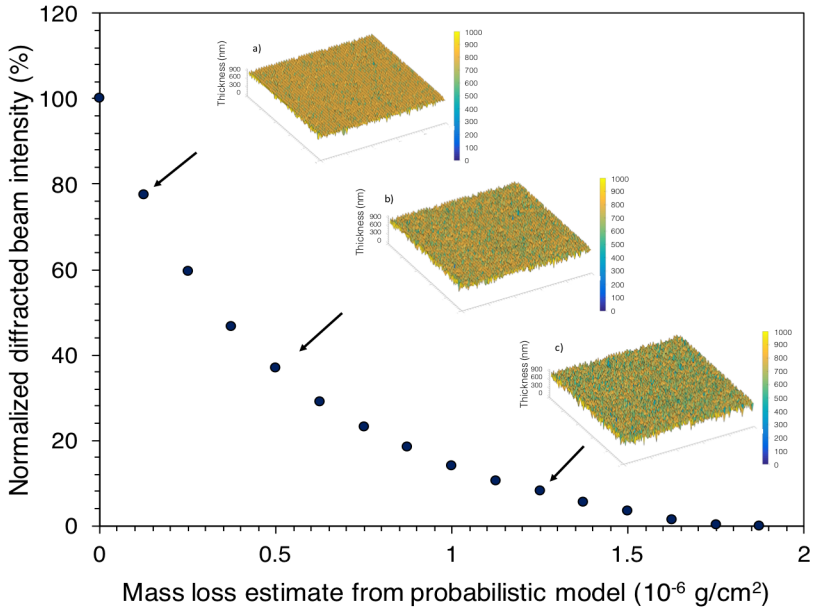

Figure 4.4 The intensity vs. mass loss plot and representative polymer surface profiles obtained from the probabilistic model. Surface profile with (a) 1000 volume elements removed, (b) 4000 volume elements removed, (c) 10000 volume elements removed. Volume elements of dimensions 800 nm x 800 nm x 125 nm were randomly removed according to an equal probability, independent of location on the surface.

Processing Conditions and Degradation Rate

The conditions under which polymer thin films are processed influence properties such as crystallinity, which in turn impact degradation and stability. Due to the small mass of thin films, it is challenging to characterize the relationship between these parameters. Therefore, we used the diffraction approach to test the effect of processing temperature (and consequently crystallinity) on the degradation rate of PHB thin films of thickness ~ 925 nm. Samples with varying crystallinity were prepared by solvent casting PHB films at different temperatures; these samples were then incorporated into the degradation sensors. Figure 4.5.a shows the X-ray diffraction patterns of these films, where the amplitude of the crystalline peaks increases with temperature. At higher temperatures, there is more thermal energy and mobility available to the polymer chains to form ordered structures[39], and crystallinity increases from about 25% at 80˚C to about 28% at 140˚C. Figure 4.5.b shows the combined plot of the change in diffraction beam intensity versus time for these PHB films. The inlay shows the $\Delta i/\Delta t$ and estimated mass loss rate ($\Delta m/\Delta t$) for the different samples. The change in diffraction intensity, and the total time for degradation of the gratings were found to increase with increasing crystallinity.

The results indicate that the films processed at elevated temperatures tend to be more crystalline (Figure 4.5.a), and degrade slower than the samples prepared at low temperatures (Figure 4.5.b). This behavior is in agreement with previous work [47] conducted on 50 μm thick PHB films. In that work, mass data was only collected at two timepoints (0 hrs and 19 hrs), since mass changes in the order of milligrams were

required for consistent measurements using a micro-balance. As an additional verification, we also monitored the degradation of PHB films (processed at 80˚C) in an enzyme solution (~ 0.2 µg/ml) using a micro-balance. Statistically significant changes in mass were observed after 2 hours of degradation. The mass loss rates per unit area observed (~ 17 µg/hr.cm^2) were on-par with the values that we estimated for the diffraction-based sensor. However, both longer testing times (including at least 2 hours of enzymatic degradation for measurable mass loss and 24 hours for drying prior to measurement) and larger samples (with a mass of 0.014 g and total surface area of 4 cm^2) were required to achieve measurable changes in mass in the time reported.

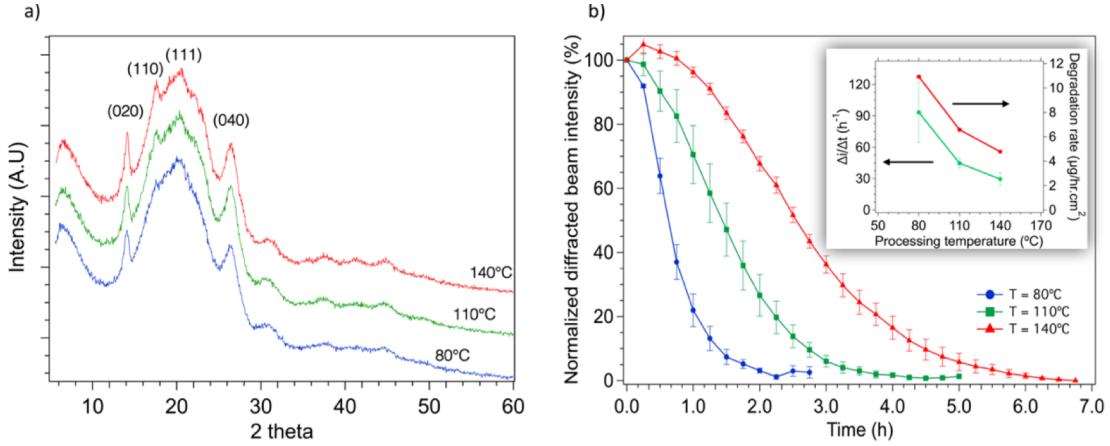

Figure 4.5 Plots showing the degradation behavior of PHB samples prepared at different solvent casting temperatures. (a) XRD patterns for PHB samples prepared at different solvent casting temperatures. The amplitude of the (202), (110) and (040) crystalline peaks increases with increasing processing temperature. (b) The plot of decrease in diffracted beam intensity with time. The inset graph shows the slope of the diffracted intensity over time and the equivalent degradation rate as a function of solvent casting temperatures.

Using the degradation sensor, we were able to detect changes in degradation rate for a range of PHB samples. The simplicity of this technique allowed us to measure differences in degradation stability of polymer thin films with minimal sample preparation and shorter testing times than possible with advanced gravimetric techniques.

Applications

The diffraction-based degradation sensor can thus be utilized to characterize polymer thin films and to determine how different variables impact their degradation and stability. These variables can include both properties of the polymer (composition, processing conditions, thermal history, etc.) and environmental conditions (temperature, humidity, pH, enzyme concentration, etc.). For example, we used the diffraction sensor to observe how differences in enzyme concentration affect the degradation of PHB (Figure 4.6). Enzymatic degradation is a complex process, which includes adsorption and desorption of the enzyme to the surface of a film, and a hydrolysis process. In our experiments, we found that the two highest enzyme concentrations we used (1.36 and 0.78 μg/mL) resulted in nearly identical degradation rates (as determined by the slope of the intensity-time curve), while at lower enzyme concentration a slower rate was observed. The slope of these curves plotted against the enzyme concentration is shown as inset in Figure 4.6, which indicates that the degradation rate follows a saturation trend characteristic of enzyme-mediated surface degradation[48]. The degradation rate resulting from different enzyme concentrations are easily discerned in a few hours, providing an alternative method to mass loss experiments – which are time-consuming, and are less sensitive and reproducible.

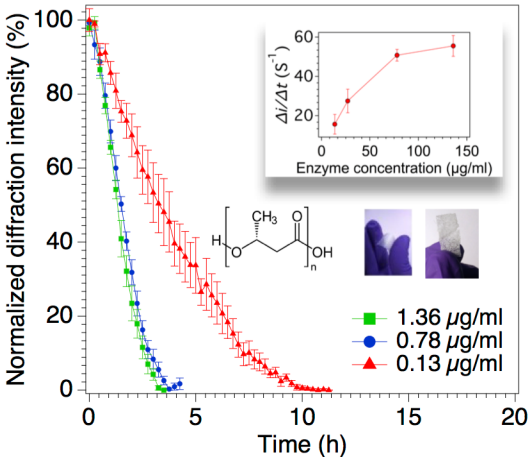

Figure 4.6 Degradation stability of PHB films exposed to solutions of depolymerase enzymes (PhaZCte) at various concentrations. Inlay plot provides a measure of the degradation rate as a function of enzyme concentration. The appearance of PHB film before (smooth and flexible) and after (porous and fragile) enzymatic degradation is shown in the inlay images.

Beyond degradation, these sensors can be used to study the impact of environmental factors such as moisture on the degradation/dissolution of materials used in transient devices, such as silk. From the literature, it is known that the dissolution characteristic of silk is dependent on the proportion of β-sheet structures and that a simple physical/chemical treatment can be used to affect this proportion[49]. To compare the effect of different treatments, we fabricated silk gratings and exposed these films to different chemical and thermal treatments. Figure 4.7 shows how methanol and thermal treatments affect the dissolution stability of silk films of thickness ~ 15 μm in water. Sensors were constructed using the following samples as the polymer diffraction grating:

1. An untreated, amorphous silk film prepared by aqueous solvent casting and drying for 24 hours at 23˚C that readily dissolves in water. The normalized diffracted beam intensity for this sample upon complete dissolution (which occurred within a second after exposure) in water was set as 0%.
2. A silk film (~ 15 μm thick) solvent cast at 60˚C for 1 hour that is partially stable to dissolution in water. The normalized diffracted beam intensity obtained for this sample was 28%.
3. A silk film (~ 15 μm thick) solvent cast at 100˚C for 1 hour that is partially stable to dissolution in water. The normalized diffracted beam intensity obtained for this sample was 55%.
4. An amorphous silk film (~ 15 μm thick) treated by methanol exposure for 1 hour to render it insoluble in water. The normalized diffracted beam intensity of this sample upon immersion in water was taken as 100% since this sample was insoluble in water.

The average diffracted intensity over the time period of interest for an insoluble sample (methanol-treated silk film) and for an entirely soluble sample (untreated silk) is used as the reference for 100% and 0% normalized intensities respectively. The dissolution of silk film is rapid process taking place within microseconds. Therefore, in these Figures, the exponential decay of intensity is not observed due to the fast time-scale of the process. Rather, the value plotted corresponds to the steady-state value of the diffraction intensity after the partial dissolution of the samples. Using these values, it is possible to compare the dissolution stability of all the intermediate, partially soluble

samples. The real-time diffraction intensity measurements were able to differentiate clearly between all these samples (Figure 4.7), each of which achieved a different stable diffraction intensity when exposed to water. From these results it can be seen that heat and methanol treatments improve the dissolution-resistance of silk, with the film exposed to the higher temperature treament undergoing lower dissolution than the film exposed to the lower temperature treatment. Such small changes in the surface stability between samples is challenging to measure using existing approaches and only a few specialized techniques[16] are currently available for such analysis. The degradation sensor thus opens up possibilities for rapid screening of resorbable polymer materials for use in transient devices.

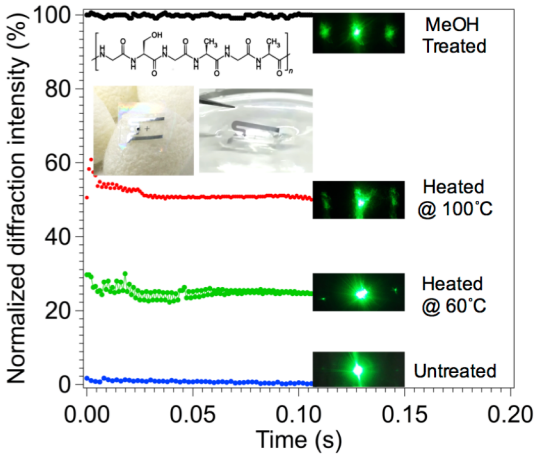

Figure 4.7 Characterization of dissolution stability of silk films. The silks films were made more resistant to dissolution in water by heat treatment or methanol treatment. Inlay images are representative diffraction patterns for each silk film. Images show a transient electronic device on silk substrate and the dissolution of the device in water.

4.5. Discussion

Depending on the nature of degradation processes and the optical properties of the polymer, the degradation sensor can be altered to obtain suitable information for a variety of materials and conditions. For instance, an opaque polymer surface could be studied by converting the setup to work in reflection mode. Similarly, if the polymer or the surrounding environment (*e.g.* solutions) absorbs visible light, the wavelength of the light and the periodicity of the gratings could be altered with similar outcomes.

The automated diffraction intensity measurement thus enables us to determine the degradation kinetics with high sensitivity and reliability. Alternatively, we could use the macroscopic optical properties – diffraction at a specific angle and the rainbow-like coloration under white light (Figure 4.1.a & 1.b) – of the diffraction gratings to qualitatively observe the environmental stability of polymers, providing us an simple, rapid method to analyze different polymeric materials.

One limitation of the diffraction method is that materials that absorb significant amounts of water during the degradation or undergo physical, surface redistribution without degradation (like starch and proteins) may be challenging to characterize, as the absorption of water and surface redistribution can distort the grating and cause varitions in optical properties without actual degradation/removal of material. Therefore, prior knowledge of the material being tested and further characterization is required to determine if useful results could be obtained for these types of materials, which would be equally challenging to monitor using other existing methods.

To increase the utility of the sensor, and to directly relate a given change in intensity to a change in mass, a precise knowledge of the relationship between the intensity of the diffracted beam and the shape of the grating is required. Further modeling should be undertaken to explore how the changing shape of the diffraction grating affects the intensity of the diffracted beam.

4.6. Conclusion

As polymer thin films occupy more and more space in the technological landscape, and as the reduction in the dimensions of these films brings forth new or different properties, it becomes crucial to appropriately characterize these materials and understand their properties. One property that may be different or amplified at the small scale is degradability, which may or may not be desirable, depending on the application. Unfortunately, many of the conventional metrologies are not amenable to accurately evaluate thin film properties such as degradation rate and stability due to the small masses of the films. We have demonstrated how a simple diffraction-based degradation sensor can be used to evaluate these very properties in polymeric thin films that degrade by a surface erosion process. The sensor was used to compare the effects of polymer crystallinity and depolymerase concentration on PHB biodegradation, and to monitor the dissolution stability of silk films, all for films with thicknesses at the nano- and micro-scale. A probabilistic model was also developed to explore how the diffracted beam intensity changes as a function of mass loss during degradation, and to estimate the rate of mass loss. The power of the method lies in the fact that the small changes in

the shape and surface of the grating lead to measurable changes in the intensity of the first-order diffraction beam. In addition, the intensity of this beam may be monitored in situ, simplifying the monitoring and the sample handling required to collect data (as compared with advanced gravimetric or chromatographic analysis). The potential applications of the degradation sensor are numerous and their number should continue to grow as new materials and properties are developed, and as interest in degradable materials continues to grow.

Acknowledgements

The authors would like to thank Alberta Agriculture and Forestry for providing funding for this research.

Author Contributions

P.A designed and performed experiments, D.M.T produced and characterized enzymes, A.L.E. and D.S. supervised the work, and contributed to designing the research and to writing the manuscripts.

4.7. References

1. Frank, C. W. *et al.* Structure in Thin and Ultrathin Spin-Cast Polymer Films. *Science (80-.).* **273,** 912–915 (1996).
2. Eason, R. *Pulsed Laser Deposition of Thin Films: Applications-Led Growth of Functional Materials*. (John Wiley & Sons, 2007).
3. Berggren, M. & Richter-Dahlfors, A. Organic bioelectronics. *Adv. Mater.* **19,** 3201–

3213 (2007).

4. Kim, D.-H. *et al.* Epidermal electronics. *Science* **333,** 838–43 (2011).

5. Rogers, J. A., Someya, T. & Huang, Y. Materials and mechanics for stretchable electronics. *Science* **327,** 1603–7 (2010).

6. John A. Rogers, Dae Hyeong Kim, Joshua D. Moss, David J. Callins, Brian Litt, J. V. High-Speed, High-Resolution Electrophysiology In-Vivo Using Conformal Electronics. (2012).

7. Kim, D.-H. *et al.* Dissolvable films of silk fibroin for ultrathin conformal bio-integrated electronics. *Nat. Mater.* **9,** 511–7 (2010).

8. Dagdeviren, C. *et al.* Transient, biocompatible electronics and energy harvesters based on ZnO. *Small* **9,** 3398–404 (2013).

9. Acar, H. *et al.* Study of Physically Transient Insulating Materials as a Potential Platform for Transient Electronics and Bioelectronics. *Adv. Funct. Mater.* **24,** 4135–4143 (2014).

10. Kaltenbrunner, M. *et al.* An ultra-lightweight design for imperceptible plastic electronics. *Nature* **499,** 458–63 (2013).

11. Irimia-Vladu, M. *et al.* Biocompatible and Biodegradable Materials for Organic Field-Effect Transistors. *Adv. Funct. Mater.* **20,** 4069–4076 (2010).

12. Kang, S.-K. *et al.* Bioresorbable silicon electronic sensors for the brain. *Nature* **530,** 71–76 (2016).

13. Zelikin, A. N. Drug Releasing Polymer Thin Films new Era of Surface-Mediated Drug Delivery. *ACS Nano* **4,** 2494–2509 (2010).

14. Tokiwa, Y., Calabia, B. P., Ugwu, C. U. & Aiba, S. Biodegradability of Plastics. *Int.*

J. Mol. Sci. **10,** 3722–3742 (2009).

15. Liu, Y. X. & Chen, E. Q. Polymer crystallization of ultrathin films on solid substrates. *Coord. Chem. Rev.* **254,** 1011–1037 (2010).
16. Jeon, H.-Y. *et al.* Array-Based High-Throughput Analysis of Silk-Elastinlike Protein Polymer Degradation and C-Peptide Release by Proteases. *Anal. Chem.* **88,** 5398–5405 (2016).
17. Millan, M. D., Locklin, J., Fulghum, T., Baba, A. & Advincula, R. C. Polymer thin film photodegradation and photochemical crosslinking: FT-IR imaging, evanescent waveguide spectroscopy, and QCM investigations. *Polymer (Guildf).* **46,** 5556–5568 (2005).
18. Marx, K. A. Quartz crystal microbalance: a useful tool for studying thin polymer films and complex biomolecular systems at the solution-surface interface. *Biomacromolecules* **4,** 1099–120 (2003).
19. Li, M., Tang, H. X. & Roukes, M. L. Ultra-sensitive NEMS-based cantilevers for sensing, scanned probe and very high-frequency applications. *Nat. Nanotechnol.* **2,** 114–20 (2007).
20. Boisen, A., Dohn, S., Keller, S. S., Schmid, S. & Tenje, M. Cantilever-like micromechanical sensors. *Reports Prog. Phys.* **74,** 36101 (2011).
21. Wang, F. C.-Y. Polymer analysis by pyrolysis gas chromatography. *J. Chromatogr. A* **843,** 413–423 (1999).
22. Sundarrajan, S., Surianarayanan, M. & Srinivasan, K. S. V. Synthesis and characterization of saturated and unsaturated polysulfide polymers and their thermal degradation processes investigated by flash pyrolysis-gas

chromatography/mass spectrometry. *J. Polym. Sci. Part A Polym. Chem.* **43,** 638–649 (2005).

23. Rizzarelli, P. & Carroccio, S. Modern mass spectrometry in the characterization and degradation of biodegradable polymers. *Anal. Chim. Acta* **808,** 18–43 (2014).
24. Mukai, K., Yamada, K. & Doi, Y. Kinetics and mechanism of heterogeneous hydrolysis of poly[(R)-3-hydroxybutyrate] film by PHA depolymerases. *Int. J. Biol. Macromol.* **15,** 361–366 (1993).
25. Yoshie, N., Oike, Y., Kasuya, K., Doi, Y. & Inoue, Y. Change of Surface Structure of Poly (3-hydroxybutyrate) Film upon Enzymatic Hydrolysis by PHB Depolymerase. *Biomacromolecules* **3,** 1320–1326 (2002).
26. O'Shea, D. in *Diffractive optics: design, fabrication, and test* **1,** 17–35 (SPIE, 2004).
27. Zappe, H. in *Fundamentals of Micro-Optics* 265–310 (Cambridge University Press, 2010).
28. Loewen, E. G. & Popov, E. *Diffraction Gratings and Applications*. (CRC Press, 1997).
29. Stafford, C. M. *et al.* A buckling-based metrology for measuring the elastic moduli of polymeric thin films. *Nat. Mater.* **3,** 545–550 (2004).
30. Bhatta, D., Christie, G., Blyth, J. & Lowe, C. R. Development of a holographic sensor for the detection of calcium dipicolinate-A sensitive biomarker for bacterial spores. *Sensors Actuators, B Chem.* **134,** 356–359 (2008).
31. Kabilan, S. *et al.* Holographic glucose sensors. *Biosens. Bioelectron.* **20,** 1602–1610 (2005).

32. Christopher Robin Lowe, Roger Bradley Millington, J. B. and A. G. M. Hologram containing sensor. (1999).

33. Marshall, A. J., Kabilan, S., Blyth, J. & Lowe, C. R. Analyte-responsive holograms for (bio)chemical analysis. *J. Phys. Condens. Matter* **18,** S619–S626 (2006).

34. Bhatta, D., Christie, G., Madrigal-González, B., Blyth, J. & Lowe, C. R. Holographic sensors for the detection of bacterial spores. *Biosens. Bioelectron.* **23,** 520–527 (2007).

35. Mayes, A. G., Blyth, J., Millington, R. B. & Lowe, C. R. Metal Ion-Sensitive Holographic Sensors. *Anal. Chem.* **74,** 3649–3657 (2002).

36. Wang, X., Liu, X. & Wang, X. Hydrogel diffraction grating as sensor: A tool for studying volume phase transition of thermo-responsive hydrogel. *Sensors Actuators B Chem.* **204,** 611–616 (2014).

37. Chen, G.-Q. & Wu, Q. The application of polyhydroxyalkanoates as tissue engineering materials. *Biomaterials* **26,** 6565–78 (2005).

38. Khorasani, M. T., Mirmohammadi, S. A. & Irani, S. Polyhydroxybutyrate (PHB) Scaffolds as a Model for Nerve Tissue Engineering Application: Fabrication and In Vitro Assay. *Int. J. Polym. Mater.* **60,** 562–575 (2011).

39. Anbukarasu, P., Sauvageau, D. & Elias, A. Tuning the properties of polyhydroxybutyrate films using acetic acid via solvent casting. *Sci. Rep.* **5,** 17884 (2015).

40. Xia, Y. & Whitesides, G. M. Soft Lithography. *Annu. Rev. Mater. Sci.* **28,** 153–184 (1998).

41. Xia, Y. *et al.* Complex Optical Surfaces Formed by Replica Molding Against

Elastomeric Masters. *Science (80-.).* **273,** 347–349 (1996).

42. Rockwood, D. N. *et al.* Materials fabrication from Bombyx mori silk fibroin. *Nat. Protoc.* **6,** 1612–1631 (2011).

43. Li, J. *et al.* Self-assembled supramolecular hydrogels formed by biodegradable PEO–PHB–PEO triblock copolymers and α-cyclodextrin for controlled drug delivery. *Biomaterials* **27,** 4132–4140 (2006).

44. Lee, S. G., Choi, S.-S., Park, W. H. & Cho, D. Characterization of surface modified flax fibers and their biocomposites with PHB. *Macromol. Symp.* **197,** 089–100 (2003).

45. Anne, A. & Demaille, C. Kinetics of enzyme action on surface-attached substrates: a practical guide to progress curve analysis in any kinetic situation. *Langmuir* **28,** 14665–71 (2012).

46. Bruckenstein, S. & Shay, M. Experimental aspects of use of the quartz crystal microbalance in solution. *Electrochim. Acta* **30,** 1295–1300 (1985).

47. Kumagai, Y., Kanesawa, Y. & Doi, Y. Enzymatic degradation of microbial poly(3-hydroxybutyrate) films. *Die Makromol. Chemie* **193,** 53–57 (1992).

48. Mukai, K., Yamada, K. & Doi, Y. Kinetics and mechanism of heterogeneous hydrolysis of poly[(R)-3-hydroxybutyrate] film by PHA depolymerases. *Int. J. Biol. Macromol.* **15,** 361–366 (1993).

49. Hu, X. *et al.* Regulation of silk material structure by temperature-controlled water vapor annealing. *Biomacromolecules* **12,** 1686–96 (2011).

5. Enzymatic Degradation of Dimensionally Constrained Polyhydroxybutyrate Films

This manuscript characterizes the degradation of PHB films of different thicknesses utilizes the diffraction-based degradation sensor discussed in Chapter 4. The effect of nanoscale dimensional constraint on the degradation of polymer thin films has not been characterized in the literature, since there were previously no suitable techniques to determine degradation in samples with small mass and dimensions. In this manuscript, solvent casting process was used to prepare films ranging from 10's of μm to 10's of nm and the degradation characteristics of each film was determined using the diffraction sensor. The results indicated an inhibition of enzymatic degradation when the PHB films were constrained down to the nanoscale. This paper compares the degradation characteristics of the films of different thicknesses and discusses the underlying mechanisms behind the degradation characteristics exhibited by polymer films constrained down to the nanoscale.

This article was published in the journal *Physical Chemistry Chemical Physics* under the title, **"Enzymatic degradation of dimensionally constrained polyhydroxybutyrate films".** The contents are reproduced here in accordance with the author's rights and copyright policies of the publisher, The Royal Society of Chemistry, and the Journal Physical Chemistry Chemical Physics.

Enzymatic degradation of dimensionally constrained polyhydroxybutyrate films

Preetam Anbukarasu, Dominic Sauvageau, Anastasia Elias

Department of Chemical and Materials Engineering, University of Alberta, Edmonton, Alberta, Canada.

5.1. Abstract

The effect of dimensional constraint, imparted by the variation in film thickness, on the enzymatic degradation of polyhydroxybutyrate (PHB) is reported. The characterization of the crystalline structure and the surface topography of solvent-cast PHB thin films revealed strong correlations between film thickness and both crystallinity and crystal anisotropy, with the polymer film becoming more amorphous with decreasing thickness. The enzymatic degradation of PHB films was characterized using a high precision diffraction metrology, which enabled the visualization of small variations in the degradation behavior. The results show that the degradation rate increases with decreasing thickness, due to a corresponding decrease in crystallinity. However, in a nanoscopic ultra-thin PHB specimen, produced by μ-transfer molding, enzymatic degradation was impeded. The enzymatic degradation rate of PHB films therefore was found to exhibit a discontinuous trend with respect to film thickness, initially increasing as film thickness was reduced, then decreasing dramatically once the thickness was reduced to tens of nanometers. In this regime, enzymatic degradation was hindered by the absence of crystalline regions in the films. These results show that a nanoscale

dimensional constraint on PHB films can result in specimen with a tunable response to extracellular enzymes.

5.2. Introduction

Ultrathin polymer films are used in advanced applications such as organic electronics[1–5], functional coating[6] and drug delivery systems[7,8]. As a result, considerable attention has been paid to characterizing the properties of highly constrained polymer films[11–17]. The physical constraint of sample thickness has been shown to affect properties such as molecular mobility[16,17], crystal growth rate[10,11,16], crystallinity and surface energy. As polymer films become more dimensionally constrained – through a reduction in thickness – both the extent and the rate at which the polymer chains can form crystalline structures decrease. For biodegradable films, these variations can in turn affect the degradation behavior.

Polyhydroxybutyrate (PHB) is a polymer of biological-origin[18,19] (produced by certain types of bacteria and fungi) that has been the subject of extensive research as a model system to understand crystallization kinetics[20] and enzymatic degradation[9,21]. PHB obtained from its natural source is known to have high stereo-regularity[22] and purity[23], which makes it susceptible to crystallization once it is extracted from microbial cells[19]. Its relatively low glass transition temperature (T_g, ~ 2°C) also allows for cold crystallization at room temperature[24]. These factors result in a high degree of crystallinity and a strong tendency towards the formation of large (up to 100's of μm) thermodynamically stable super-structures known as spherullites[25], which are composed of juxtaposed layers of ordered lamellar structures and randomly coiled

amorphous regions. In an unconstrained thick sample, spherulitic structures are formed without inhibition. However, when the sample is dimensionally constrained (as in the case of thin films), crystals tend to grow in a discontinuous fashion, resulting in lamellar structures that can be visualized as plate-like features on the polymer surface[26,27]. Such a constraint on the polymer leads to a host of microstructures and properties rarely observed in bulk PHB.

Studies on the crystallization behavior of spin-cast PHB films have shown that when film thickness decreases, both the crystalline structure and the degree of crystallinity are affected[11]. Both the slow crystallization rate and low degree of crystallinity observed for PHB films in these studies were attributed to two factors: (1) below certain values, the thickness of the polymer film was small when compared to the critical nucleus size, thus inhibiting the formation of stable nuclei, and (2) polymer chain mobility was reduced in thin samples, impeding the crystallization process[15].

PHB can be degraded by enzymes known as PHA depolymerases[28–32], and this degradation process is dependent on the structure and the properties of the polymer film[33]. In particular, the crystallinity of PHB is known to impact its enzymatic degradation behavior[34,35]. In previous work PHB samples with lower crystallinity were shown to undergo faster enzymatic degradation than highly crystalline samples[35].

Although many previous studies have characterized the crystallization kinetics of polymer thin films[11,16], the enzymatic degradation of dimensionally constrained polymer

films has not been systematically studied. One of the main factors that preclude the characterization of degradation in polymer thin films is the inability of existing characterization techniques – such as gravimetry and spectroscopy – to monitor the degradation of thin film samples with small masses. We have recently demonstrated a method to monitor the degradation of polymer thin films based on diffraction[36]. This method can qualitatively track the degradation of polymer thin films, allowing the effects of different processing conditions, film properties, or degradation environments on degradability to be discerned[36]. In this method (Figure 5.1), the surface of the polymer is patterned with microscopic grooves to form a grating. When this grating is illuminated with a laser, the light is diffracted and the intensity of the diffraction pattern can be monitored. As the polymer grating degrades, the intensity of the diffraction pattern decreases, and this change in the diffraction intensity can be used as a qualitative measure of the degradation rate. This diffraction-based degradation sensor affords the ability to characterize samples of extremely small mass and dimensions, including thin films, as long as consistent diffraction gratings can be patterned/replicated on the surface[36]. Here, we use this technique to determine the effect of reducing the film thickness (down to ~ 40 nm) on the degradation rate.

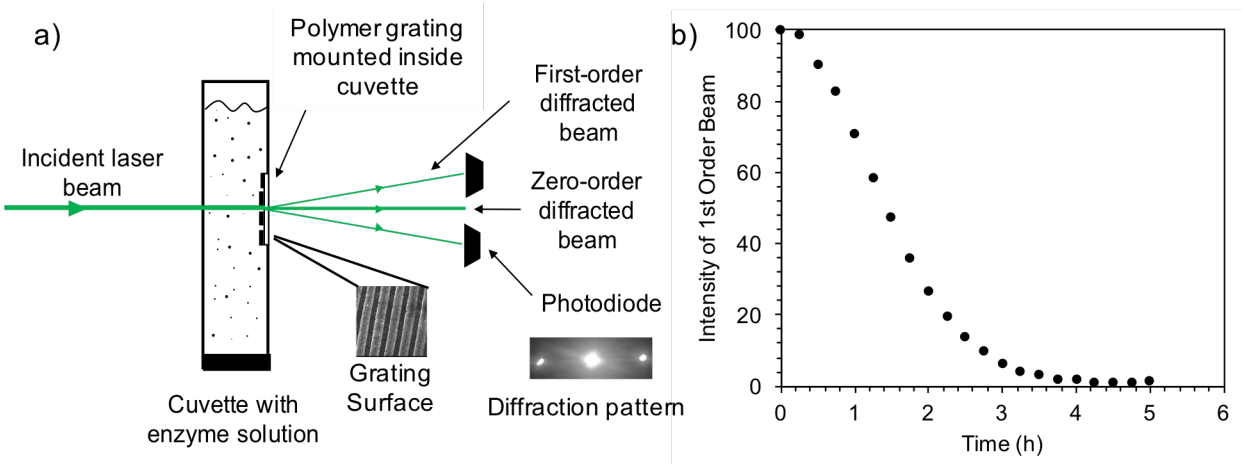

Figure 5.1 The diffraction-based degradation method. a) The schematic that shows the essential components of the degradation sensor, which includes a light source, degradation environment, polymer film patterned with diffraction grating and photodiodes to measure.

In this paper, we characterize the effect of dimensional constraints on the properties of PHB films and the resulting enzymatic degradation behavior. Samples of different thicknesses with gratings on their surface were prepared by solvent casting PHB from acetic acid on a polydimethylsiloxane (PDMS) grating. The physical properties of the samples were characterized by X-ray diffraction and atomic force microscopy (AFM). The enzymatic degradation of these samples was then measured using the diffraction-based technique described above. To produce nanoscale films constrained in two dimensions, PHB samples were prepared using μ-transfer molding, which resulted in a periodic array (center to center spacing of 2 μm) of PHB micro-rods with thickness of 40-50 nm. The properties of this sample were also characterized and compared with thicker PHB films.

5.3. Materials and Methods

The PHB (98%) used for the work was obtained as thermally processed pellets (BRS Bulk Bio-pellets, Bulk Reef Supply, Golden Valley, USA). The purity of as-received PHB was established to be 98% in our previous work[37]. The PHB pellets were washed with isopropyl alcohol and otherwise used as received. Acetic acid (99%) was obtained from Sigma-Aldrich, Canada. The PDMS (Sylgard 184, Dow Corning, Canada) with diffraction gratings on its surface was used as the substrate for solvent casting of PHB thin film. PDMS substrates were prepared by mixing part A and part B solutions in 1:10 ratio, as recommended by the supplier.

Fabrication of PHB thin films with gratings on surface

The PHB thin films were prepared by using acetic acid as solvent using an established protocol[37]. Briefly, PHB was dissolved in acetic acid (~0.05 g/ml) by boiling the solution (boiling point of 118ºC) in a sealed beaker for 40 minutes (while stirring) to create a homogenous solution. The solution was then diluted with acetic acid to the required concentration to prepare PHB films of different thicknesses. In this work, solution concentrations of 0.01, 0.001 and 0.0001 g/ml were used to prepare PHB films of thicknesses of 3 μm, 600 nm, and 150 nm, respectively.

A PDMS master mold with microscopic grooves on the surface with a periodicity of 2 μm, height of 120 nm, and fill factor of 50% was used as the substrate to prepare PHB films patterned with diffraction gratings suitable for the enzymatic degradation experiments. Approximately 0.3 ml of PHB acetic acid solution was poured and allowed

to dry on the PDMS substrate maintained at 140˚C. 30 seconds after the film was completely dry (as determined by visual observation), the substrate was removed from the hotplate and allowed to cool to room temperature. The PHB film was then transferred onto a glass slide and sectioned into 1-cm^2 samples. The samples were aged for 7 days before characterization and degradation studies.

Fabrication of PHB micro-rods by μ-transfer molding

The ultra-thin PHB micro-rods were prepared using a solvent assisted μ-transfer molding technique[38]. Approximately 0.3 ml of dilute PHB acetic acid solution (0.0001 g/ml) was poured on a PDMS substrate patterned with diffraction gratings. The substrate was then flipped onto a glass surface to allow the PHB solution to spread and fill the microchannels formed between subsequent peaks of the PDMS gratings and the glass surface. The filled sample was heated at 140˚C for 3 minutes to remove any excess solvent. Thus, micro-rods of PHB were formed on the glass surface after the removal of the PDMS mold. The samples were aged for 7 days before characterization and degradation studies.

Optical Microscopy

The superstructural features on the PHB surfaces were visualized using a Leica DM4 P microscope with cross polarizer filters. Cross-polarized images were obtained with a full wave λ plate to improve contrast between crystalline and amorphous regions. Solvent-cast PHB films of different thicknesses were placed in conformal contact with a glass slide and were imaged at magnifications of 200× and 400×. To facilitate the

visualization of the crystalline regions, PHB films of different thickness were prepared without diffraction gratings on the surface and imaged under cross-polarized microscopy.

X-ray diffraction (XRD)

The crystalline peaks of the various PHB thin films were determined using a Rigaku X-ray diffraction (XRD) system in glancing incidence angle mode. An Ultima VI goniometer fitted with a thin film attachment was used to characterize the samples. Scans were carried out between 5º and 40º at a rate of 2º/min using Cu Kα X-rays at 44 kV. An X-ray beam spot of 5 mm diameter was used for all scans. The samples were mounted on a glass slide to keep them as flat as possible. Baseline correction from the XRD pattern was carried out using the software Igor Pro 6.35A5.

Atomic Force Microscopy (AFM)

The surface morphology and the 2D cross-section of PHB thin film surfaces were determined using a Bruker Nano Dimension Edge AFM. It was operated in tapping mode using a tip with a spring constant of 40 N/m. The images were obtained over 20 μm × 20 μm areas for all samples and 2D cross-sectional profiles of PHB gratings were obtained using the NanoScope Analysis software.

Diffraction-Based Degradation Sensor

The enzymatic degradation of the PHB films of different thicknesses was carried out using a recently developed diffraction-based degradation sensor[36] (Figure 5.1). Briefly, the polymer film was patterned with a diffraction grating on its surface (as described in section 2.1). The film was mounted inside a plastic cuvette, with the surface of the grating in contact with the solution of PHA depolymerase enzyme maintained at a room temperature. A diode laser (λ = 650 ± 10 nm, power = 2.5-3 mW) was directed through the cuvette, passing through the diffraction grating at an angle of 90 degrees to the surface. A pair of photodiodes in reverse-biased configuration was placed at 10 ± 0.5 cm from the sample to collect the light from the first order diffraction spots. The entire sensor setup was maintained in complete darkness during the experiment to prevent interference from stray light. As the polymer degraded, the grooves comprising the grating became less defined, and the resulting diffraction efficiency decreased. The light source and the photodiode were controlled using a data acquisition system developed in-house based on the Arduino programming environment. The system was programmed to switch on the laser once every 15 minutes and to acquire 10 data points from each photodiode within 10 seconds. The average of these data points was reported as the diffracted beam intensity at this time point. At least 3 diffracted beam intensity measurements were used to construct the diffracted beam intensity curve. The intensity at each time point was normalized to the diffraction intensity at the beginning of the degradation reaction and plotted against degradation time, as was shown in Figure 5.1.b.

5.4. Results and Discussion

Appearance and Microstructure of PHB films

PHB films of different thicknesses (3 μm, 600 nm, and 150 nm) were solvent cast on flat glass substrates from solutions at different concentrations and the microstructural variations were characterized using optical microscopy. Visually, all the films were observed to be homogeneous and translucent, with uniform, planar surfaces.

Figure 5.2 shows the microscopic features of the three different thicknesses of flat PHB thin films (without diffraction gratings) as imaged by optical microscopy. A cross-polarizer with retarder plate was used to improve contrast between the crystalline and amorphous regions of the polymer samples, wherein the blue regions correspond to ordered regions and the yellow regions to amorphous regions. Despite a similar macroscopic appearance, the microstructure and the crystallization conditions can be drastically different depending on the thickness of the film. From Figure 5.2.a, we can observe that the thicker film consists of randomly oriented, crystalline structures throughout the sample, which are commonly observed in bulk PHB samples where dimensional constraints do not play a dominant role in crystal nucleation and growth. Further reduction in the thickness of the polymer film (Figure 5.2.b and 2.c) resulted in more anisotropic structures, since three-dimensional crystalline structures (such as spherulites) become kinetically unfavorable under constrained conditions. Overall, the random distribution and extent of ordered structures were found to decrease as the film thickness was decreased. The 150-nm film (Figure 5.2.c) has a relatively feature-less surface with very few crystalline regions (blue) visible. This reduction in the relative

abundance of crystalline structure has been shown to arise from the limitation on the polymer chain mobility imparted by the dimensional constraint[17]. Previous works have confirmed these observations, where the crystalline regions become more anisotropic as thickness decreases[9,39–41].

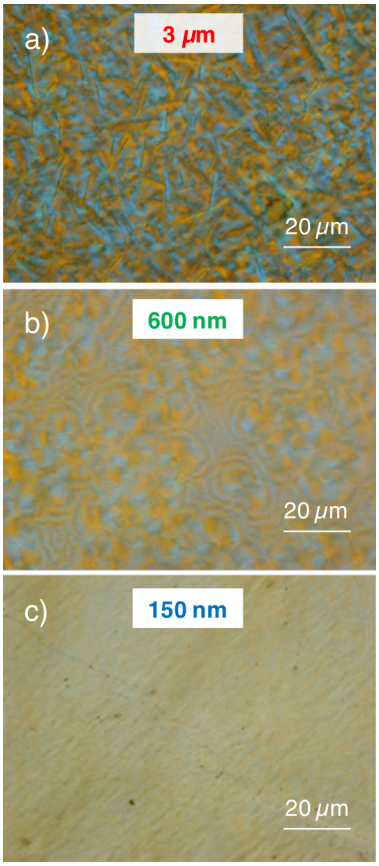

Figure 5.2 Cross-polarized microscopy images of samples of different thicknesses: a) 3 μm, b) 600 nm, and c) 150 nm.

Crystallinity and Crystal Anisotropy

The crystalline state of the polymer thin film is very important since the nature and quantity of the ordered structures play dominant roles in macroscopic properties such as degradation behavior. In this work, crystallinity and crystal anisotropy of the PHB films were characterized using thin film glancing angle X-ray diffraction (XRD) analysis.

Figure 5.3.a shows XRD patterns of PHB films of various thicknesses with gratings on their surface. The XRD patterns show a general trend where decreasing sample thickness results in the loss of certain peaks corresponding to the orthorhombic crystal planes of PHB, namely the (110) and (111) that are associated with the edge-on crystal planes. This result indicates that the crystal growth tends to be more anisotropic for dimensionally constrained (i.e. thinner films), where the crystals are forced to grow more preferentially in the plane of the polymer film direction (*i.e.* flat-on crystals result). These results agree well with a previous study investigating the crystallinity of spin-cast PHB thin films which showed that crystal anisotropy is greatly influenced by dimensional constraints, with thinner films exhibiting more anisotropy[42]. In addition, the inference from XRD patterns are consistent with the general conclusions drawn based on optical microscopy.

Figure 5.3.b shows that overall percentage crystallinity (%C), as calculated from XRD patterns. The crystallinity was found to be lower for smaller thicknesses. These results are consistent with previous studies which have shown that crystallinity decreases when the film thickness is reduced[42]. To enable optical monitoring of degradation, the surface of the polymer must be patterned with a diffraction grating. To verify that the crystallization behavior is not impacted by the formation of the diffraction gratings on the PHB surface, we also collected XRD patterns for PHB films of similar thickness without gratings (Figure 5.3.c). No significant difference was observed between films of similar thickness with gratings on the surface and without; all of the same peaks are visible with a similar pattern. Overall, the XRD patterns show that the crystallinity decreases and the crystal anisotropy increases, as PHB film thickness is reduced.

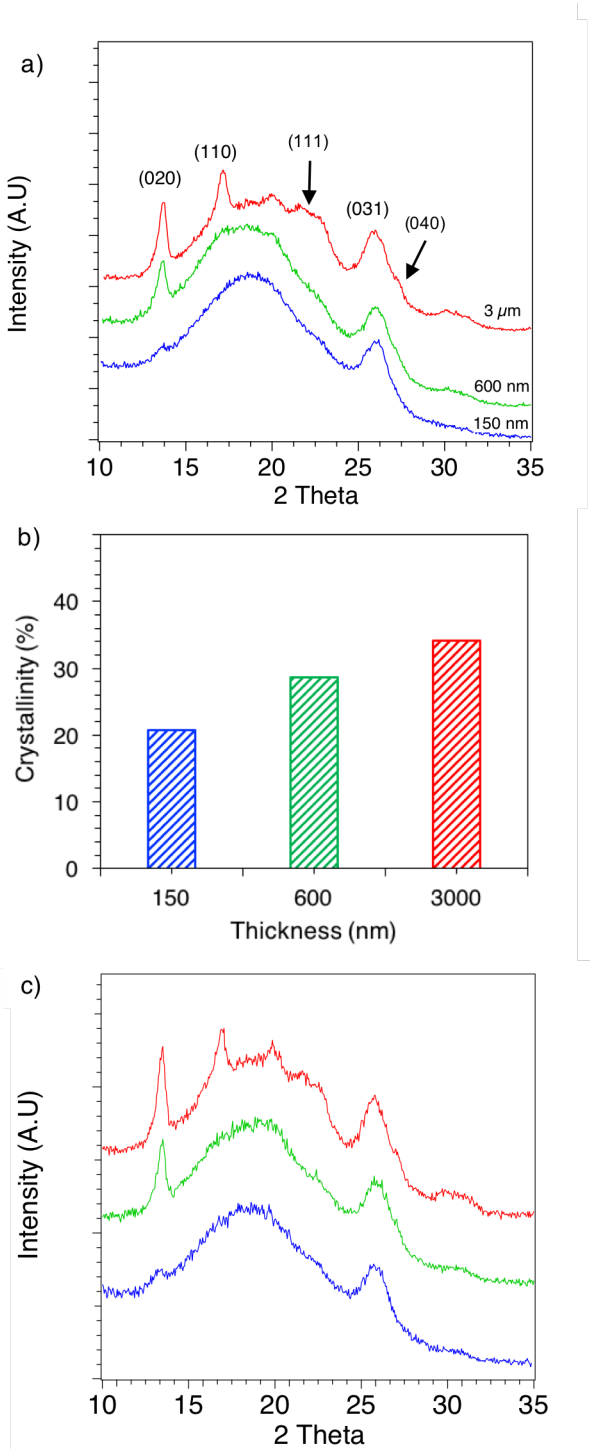

Figure 5.3 Crystalline state of the PHB thin films. a) Combined plot of XRD patterns for PHB films of different thicknesses. b) Percent crystallinity vs. film thickness calculated from XRD patterns. c) XRD pattern of PHB films without gratings patterned on their surface.

Surface Structure and Uniformity

The surface topography and the uniformity of the PHB films patterned with diffraction gratings on their surface were characterized over areas of 20 μm^2 (Figure 5.4.a) and 3 μm^2 (Figure 5.4.b) using AFM. The low magnification AFM of the PHB films show the uniform micro-grooves of the diffraction gratings formed by the replica molding process. For each case, the thickness of the grooves (120 nm) is less than the overall thickness of the sample (3 μm, 600 nm, and 150 nm). The pattern on the PHB surface was found to be identical irrespective of the overall film thickness, indicating that the thickness does not affect the replication of the diffraction gratings. The high magnification AFM images (Figure 5.4.b) show the presence of fine lamellar structures in the thick PHB films. While the thin films also contain some lamella on the surface, the relative abundance was found to decrease considerably as the film thickness decreased. These observations support the XRD results (Figure 5.3.b) indicating that the tendency to form crystalline structures decreases with reduced film thickness. Figure 5.3.c shows the phase mode AFM profiles of the different films. The images were obtained over the same area on which the height mode images were captured. The phase mode images illustrate line-like structures arranged with 8-10 nm spacing, corresponding to the lamellar layers present in the PHB crystals. The AFM images of the thickest sample (3μm, Figure 5.4.c, first column) also show the S-shaped bending profile typical of unconstrained crystal growth. Such surface features (repeating structures of the lamellae and S-shape beading patterns) become less apparent in the thinner films (second and third columns). In addition, the 150-nm thick films have a relatively smooth, featureless surface, with a few regions showing flat structures with an

average step height of ~ 10 nm (comparable to the dimension of the c-axis of the orthogonal PHB crystal). This indicates that the long-axis of the lamella is oriented parallel to the direction of the film (flat-on crystal). These observations are in agreement with the inferences made from the XRD patterns (Figure 5.3.a) which point towards the emergence of crystal anisotropy (favoring flat-on orientation) as the film thickness decreases.

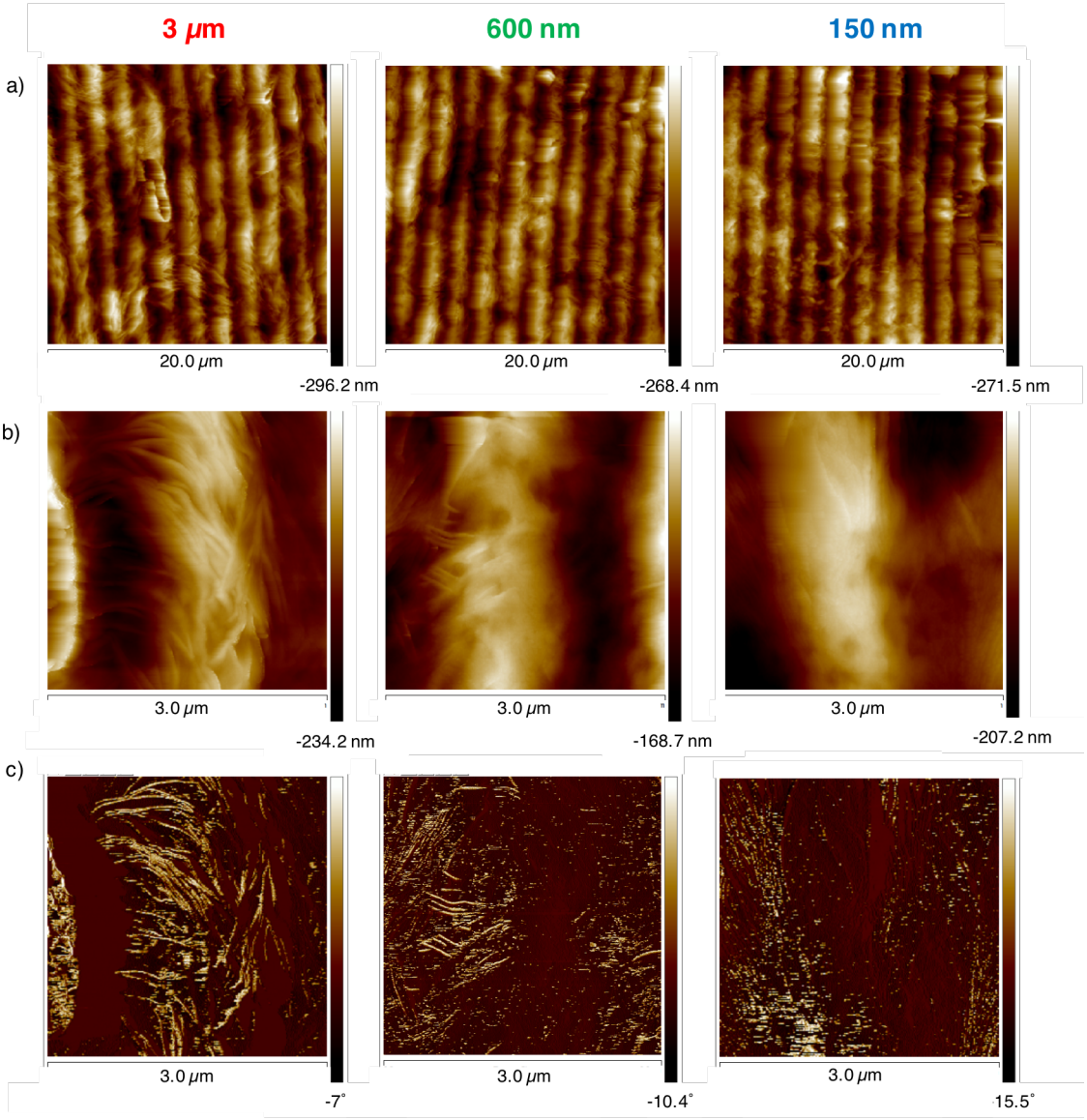

Figure 5.4 Surface profile of the PHB thin films. a) AFM surface profiles (20 μm2) of the PHB films patterned with diffraction gratings on their surfaces. b) High magnification (3 μm2) AFM profiles show the presence of crystalline lamella on the surface. c) 2D cross-sectional profiles of PHB films showing the repeating pattern concomitant with edge-on lamellar orientation in thick films and flat-on orientation in the thin films.

Enzymatic Degradation Behavior

The enzymatic degradation of PHB thin films of different thicknesses was characterized using the diffraction-based method previously developed[36]. Figure 5.5 shows a plot of the change in normalized diffraction intensity with respect to time for PHB films with surface gratings immersed in a solution containing the enzyme $PhaZ_{Cte}$. For each film, the intensity of the diffraction pattern decreases over time, due to the gradual erosion of the diffraction grating that occurs during degradation[36]. The initial thickness of the diffraction grating was the same for each film (120 nm), and the time required for the relative intensity to go from 100% to 0% is dependent on the rate at which the diffraction grating degrades from 120 nm to a few nm – at which point the intensity of first order diffracted beams is no longer observable. Considering a laser spot size of 2 mm^2 (which was used in this work) and surface density of 1.13 g/cm^3, this corresponds to a total change in mass of ~ 1 x 10^{-6} g. Thus, the rate of change of diffraction intensity provides a representation of the degradation rate. From the plot of Figure 5.5.b, we can observe that the diffracted beam intensity decreases consistently for all the thin film samples. Further, the rate of change in intensity was found to negatively correlate with the overall thickness of the PHB film, with the thicker film degrading at the slowest rate. The increasing degradation rate with decreasing film thickness (and consequent decrease in crystallinity) confirms expectations based on previous work that demonstrated that the degradation rate has an inverse relationship with crystallinity[15]. However, unusual degradation behavior may arise when the PHB thin film is constrained down to the nanoscale.

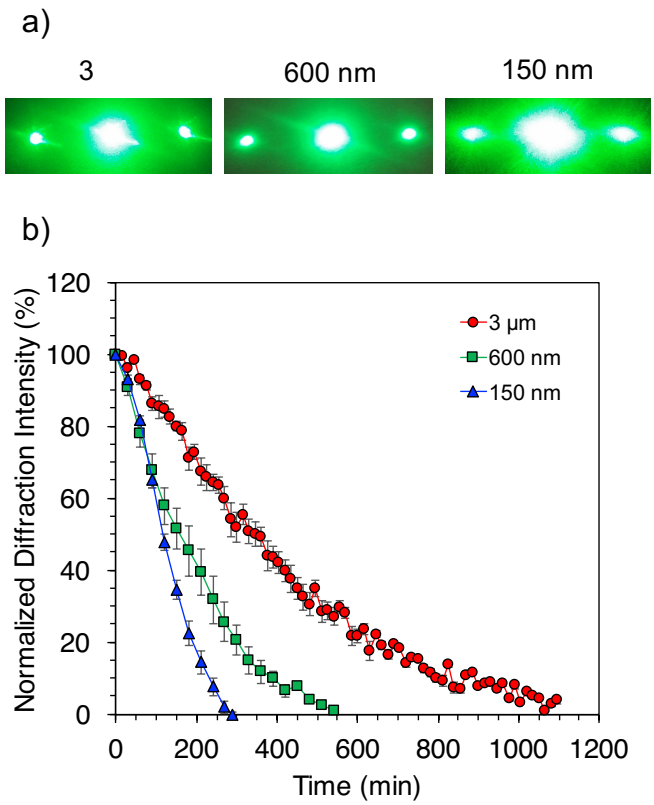

Figure 5.5 Degradation behavior of the PHB films. a) Initial diffraction patterns of PHB films of different thicknesses, and b) Normalized diffraction intensity vs. time plot obtained by exposing the PHB thin films of different thickness to a PhaZcte enzyme solution.

PHB Ultra-Thin Film Constrained to Nanoscale

It has been shown that when the thickness of a polymer sample is constrained below the critical value required for the formation of thermodynamically stable nuclei, crystallinity can be completely suppressed[15]. While this has interesting implications for the properties of PHB, monitoring the degradation behavior of such thin samples is challenging using traditional techniques. To the best of our knowledge, no previous work has characterized the degradation behavior of nanoscale polymer films. To

evaluate the effect of nanoscale constraint on enzymatic degradability, we used solvent casting and μ-transfer molding to produce periodic μ-rods of PHB, which, while being highly constrained in two dimensions, can still produce a consistent diffraction pattern. This enables us to use the diffraction method to characterize the degradation behavior of the PHB nanostructure in a holistic manner. Figure 5.6.a and 6.b shows the AFM image and cross-sectional profile of the PHB nanostructures fabricated by μ-transfer molding. These images show that the surface consists of microscopic lines of PHB (40-50 nm in height) with a periodicity of 2 μm.

The crystalline state of the μ-transfer molded PHB is a critical factor influencing its degradation behavior. Figure 5.6.c shows the XRD pattern obtained for the μ-transfer molded PHB surface. which only shows a broad, amorphous halo and no crystalline peaks, indicating the absence of crystalline structures. The complete absence of crystalline regions in the sample can influence the enzymatic attachment process – which usually takes place in the crystalline regions of the polymer while hydrolysis takes place in the amorphous regions – and result in unexpected degradation properties. The PHB micro-rods were exposed to enzyme solutions and the diffraction intensity was monitored to determine their degradation behavior. Figure 5.6.d and 6.e show the surface profile of μ-transfer molded PHB before and after 4 hours of exposure to the enzyme solution. The surface structure of the 150 nm thick PHB films before and after 4 hours of degradation is depicted in Figure 5.6.f and 6.g. Surprisingly, the μ-transfer molded PHB did not exhibit visible degradation after 4 hours, whereas the 150-nm thick film showed substantial degradation over the same time period. The minimal variation

on the μ-transfer molded PHB surface after 4 hours of exposure to the enzyme solution is in total contrast to the appearance of the 150-nm sample, which experienced considerable surface erosion over the same period of time. The respective diffraction intensity vs time relationships are shown in Figure 5.6.h. It can be observed that the diffraction intensity essentially stays constant over 4 hours for the μ-transfer molded PHB. These results show that the μ-transfer molded PHB, containing no crystalline structure, does not have short term susceptibility to enzymatic degradation by $PhaZ_{Cte}$.

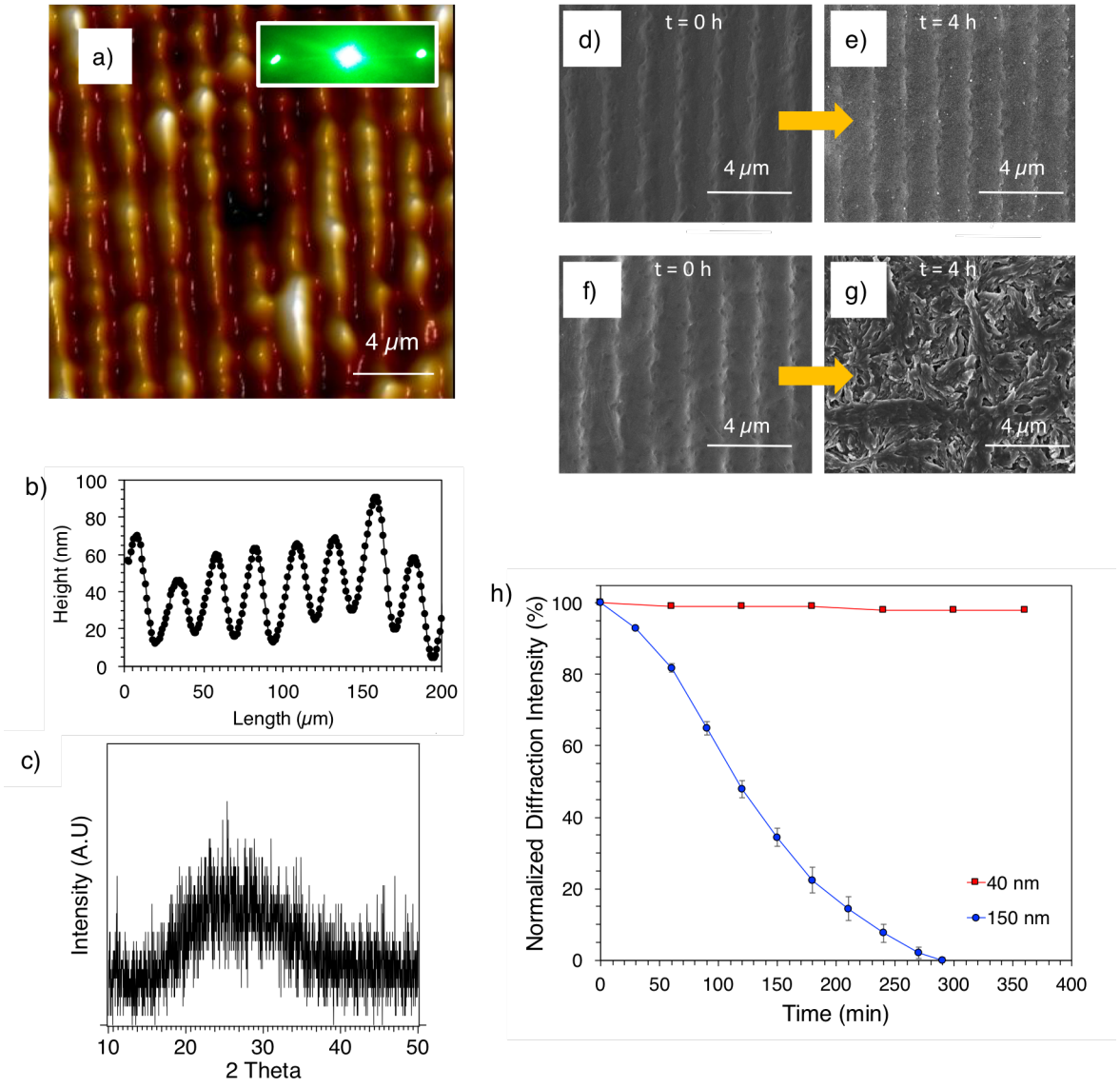

Figure 5.6 Appearance and properties of PHB ultra-thin films prepared by μ-transfer molding on a glass substrate. a) Surface topography obtained by AFM. Inset shows the corresponding diffraction pattern of the ultra-thin PHB sample; b) 2D cross-sectional profile of the PHB surface; c) XRD pattern of the ultra-thin PHB film; d) the surface of μ-transfer molded PHB film at the start of degradation; e) the surface after 4 hours; f) the surface profile of 150-nm thick PHB film at the start of degradation; g) the surface after 4 hours of degradation; h) the plot comparing change in diffraction intensity of the μ-transfer molded film and the 150-nm thick film.

Such resistance to enzymatic degradation has been found in previous studies for synthetic, atactic PHB which is intrinsically amorphous and is incapable of crystallizing[43,44]. The observations in the present work involve PHB which can crystallize readily in unconstrained states. To the best of our knowledge, this is the first study in which a crystallizable form of PHB has been constrained sufficiently to preclude crystallization and enzymatic degradation. No other previous study has studied the degradation of such heavily constrained PHB samples.

This resistance to enzymatic degradation of nanoscale PHB can be explained based on the mechanism of the enzymatic degradation process. The enzymatic degradation is a two-step process involving: 1) attachment of the enzyme to the polymer surface by the binding domain and 2) hydrolysis of the polymer chain in amorphous regions by the catalytic domain. The degradation cannot proceed with high specificity and at an elevated rate without the binding step[45], which is where the nanoscale constraint on the PHB ultra-thin film intervenes. Typically, the binding domain of the enzyme can attach to PHB only in the presence of a stable, repeating molecular arrangement (such as the crystalline regions of the polymer)[43]. The absence of crystal structures in a μ-transfer molded PHB film makes it a challenge for the enzymes to bind to the polymer surface, which is an important first step in the degradation process. Therefore, the high specificity and increased degradation rate afforded by the enzymatic binding process is impeded. In addition, the crystalline domains can act as pinning agents for the amorphous polymer chains and can increase the probability of enzyme attachment, which facilitates the degradation process[19]. It is well understood from

previous work that polymer chain dynamics and glass transition temperature can experience a sudden transformation if the polymer is constrained to be completely amorphous[46]. This phenomenon can cause the degradation behavior to follow a discontinuous trend as the PHB film thickness is decreased to the nanoscale.

These results highlight how dimensional constraints afford the ability to control and tune the biodegradation rate of the polymer depending on the application and material requirements.

5.5. Conclusion

As polymer thin films have become more technologically important, the interest in studying and characterizing their degradation and stability has increased significantly. PHB, with its unique set of properties such as biodegradability, near-ideal crystallization behavior, and bio-sustainability, is an extremely relevant material to study under different dimensionally constrained states. Studying the effect of dimensional constraints on a fundamental property — namely, enzymatic degradation behavior — is of great relevance from both a fundamental and application point of view. This work characterized the degradation behavior of PHB films with thickness ranging from 40 nm to 3 μm. The studies showed that the degradation behavior of the PHB film could be influenced and tuned by altering dimensional constraints. Further, these results show how PHB becomes resistant to enzymatic attack when the constraints are high enough to preclude crystallization. The properties explored in this work can be utilized to create

PHB-based systems that have a controllable set of degradation behavior and properties, by changing the physical dimensions of the polymer film.

Acknowledgements

Funding from Alberta Agriculture and Forestry and the Natural Sciences and Engineering Council of Canada (NSERC) is gratefully acknowledged. The authors thank Diana Martínez-Tobón for supplying the enzymes for testing.

Author Contributions

P.A designed and performed the experiments. A.L.E. and D.S. supervised the work, and contributed to designing the research and to writing the manuscripts.

5.6. References

1. Berggren, M. & Richter-Dahlfors, A. Organic bioelectronics. *Adv. Mater.* **19,** 3201–3213 (2007).
2. Kaltenbrunner, M. *et al.* An ultra-lightweight design for imperceptible plastic electronics. *Nature* **499,** 458–63 (2013).
3. Rogers, J. A., Someya, T. & Huang, Y. Materials and mechanics for stretchable electronics. *Science* **327,** 1603–7 (2010).
4. Kim, D.-H. *et al.* Dissolvable films of silk fibroin for ultrathin conformal bio-integrated electronics. *Nat. Mater.* **9,** 511–7 (2010).
5. Tao, H. *et al.* Silk-based conformal, adhesive, edible food sensors. *Adv. Mater.* **24,** 1067–72 (2012).

6. Knoll, W. & Advincula, R. C. *Functional Polymer Films*. *Functional Polymer Films* **1–2,** (Wiley-VCH, 2011).
7. Zelikin, A. N. Drug Releasing Polymer Thin Films new Era of Surface-Mediated Drug Delivery. *ACS Nano* **4,** 2494–2509 (2010).
8. Williams, P. M. Degradation of a Thin Polymer Film Studied by Simultaneous in situ Atomic Force Microscopy and Surface Plasmon Resonance Analysis. *Drug Deliv.* (1995).
9. Khasanah *et al.* Evolution of Intermediate and Highly Ordered Crystalline States under Spatial Confinement in Poly(3-hydroxybutyrate) Ultrathin Films. (2016).
10. Dai, X. *et al.* A grazing incident XRD study on the structure of poly(3-hydroxybutyrate) ultrathin films sandwiched between Si wafers and amorphous polymers. *Polym. Chem.* **7,** 3705–3713 (2016).
11. Capitán, M. J., Rueda, D. R. & Ezquerra, T. a. Inhibition of the crystallization in nanofilms of poly(3-hydroxybutyrate). *Macromolecules* **37,** 5653–5659 (2004).
12. Kecskemeti, G. *et al.* Pulsed laser deposition of polyhydroxybutyrate biodegradable polymer thin films using ArF excimer laser. *Appl. Surf. Sci.* **253,** 1185–1189 (2006).
13. Khasanah *et al.* Evolution of Intermediate and Highly Ordered Crystalline States under Spatial Confinement in Poly(3-hydroxybutyrate) Ultrathin Films. *Macromolecules* acs.macromol.6b00431 (2016). doi:10.1021/acs.macromol.6b00431
14. Sun, X. *et al.* Crystal Morphology of Poly(3-hydroxybutyrate) on Amorphous Poly(vinylphenol) Substrate. (2016).

15. Frank, C. W. *et al.* Structure in Thin and Ultrathin Spin-Cast Polymer Films. *Science (80-.).* **273,** 912–915 (1996).

16. Napolitano, S.; Wübbenhorst, N. Deviation from bulk behaviour in the cold crystallization kinetics of ultrathin films of poly(3-hydroxybutyrate). *J. Phys. Condens. Matter* **19,** 205121 (2007).

17. Wang, M., Braun, H., Meyer, E. & Zhu, J. Morphogenesis and Chain Behaviors Related to Crystallization in Ultrathin Polymer Films ∗. 1–11

18. Chen, G.-Q. A microbial polyhydroxyalkanoates (PHA) based bio- and materials industry. *Chem. Soc. Rev.* **38,** 2434–46 (2009).

19. Orts, W. & Nobes, G. Poly (hydroxyalkanoates): biorefinery polymers with a whole range of applications. The work of Robert H. Marchessault. *Can. J. …* **86,** 628–640 (2008).

20. Tomasi, G. & Scandola, M. X-Ray investigation on melt-crystallized bacterial. **0,** 71–80 (1997).

21. Khasanah *et al.* Evolution of Intermediate and Highly Ordered Crystalline States under Spatial Confinement in Poly(3-hydroxybutyrate) Ultrathin Films. *Macromolecules* acs.macromol.6b00431 (2016). doi:10.1021/acs.macromol.6b00431

22. Yu, J., Plackett, D. & Chen, L. X. L. Kinetics and mechanism of the monomeric products from abiotic hydrolysis of poly [(R) -3-hydroxybutyrate] under acidic and alkaline conditions. **89,** (2005).

23. Barham, P. J. & Keller, A. The Relationship between Microstructure and Mode of Fracture in Polyhydroxybutyrate. **24,** 69–77 (1986).

24. Gunaratne, L. M. W. K., Shanks, R. a. & Amarasinghe, G. Thermal history effects on crystallisation and melting of poly(3-hydroxybutyrate). *Thermochim. Acta* **423,** 127–135 (2004).

25. Kumagai, Y. films. **57,** 53–57 (1992).

26. Crist, B. in *Handbook of Polymer Crystallization* 73–124 (John Wiley & Sons, Inc., 2013). doi:10.1002/9781118541838.ch3

27. Müller, A. J., Arnal, M. L. & Lorenzo, A. T. in *Handbook of Polymer Crystallization* 347–378 (John Wiley & Sons, Inc., 2013). doi:10.1002/9781118541838.ch12

28. Hiraishi, T. *et al.* Degradation and adsorption characteristics of PHB depolymerase as revealed by kinetics of mutant enzymes with amino acid substitution in substrate-binding domain. *Biomacromolecules* **11,** 113–119 (2010).

29. Iwata, T. *et al.* Enzymatic Degradation and Adsorption on Poly[(R)-3-hydroxybutyrate] Single Crystals with Two Types of Extracellular PHB Depolymerases from Comamonas acidovorans YM1609 and Alcaligenes faecalis T1. *Macromolecules* **30,** 5290–5296 (1997).

30. Kasuya, K., Inoue, Y., Yamada, K. & Doi, Y. Kinetics of surface hydrolysis of poly[(R)-3-hydroxybutyrate] film by PHB depolymerase from Alcaligenes faecalis T1. *Polym. Degrad. Stab.* **48,** 167–174 (1995).

31. Iwata, T. *et al.* Enzymatic Degradation and Adsorption on Poly[(R)-3-hydroxybutyrate] Single Crystals with Two Types of Extracellular PHB Depolymerases from Comamonas acidovorans YM1609 and Alcaligenes faecalis T1. *Macromolecules* **30,** 5290–5296 (1997).

32. Iwata, T., Doi, Y., Kasuya, K. & Inoue, Y. Visualization of Enzymatic Degradation

of Poly[(R)-3-hydroxybutyrate] Single Crystals by an Extracellular PHB Depolymerase,Ä†. *Macromolecules* **30,** 833–839 (1997).

33. Abe, H. *et al.* Microscopic visualization on crystalline morphologies of thin films for poly [(R) -3-hydroxybutyric acid] and its copolymer. **41,** 867–874 (2000).
34. Mochizuki, M. *et al.* Structural Effects upon Enzymatic Hydrolysis of Poly(butylene succinate-co-ethylene succinate)s. *Macromolecules* **30,** 7403–7407 (1997).
35. Kumagai, Y., Kanesawa, Y. & Doi, Y. Enzymatic degradation of microbial poly(3-hydroxybutyrate) films. *Die Makromol. Chemie* **193,** 53–57 (1992).
36. Anbukarasu, P., Martínez-Tobón, D. I., Sauvageau, D. & Elias, A. L. A diffraction-based degradation sensor for polymer thin films. *Polym. Degrad. Stab.* (2017). doi:10.1016/j.polymdegradstab.2017.05.020
37. Anbukarasu, P., Sauvageau, D. & Elias, A. Tuning the properties of polyhydroxybutyrate films using acetic acid via solvent casting. *Sci. Rep.* **5,** 17884 (2015).
38. Xia, Y. & Whitesides, G. M. Soft Lithography. *Annu. Rev. Mater. Sci.* **28,** 153–184 (1998).
39. Liu, Y. X. & Chen, E. Q. Polymer crystallization of ultrathin films on solid substrates. *Coordination Chemistry Reviews* (2010). doi:10.1016/j.ccr.2010.02.017
40. Y. Wang, † *et al.* Crystallization in the Thin and Ultrathin Films of Poly(ethylene−vinyl acetate) and Linear Low-Density Polyethylene. (2004).
41. Kossack, W., Seidlitz, A., Thurn-Albrecht, T. & Kremer, F. Interface and Confinement Induced Order and Orientation in Thin Films of Poly(ϵ-caprolactone).

(2016).

42. Napolitano, S. & Wübbenhorst, M. Slowing Down of the Crystallization Kinetics in Ultrathin Polymer Films: A Size or an Interface Effect? *Macromolecules* **39,** 5967–5970 (2006).

43. He, Y., Shuai, X., Kasuya, K. I., Doi, Y. & Inoue, Y. Enzymatic degradation of atactic poly(R,S-3-hydroxybutyrate) induced by amorphous polymers and the enzymatic degradation temperature window of an amorphous polymer system. *Biomacromolecules* **2,** 1045–1051 (2001).

44. Abe, H., Matsubara, I., Doi, Y., Hori, Y. & Yamaguchi, A. Physical Properties and Enzymic Degradability of Poly(3-hydroxybutyrate) Stereoisomers with Different Stereoregularities. *Macromolecules* **27,** 6018–6025 (1994).

45. Sanjay Kumar Sharma, Ackmez Mudhoo, J. H. C. in *A Handbook of Applied Biopolymer Technology: Synthesis, Degradation and Applications* 322 (Royal Society of Chemistry, 2011).

46. Forrest, J. A. & Dalnoki-Veress, K. The glass transition in thin polymer films. *Adv. Colloid Interface Sci.* **94,** 167–195 (2001).

6. Time-temperature indicator based on enzymatic degradation of dye-loaded

This manuscript proposes a time-temperature indicator based on the degradation of a dye-loaded PHB film (as developed and characterized in Chapters 3 thru 5), which can be used to determine the change in quality of food products in the supply chain. The kinetic parameters of the TTI device were determined by observing the rate of release of the dye from the PHB matrix due to enzymatic degradation. The article is the first instance of a TTI being developed based on a dye-loaded polymer that can easily be produced roll-to-roll, enabling the possibility of a commercially viable TTI, that is also kinetically accurate. Further, the kinetic parameters were found to be in line with the decay kinetics of some fresh meat and dairy products which indicate the potential for the proposed TTI for monitoring a range of fresh food products.

The article has been published in *Biotechnology Journal* under the title, **"Time-temperature indicator based on enzymatic degradation of dye-loaded polyhydroxybutyrate".** The contents are reproduced here in accordance with the author's rights and copyright policies of the publisher, Wiley, and Biotechnology Journal.

Time-Temperature Indicator Based on Enzymatic Degradation Of Dye-Loaded Polyhydroxybutyrate

Preetam Anbukarasu, Dominic Sauvageau, Anastasia Elias*

Department of Chemical and Materials Engineering, University of Alberta, Edmonton, Alberta, Canada.

6.1. Abstract

We describe an enzyme activated time-temperature indicator (TTI) which produces a direct colour change concomitant to variations in integrated time and temperature conditions. This direct colour change is realised by degrading a dye-loaded polyhydroxybutyrate (PHB) film by a depolymerase enzyme. The degradation of the PHB film by the enzyme causes the release of the dye in solution, which in turn undergoes an optical transition from clear to coloured with elapsing time. Macroscopic and microscopic optical observations confirmed the uniform distribution of the dye in the PHB film. The dye release kinetics, mediated by the enzymatic reaction, were tested at different temperatures ranging from 4°C to 37°C, and were used to determine the suitability of a dye-loaded PHB as a time-temperature indicator for fresh food products based on kinetic parameters previously reported. The kinetic analysis showed that the activation energy of the dye release process was 74 kJ/mol, and that, at 37°C, the dye would be totally released within 6 hours. However, when incubated at 4°C, the TTI requires in the range of 168 hours (7 days) to release all the dye. These kinetics values highlight the potential of the TTI for monitoring fresh food products that have optimum shelf life around 4°C.

6.2. Introduction

Time and temperature are primary factors that affect the shelf-life of perishable products such as meat [1–3], dairy [4] and vegetables [5–8]. Time-temperature indicators (TTI) are devices that can monitor the integrated effects of time and temperature and produce a measurable response, which makes them useful for quality and shelf-life assessment of such products [9–11]. Ideally, the relationship between this response and the degradation of the product monitored should be directly proportional.

Several TTIs for food product monitoring can be found both in the literature and as commercial products. These TTIs can be classified based on the mechanism used to measure the effects of time and temperature: this includes bio-chemical TTIs (microbial [12,13] & enzymatic [14–16]), and physico-chemical TTIs (diffusion-based TTIs [17–19], polymerization reaction, thermochromic reaction, etc.) [20–22]. Among these, bio-chemical TTIs have the most suitable kinetics for monitoring fresh food products, since both bacterial and enzymatic activity are good markers of microbial growth, food degradation processes, and, thus, of the resulting loss in quality. The literature shows interesting implementations of bacterial TTIs [12,13,23], where a bacterial culture is grown inside the TTI, and the changes in the pH/chemical composition are used to indicate the loss of quality. However, bacterial TTIs have practical difficulties in manufacturing, handling and safety that make them unsuitable for food products. Enzymatic TTIs, in contrast, have most of the advantages of microbial systems while being more robust and easier to implement in a compact package. Consequently, some enzymatic TTIs have been developed and commercialised, such as VITSAB Smart TTI seafood label [9], i-Point and

the Bio-Medical Sciences Inc. TTI [24]. Enzymatic TTIs are also described in the literature. Ramstad *et al.* developed one of the first enzymatic TTIs in which an oxidizing enzyme was used to degrade a phenolic compound [14]. Yan *et al.* have proposed a urease-based TTI [25], while Yan *et al.* have developed an amylase-based TTI [16]. Wu *et al.* have used lipase to break down glyceryl tributyrate, and visualised the degradation using a pH strip that changed colour as the enzyme solution became more acidic due to the release of degradation products [26]. In this approach, it can be challenging to determine the useful life left in the product since the pH strip changes colour drastically when the acidity of the solution exceeds a threshold. Further, the use of additional components (pH strip and barrier materials) in the TTI increases the manufacturing cost and complexity of the device.

In this work, we describe an enzymatic TTI that undergoes a colourimetric change based on the degradation of polyhydroxybutyrate (PHB) by a PHB depolymerase enzyme (from *Comamonas testosteroni*), $PhaZ_{Cte}$. PHB is a thermoplastic, biodegradable polymer of bacterial origin, which can be processed into uniform films by both thermal and solvent-assisted processing [26–30]. PHB is inexpensive, chemically resistant to most solvents, and can be degraded by a wide array of PHB depolymerase enzymes [28,29], suggesting that it could be useful for TTI applications. The hydrolysis reactions catalyzed by PHB depolymerases are known to have activation energies in the range of 70 to 85 kJ/mol [31,32]. Since these values are in the vicinity of the activation energies of the degradation processes of perishable products such as fresh

meats, some vegetables and dairy products [33], PHA depolymerases are good candidates to monitor their loss in quality.

The TTI presented herein is comprised of a dye-loaded PHB film exposed to an enzyme solution, which *directly* undergoes a change in colour upon exposure to an enzyme solution. The degradation of the polymer releases dye into the solution, causing its colour to change gradually from clear to coloured at a rate determined by the temporal and thermal exposure history of the device. Figure 6.1.a shows a schematic of the enzymatic degradation of dye-loaded PHB film which results in blue coloration of the enzyme solution with progressing time. A conception of the TTI device suitable for deployment in commercial products is also shown in Figure 6.1.b. Figure 6.1.c shows the photographs of a prototype device.

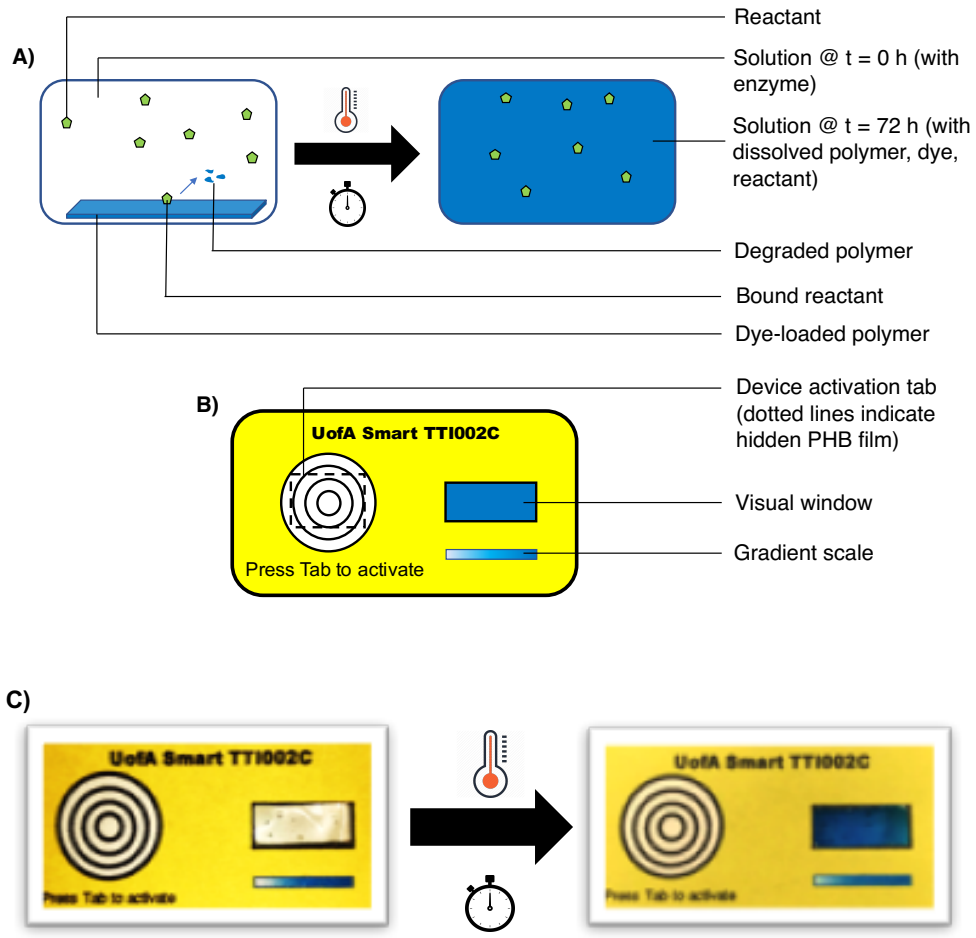

Figure 6.1 Schematic showing the enzymatic degradation of the dye-loaded PHB film and its applications as a time-temperature indicator. A) The process of enzymatic degradation and change in color of the enzyme solution which is related to the temporal and thermal exposure history. B) Schematic conception of a TTI device. The device can be activated by pressing the tab which brings the PHB film in contact with the enzyme solution. The change in color of the solution can be observed through the visual window and the gradient scale can be used to estimate the remaining shelf life of the product. C) Photographs of a simple prototype TTI based on the enzymatic degradation of dye-loaded PHB. With passing time, the display window shows more intense blue colours, which is concomitant with the time and temperature conditions experienced by the product that is monitored.

In this study, we investigated the preparation and characterization of the dye-loaded PHB film from which the dye is released, and its enzymatic degradation behaviour. The degradation experiments performed with the dye-loaded PHB were carried at temperatures ranging from 4°C to 37°C to determine the dye release rate and activation energy of degradation. From these results, the suitability of using the dye-loaded PHB, degraded by the enzymatic solution for monitoring the shelf-life and loss of quality of food products was evaluated.

6.3. Materials and Method

The PHB (M_n ~ 79,000 ± 1230, as determined by gel permeation chromatography) used for the work was obtained as thermally processed pellets (BRS Bulk Bio-pellets, Bulk Reef Supply, Golden Valley, USA). The purity of as-received PHB was established to be 98% in our previous work [34]. The PHB pellets were washed with isopropyl alcohol and otherwise used as received. Acetic acid (99%) was obtained from Sigma-Aldrich, Canada.

The blue dye (Brilliant Blue FCF) was obtained from Sigma Aldrich (Canada, product no. 80717-100MG) and mixed with deionized water (3.3 mg/ml) to form a homogenous solution, and used to prepare the dye-loaded PHB films. Polydimethylsiloxane (PDMS) (Sylgard 184, Dow Corning, Canada) was used to prepare the substrate for solvent casting the PHB thin film. The PDMS substrate was prepared by mixing part A and part B in a 1:10 ratio, as recommended by the supplier.

Preparation of dye-loaded PHB film

The PHB pellets were dissolved in boiling acetic acid (boiling point of 118°C) on a hot plate while stirring, as described in our previous work [34]. The solution was then diluted down to a concentration of 0.005 g of PHB per 1 ml of acetic acid. The solution was cooled to 25°C, and 1µL of the Brilliant Blue dye solution was added to each 1 ml of PHB-acetic acid solution. The coloured PHB solution (0.3 ml) was then poured on the PDMS substrate (19.5 mm × 19.5 mm) maintained at 80°C, and the solution was allowed to dry for 5 minutes to assist evaporation of the solvent. After drying and complete removal of the solvent, a uniform PHB thin film containing the brilliant blue dye was formed on the substrate; the typical thickness of the resulting film was about 900 µm. The film was then cooled to room temperature, peeled from the substrate, and cut into rectangles of 1 cm^2 dimension. The PHB film was then mounted on the inside surface of a disposable UV-VIS micro-cuvette (Sigma Aldrich, Canada). Care was taken to mount the film away from the optical path of the cuvette. All dye-loaded PHB films were aged for at least 21 days before the experiments. The molecular weight of the PHB films after solvent casting was measured using gel permeation chromatography. No statistically significant variations between as-received and solvent cast PHB (MW of as-received PHB: 79,000 ± 2130; MW of PHB film: 81,200 ± 2300) was observed.

Preparation of PHB depolymerase enzyme

Comamonas testosteroni (DSMZ 6781) was grown under the cultivation conditions recommended by the provider (Tryptic Soy Broth – TSB, Becton Dickinson, 30°C, 150 rpm) until it reached an approximate optical density at 600 nm (OD600) of 4.

Shake flasks (250 mL) containing 1% w/v of bulk PHB film suspended in a mineral medium (medium 457 DSMZ – Brunner) were inoculated with 10% v/v of bacterial culture for a total volume of 40 mL. The cultures (in which PHB was the only carbon source) were incubated at 30°C and 150 rpm for 3 days until they reached an average OD600 of 5.4. The cultures were centrifuged (Sorval RC 6 PLUS, Thermo) at 10,000×g and 4°C for 30 min. Supernatants were pooled, filter sterilized, and stored at 4°C to be used as the enzyme solution. Preliminary PHB degradation experiments were conducted using different enzyme concentrations (0.25 µg/ml, 0.025 µg/ml and 0.0025 µg/ml) on the dye-loaded PHB processed at 80°C. From these results, the enzyme solution concentration of 0.25 µg/ml was found to be the most appropriate for monitoring fresh milk and meat products, and was used in all subsequent experiments.

Preparation of enzymatic TTI and kinetics studies

To characterize the response of the TTI, the dye-loaded PHB film was mounted inside a clear plastic cuvette. The TTI was activated by adding the extracellular enzyme solution into the cuvette, so as to bring the PHB film in contact with the enzyme. As the PHB degraded, the dye contained within the film was released into the enzyme solution. This color change rate was taken as the dynamic response parameter, $F(t,T)$ of the TTI. The kinetics of dye release were determined by placing TTIs in a climate-controlled incubator maintained at temperatures ranging from 4°C to 37°C (deviation of ±1°C). The dye release rates were measured quantitatively at a time interval of 15 minutes by using a UV-VIS spectrometer (Ultraspec50, Biochrom, Cambridge, UK), such that the beam path transected the solution but not the film. Similarly, the dynamic response of the TTI

was characterized for all relevant temperatures at constant time intervals as the colour transitioned from clear at the initiation of TTI to deep blue at the completion of the dye release process.

UV-VIS Spectroscopy

The color of the solutions was monitored as a function of time using a UV-VIS spectrometer (Ultraspec50, Biochrom, Cambridge, UK). The absorbance values of the degrading solution were obtained at the wavelength 628-630 nm, corresponding to the peak absorbance wavelength of the brilliant blue dye used in this work. The optical absorbance was used as the dynamics colour change parameter to determine the kinetics of the reaction.

The UV-VIS spectrometer was also used to obtain a spectrum scan (200 nm to 800 nm) for the degradation solution at different times to confirm the release of the dye as the degradation process took place.

Optical microscopy and visual observation

The dye-loaded PHB films were observed under a transmission mode optical microscope (Zeiss Axio Imager 2) to determine the uniformity and distribution of the dye in the PHB matrix. The images were obtained at different magnifications to determine the size and distribution of dye agglomerates within the sample.

Scanning Electron Microscope

The surface morphology of the dye-loaded PHB film at different stages of the degradation process was studied using a field emission scanning electron microscope (JEOL, USA). The images were obtained under secondary electron mode at a beam potential of 5 kV, to bring out the variations in the surface morphology of the PHB film as it degrades over time.

6.4. Results

Characterization of dye-loaded PHB

The appearance and homogeneity of the dye-loaded PHB was determined using visual observation and a transmission mode optical microscope. Figures 6.2.a and 2.b shows an image of a dye-loaded PHB film beside a colourless, control PHB film, contrasting the difference in appearance. The control PHB film was found to have a mildly cloudy appearance with no traces of colouration, while the dye-loaded film was blue, with similar opacity. At the macroscopic scale, the distribution within the dye-loaded sample was found to be uniform, and no apparent agglomeration of the dye particles was observed. Figures 6.2.c to 2.e show optical microscope images of the dye-loaded PHB at three different magnifications. At low magnification (50×, Figure 6.2.c), the dye appears to be uniformly distributed in the polymer matrix. Particles with a range of sizes can be seen, with diameters of up to approximately 20 μm. At high magnifications (>200×), individual dye particles were clearly visible; these particles were

uniformly dispersed. Overall, the diameter of the dye particles was observed to range from 2-20 µm.

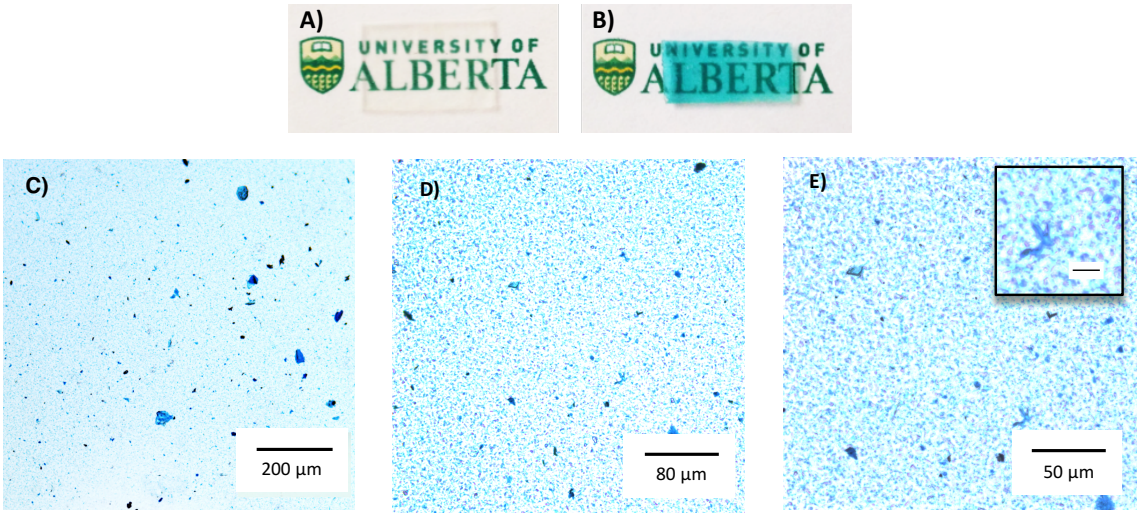

Figure 6.2 Photographs and optical micrographs of the PHB films loaded with dye. A) PHB without dye, B) PHB loaded with Brilliant Blue FCF. C) 50x magnification showing the presence of small agglomerates. Some sparsely distributed, larger agglomerates (> 10 µm) were also observed in the sample. D) 125x magnification and E) 200x magnification which show the size of the smaller agglomerates and the uniform distribution of the dye within the sample. The inset image shows the individual particles of dye embedded in the matrix (Inset scale bar: 5 µm).

To verify the stability of the dye under non-enzymatic conditions, dye-loaded films were washed repeatedly with water and soaked in mineral medium for several days. Under these conditions, there was no apparent discoloration of the sample, (or coloration of the water), indicating that the dye was securely contained by the PHB matrix. This result shows that the dye does not migrate readily out of the PHB matrix without the enzyme solution.

As described above, the TTI was activated by exposing the dye-loaded PHB to the depolymerase enzyme solution that causes the degradation of the PHB, resulting in a controlled release of the dye contained within the matrix. Figure 6.3.a shows a schematic of the degradation process and the consequent release of dye from the PHB matrix at different stages of degradation. Figure 6.3.b shows a representative sample for which half of the film was exposed to the enzyme solution and the other half was exposed to air for 24 hours. The half that was exposed to the enzyme appeared colourless, since most of the dye was released into the solution due to the degradation process. The unexposed half of the PHB film, in contrast, retained the loaded dye. These results show that the deterioration of PHB matrix can lead to the release of the dye. If the solution is confined to a small enough volume, its colour is expected to change considerably, providing a direct reporting mechanism.

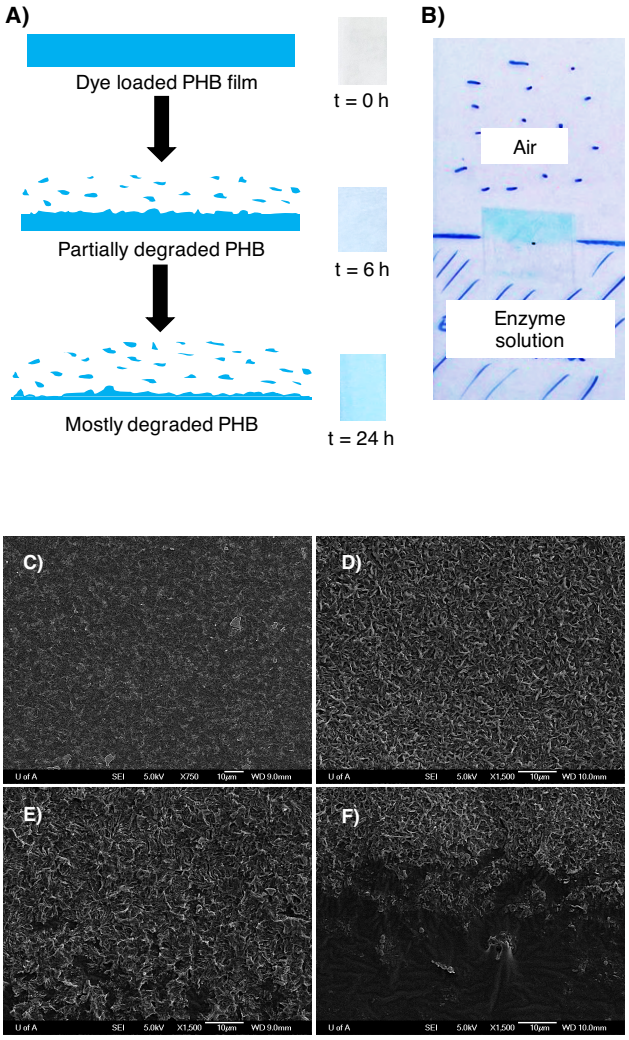

Figure 6.3 Schematics, images and scanning electron microscopy (SEM) of the PHB film loaded with dye and degraded for different times. A) Schematic (left) and corresponding optical images (right) showing the release of the dye from the PHB during degradation. The images depict the enzyme solution, which goes from clear to blue as the dye is released. B) Photograph of a PHB film loaded with dye; the bottom half of the sample was exposed to a degrading enzyme solution and the top half was exposed to air. The part of the film exposed to enzyme has degraded and released all the dye while the dye in the top half remained in the sample. C) SEM of as-fabricated PHB film. SEM of film exposed to enzyme D) for 6 h, E) for 16 h and F) for 24 h.

To fabricate a TTI based on the degradation of a dye-loaded PHB, it is important to understand the nature and uniformity of degradation of the polymer matrix at various stages of the process. Figure 6.3.C to 3.F show the surface morphology change that occurs in the dye-loaded PHB film at different stages of degradation, as observed by SEM. The as-fabricated PHB film (Figure 6. 3.C) was found to have a relatively smooth, uniform surface profile. When exposed to the enzyme solution, the polymer chains hydrolyzed and eroded away during the early stages of degradation. Consequently, the surface became more irregular (Figure 6. 3.D). As the degradation proceeded beyond 16 hours (Figure 6. 3.E and 3.F), most of the PHB film eroded away and the backing layer used to mount the PHB film started to be exposed (darker regions). The SEM images thus clearly depict the surface degradation, the evolution of porosity in the film, and the overall roughness with time.

Kinetics of dye release from PHB matrix

To investigate the rate of colour change of the solution resulting from the degradation of dye-loaded PHB, samples were incubated in enzyme solutions for various times and at various temperatures, and the colour of the solutions was monitored using UV-VIS spectrometry. During the degradation process, the solutions transitioned from clear to coloured as the samples released the dye. Figure 6.4 shows the change in optical absorbance vs. wavelength at different degradation times for a sample incubated in enzyme solution at 24°C. The plot shows that the maximum absorbance occurred at 628 nm (OD628), which is the peak absorbance wavelength of the Brilliant Blue FCF dye. Therefore, all kinetic experiments were carried out by

measuring the change in optical absorbance at 628 nm and using it as the colour response parameter.

At a constant temperature, the colour response of the TTI, $F(t)_T$, can be expressed as follows:

$$dF(t)_T = k\, dt$$

Where k is the rate constant of the dye release process, and t is the time for which the TTI is active. The optical absorbance at 628 nm as a function of time is shown inset in Figure 6.4, and corresponds to the color response function $F(t)_T$. This curve $F(t)_T$ is initially linear (indicating that the color changes at a constant rate) and then reaches a plateau once all of the dye is released (in this case, after around 6 hours). The linear region of the graph is consistent with pseudo-zero-order kinetics for a surface degraded by an enzyme at elevated concentrations, and the slope of this region is the rate constant, k.

The temperature dependence of the rate constant (k) and the activation energy of the dye release process (as mediated by PHB degradation) can be determined by incubating the dye-loaded PHB in enzyme solution at different temperatures and measuring the rate constant (k) for each temperature. The activation energy can then be determined using an Arrhenius equation, which is expressed in the natural logarithm form:

$$\ln k = \ln k_A - E_A/RT$$

Where k_A is the pre-exponent factor, and E_A is the activation energy of the dye release process. Plotting *ln k* against *1/T* will produce a straight line, the slope of which is the activation energy and the intercept gives the pre-exponent factor.

The optical response of the dye-loaded PHB exposed to enzyme was measured at 4°C, 15°C, 24°C and 37°C to estimate the kinetic parameters of the of the TTI. Similar to the representative plot in Figure 6.4, absorbance was found to increase monotonically with increasing degradation time for all experimental temperatures. Figure 6.5.a shows this linear relationship between the optical response function vs time for samples incubated at different temperatures. The plot also shows that the rate of change in optical absorbance (rate constant, *k*) increases with increasing degradation temperature.

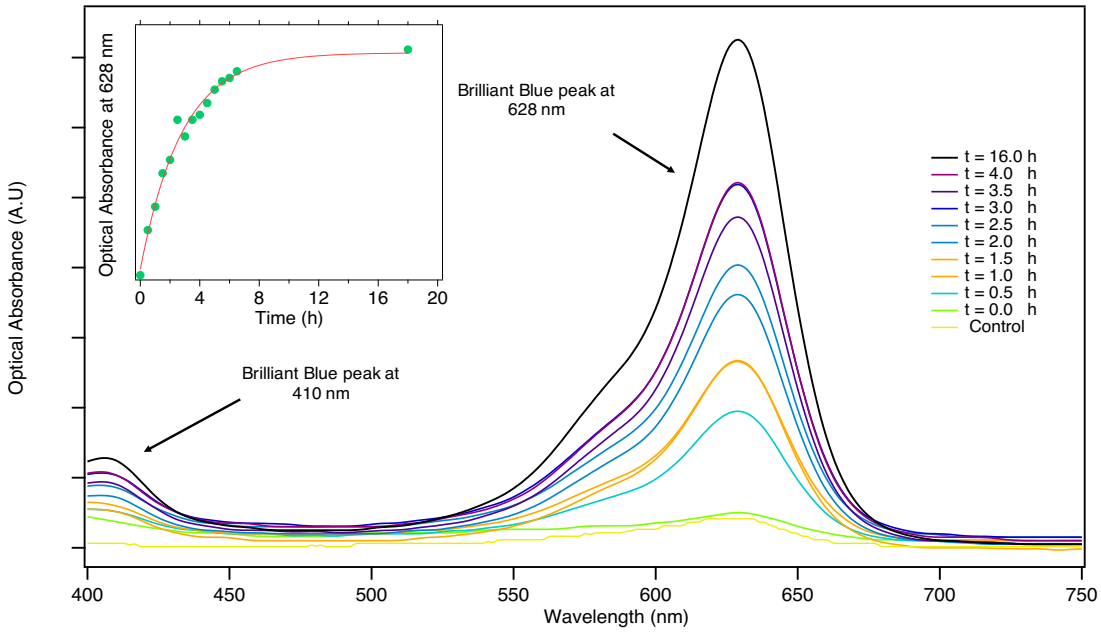

Figure 6.4 A combined plot of the UV-VIS spectrum of the degrading solution exposed to the PHB loaded with Brilliant Blue FCF dye for different time spans. The plot shows a maximum peak at 628-630 nm, which corresponds to the absorption wavelength of the blue dye. The negative control sample exposed to water for 24 hours showed minimal optical absorbance at 630 nm, indicating that the enzyme in the solution is necessary for rapid dye release. The inset plot shows the monotonic increase in optical absorbance at 628 nm with the passage of time.

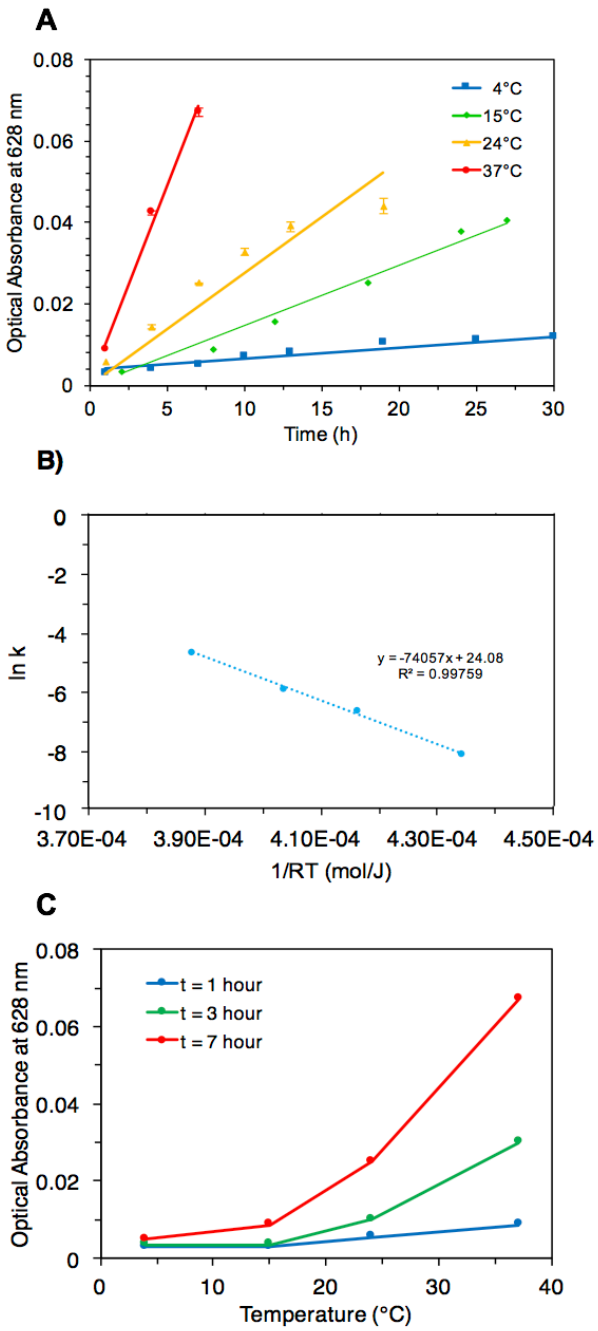

Figure 6.5 Kinetics of the TTI based on dye-loaded PHB films. A) Combined plot of optical absorbance (absorbance) at 628 nm of the degrading solution versus time. Each curve was obtained at different temperatures to find the rate of dye release and the total time required for complete release of the dye with respect to temperature. B) Plot of ln k vs 1/RT, which was used to determine the activation energy. C) Plot of optical absorbance vs. temperature at different degradation times.

Figure 6.5.b shows the natural log of *k* vs. 1/RT, which was used to determine the activation energy of the dye-release process. The activation energy calculated from the slope of the curve is E_A ~ 74 kJ/mol. Figure 6.5.c shows a combined plot of optical absorbance vs. temperature obtained at different times during degradation, which shows how the OD follow an exponential trend, as is typical for reactions that can be modeled by Arrhenius equation.

6.5. Discussion

Dye-loaded PHB in enzyme solution changes color intensity at a linear rate

A TTI with widespread applicability must undergo a gradual and predictable change in color as a function of both time and temperature. In our work, this color change results, as the dye-loaded polymer matrix is degraded by exposure to enzyme solution, releasing dye into the solution itself. We found this dye release rate and the color intensity change to be linear at a given temperature for a predictable period of time (Figure 6.5.a), eventually rolling off to a saturation trend as the PHB was completely degraded and the dye was fully released into the solution (Figure 6.4, inset). This linearity can be attributed to a number of factors, as discussed below.

A uniform distribution of the dye in the polymer matrix is desirable to ensure a constant rate of dye release as PHB degrades. As shown in Figure 6.2, the dye particles (with sizes in the range from 2 to 20 μm) were found to be dispersed throughout the matrix. In addition, we found that the dye was stable in the polymer

matrix under normal storage conditions. PHB films exposed to water for over 7 days did not experience any color change whereas the samples exposed to enzyme solution resulted in complete degradation of the PHB films and release of all the dye dispersed in the polymer matrix (Figures 6.3.a and 3.b). We attribute this stability to the relatively high molecular weight and consequent hydrophobicity of the PHB (which limits the amount of water that can diffuse into the matrix and dissolve the dye). This uniformity and stability facilitates a gradual release of the dye as the PHB film is degraded by the enzyme.

Enzymatic degradation of PHB is a surface-mediated reaction, suggesting that the dye in the polymer will be released at a constant rate as long as the surface area of PHB film remains relatively constant through the degradation process. In the case at hand, even if small variations in the surface area were initially observed due to preferential erosion of amorphous regions of the polymer matrix by extracellular PHB depolymerase enzymes such as $PhaZ_{Cte}$ [35] (Figure 6.3.c thru 3.f)), the dye was released at a linear rate and no apparent deviation from linearity was observed until the PHB film was all completely degraded. Overall, these results indicate that enzymatic degradation of a dye-loaded polymer is a viable system for the implementation of TTI devices that have a predictable response.

The response of the TTI varies with temperature

The temperature dependence of the degradation process (particularly of the rate constant, k) is the key factor allowing the enzymatic degradation of the polymer to be

leveraged to track time and temperature exposure. It has been shown previously that the highest activity for the extracellular enzyme used in this work ($PhaZ_{cte}$ from *C. testosteroni)* occurs around 70˚C (at a pH of 8.5) [36]*.* All temperatures investigated here are below this optimal value, and at higher temperatures a higher rate constant is observed than at lower temperatures. It is known from the literature that the rate of degradation is also pH dependent [41]. For simplicity, the pH in our work was kept as constant.

The results in Figures 6.5.a and 5.b show that the dye-loaded PHB degraded by a suitable enzyme can produce a visible response at a rate that varies with the temperature, indicating its utility in estimating the quality of some food products, including dairy and fresh meat. Food itself undergoes spoilage at different rates depending on the temperature of storage; the temperature dependence of this rate is described by the activation energy. The reaction in an ideal TTI should have an activation energy similar to that of food spoilage, such that it can change color at the same rate as the food spoils. Based on the kinetic analysis, the activation energy of the TTI was found to be 78 kJ/mol. This value is within the acceptable range for the activation energy of fresh meat and dairy products (~70-90 kJ/mol), as proposed by Labuza *et al.* [33]. For the system described here (using the enzyme Phaz from *C. testosteroni)*, the dye is completely released in 6 hours at 37°C, and 168 hours (7 days) at 4°C.

However, the response time and kinetic behavior of the TTI should be altered depending on the application of interest. The ability to tune the kinetics and response time can enable the TTI to be used for monitoring a wider range of products. We propose that different depolymerase enzymes can be used to tune the kinetic parameters of TTI, since many PHB depolymerases enzymes are found in nature, each with a different activation energy and optimal temperature for activity [28,37,38]. It would therefore be possible to change the rate of dye release and tailor the kinetics of the TTI for a given time and temperature combination by changing enzyme concentration and/or by using a different enzyme.

Further, the response time of a TTI can be altered simply by changing the thickness of the PHB film. The enzymatic degradation of PHB can be considered as a zero-order reaction since the surface area essentially remains a constant as the polymer surface erodes away. As the surface of the polymer film degrades, the density of active sites on the surface remains constant for most of the degradation process, and since the enzyme concentration remains constant during the reaction, the reaction will proceed as pseudo-zero order with respect to the polymer substrate. The linear response at a given temperature, as shown in Figure 6. 5.A, supports this idealization. Due to this pseudo-zero-order kinetics, an increase in PHB film thickness would result in a proportional increase in the time for complete release of the dye from polymer matrix, while maintaining the kinetic parameters a constant.

In addition to these parameters, factors such as storage temperature, pH and substrate concentration can also influence the response of an enzyme-catalyzed reaction. Typically, the enzyme activity increases with an increase in temperature, until the optimum activity is reached [36]. Beyond this point, the enzyme rapidly loses activity and becomes less effective at catalyzing the substrate [36]. Therefore, while selecting enzymes for TTI, it is important to consider the maximum temperature to which the product will be exposed and use enzymes that do not lose activity in the working temperature range and time scales of the TTI. The PhaZ from *C. testosteroni* used in this work has optimum activity at 70˚C which makes it a suitable candidate for monitoring food products that would not be exposed to elevated temperatures during storage. In addition to temperature, pH [36] and substrate concentration can also impact the apparent activity of the enzymes. However, in a TTI device the pH and substrate concentration can be considered to be invariant when a solid film with uniform surface area is available, and sufficient liquid medium is present to prevent substantial reduction in pH during degradation. Nonetheless, these parameters can also be altered to tune the response time and kinetics of the TTI. The interplay between these different factors can thus be utilized to fine tune the response of the TTI based on the specific needs of an application.

Viability and practical applicability

The proposed TTI based on the dye-loaded PHB was adapted to create a simple prototype (as shown in Figure 6. 1.C). The prototype was created by mounting the dye-loaded PHB film (out of the line of sight, behind the press tab symbol) inside a small

plastic package that contains the enzyme solution. The volume of the liquid was deliberately kept small (1 ml) and the prototype was constructed to cut out all stray light to maximize the extent of change in color as the dye is released. The colour seen in the window of the TTI intensifies with proceeding time after the device is activated, due to the release of dye into the solution. A semi-quantitative measure of the remaining useful life of the product being monitored can be obtained by comparing the coloration of the TTI with a reference gradient scale, similar to the one shown below the visual window (Figures 6.1.b and 1.c). A major advantage of our system is that the TTI that can produce a direct visual change, without depending on a secondary mechanism (like pH indicators or secondary reaction substrates) to indicate the response. This simplification in design can allow for a streamlined manufacturing process, improved reliability and a lower manufacturing cost of the TTI. One factor to consider while using enzymatic devices is the need to keep the enzyme active before its deployment in food packages. Therefore, suitable storage conditions or additives must be used to maintain stability and consistent response of the TTI, as is the case with all existing commercial enzymatic and microbial TTIs.

6.6. Conclusion

Time temperature indicators are useful devices for food quality monitoring and their utility depends on their accuracy and the ease of implementing the device in the food-packaging infrastructure. Most existing TTIs are limited in terms of cost, complexity and/or reliability. In addition, these devices typically require secondary indication mechanisms such as a pH indicator to visualize the response. In this work,

we have developed a TTI based on the enzymatic degradation of a dye-loaded PHB which has the potential to meet the needs of an accurate and cost effective TTI. The proposed device overcomes most of the disadvantages of existing TTIs and makes possible a streamlined, reliable device. We have shown that the degradation of PHB and the subsequent release of the dye into the degrading solution display kinetic properties similar to those of the loss of quality of certain food products. The kinetics of the dye release was studied and was found to yield an activation energy of 74 kJ/mol, which is suitable for monitoring many dairy and fresh meat products. PHB, which can be degraded by robust depolymerase enzymes with a wide range of activation energies, has the potential to be a good candidate for TTI applications in the food processing industry. Overall, the demonstrated devices have the potential to act as low-cost TTIs for food quality monitoring.

Acknowledgements

Funding from Alberta Agriculture and Forestry (AAF), and the Natural Sciences and Engineering Council of Canada (NSERC) is gratefully acknowledged. The authors thank Diana Martínez-Tobón for supplying the enzymes for testing.

Author Contributions

In this work, P.A designed and performed the experiments. A.L.E. and D.S. supervised the work, and contributed to designing the research and to writing the manuscripts.

6.7. References

1. Limbo, S., Torri, L., Sinelli, N., Franzetti, L. & Casiraghi, E. Evaluation and predictive modeling of shelf life of minced beef stored in high-oxygen modified atmosphere packaging at different temperatures. *Meat Sci.* **84,** 129–136 (2010).
2. Nychas, G. J. E., Skandamis, P. N., Tassou, C. C. & Koutsoumanis, K. P. Meat spoilage during distribution. *Meat Sci.* **78,** 77–89 (2008).
3. Sinelli, N., Limbo, S., Torri, L., Di Egidio, V. & Casiraghi, E. Evaluation of freshness decay of minced beef stored in high-oxygen modified atmosphere packaged at different temperatures using NIR and MIR spectroscopy. *Meat Sci.* **86,** 748–752 (2010).
4. Muir, D. D. The shelf-life of dairy products: 1. Factors influencing raw milk and fresh products. *Int. J. Dairy Technol.* **49,** 24–32 (1996).
5. Buchanan, R. L. & Klawitter, L. A. Effect of temperature history on the growth of Listeria monocytogenes Scott A at refrigeration temperatures. *Int. J. Food Microbiol.* **12,** 235–245 (1991).
6. Gonzalez-Aguilar, G. A., Ayala-Zavala, J. F., Ruiz-Cruz, S., Acedo-F??lix, E. & D??az-Cinco, M. E. Effect of temperature and modified atmosphere packaging on overall quality of fresh-cut bell peppers. *LWT - Food Sci. Technol.* **37,** 817–826 (2004).
7. Paull, R. E. Effect of temperature and relative humidity on fresh commodity quality. *Postharvest Biol. Technol.* **15,** 263–277 (1999).
8. Randolph M. Beaudry, Arthur C. Cameron, Ahmad Shirazi, and D. L. D.-L. Modified-atmosphere packaging of blueberry fruit: effect of temperature on

package O2 and CO2. *J. Am. Soc. Hortic. Sci.* **117,** 436–441 (1992).

9. Bobelyn, E., Hertog, M. L. a T. M. & Nicolaï, B. M. Applicability of an enzymatic time temperature integrator as a quality indicator for mushrooms in the distribution chain. *Postharvest Biol. Technol.* **42,** 104–114 (2006).
10. Fu, B., Taoukis, P. S. & Labuza, T. P. Predictive Microbiology for Monitoring Spoilage of Dairy Products with Time-Temperature Integrators. *J. Food Sci.* **56,** 1209–1215 (1991).
11. Smolander, M., Alakomi, H. L., Ritvanen, T., Vainionpää, J. & Ahvenainen, R. Monitoring of the quality of modified atmosphere packaged broiler chicken cuts stored in different temperature conditions. A. Time-temperature indicators as quality-indicating tools. *Food Control* **15,** 217–229 (2004).
12. Ellouze, M. & Augustin, J. C. Applicability of biological time temperature integrators as quality and safety indicators for meat products. *Int. J. Food Microbiol.* **138,** 119–129 (2010).
13. Vaikousi, H., Biliaderis, C. G. & Koutsoumanis, K. P. Applicability of a microbial Time Temperature Indicator (TTI) for monitoring spoilage of modified atmosphere packed minced meat. *Int. J. Food Microbiol.* **133,** 272–278 (2009).
14. Ramstad, D.E., Volz, F. E. Did it thaw? Gel will tell. *Food Ind.* **22,** 182–184 (1950).
15. Wu, D. *et al.* Development and characterization of an enzymatic time-temperature indicator (TTI) based on Aspergillus niger lipase. *LWT - Food Sci. Technol.* **60,** 1100–1104 (2015).
16. Yan, S. *et al.* Development and characterization of a new amylase type time-temperature indicator. *Food Control* **19,** 315–319 (2008).

17. Galotto, M. & Ulloa, P. Development and Application of Time–temperature Indicators Used on Food during the Cold Chain Logistics. *Packag. Technol. Sci.* **23,** 253–266 (2010).

18. Kim, J. U. *et al.* Kinetic modeling and characterization of a diffusion-based time-temperature indicator (TTI) for monitoring microbial quality of non-pasteurized angelica juice. *LWT - Food Sci. Technol.* **67,** 143–150 (2016).

19. Wanihsuksombat, C., Hongtrakul, V. & Suppakul, P. Development and characterization of a prototype of a lactic acid-based time-temperature indicator for monitoring food product quality. *J. Food Eng.* **100,** 427–434 (2010).

20. Brizio, A. P. D. R. & Prentice, C. Development of Aa New Time Temperature Indicator for Enzymatic Validation of Pasteurization of Meat Products. *J. Food Sci.* **80,** M1271–M1276 (2015).

21. Galagan, Y. & Su, W. F. Fadable ink for time-temperature control of food freshness: Novel new time-temperature indicator. *Food Res. Int.* **41,** 653–657 (2008).

22. Smyth, A. B., Song, J. & Cameron, A. C. Modified Atmosphere Packaged Cut Iceberg Lettuce : Effect of Temperature and O 2 Partial Pressure on Respiration and Quality. *J. Agric. Food Chem.* **46,** 4556–4562 (1998).

23. Daszczuk, A. *et al. Bacillus subtilis* Biosensor Engineered To Assess Meat Spoilage. *ACS Synth. Biol.* **3,** 999–1002 (2014).

24. Larsson, R. P. Time-temperature integrating indicator. (1974).

25. Wu, D. *et al.* Preliminary study on time-temperature indicator (TTI) system based on urease. *Food Control* **34,** 230–234 (2013).

26. Chen, G.-Q. A microbial polyhydroxyalkanoates (PHA) based bio- and materials industry. *Chem. Soc. Rev.* **38,** 2434–46 (2009).

27. Doi, Y. Microbial synthesis, physical properties, and biodegradability of polyhydroxyalkanoates. *Macromol. Symp.* **98,** 585–599 (1995).

28. Jendrossek, D. & Handrick, R. Microbial Degradation of Polyhydroxyalkanoates*. *Annu. Rev. Microbiol.* **56,** 403–432 (2002).

29. Keshavarz, T. & Roy, I. Polyhydroxyalkanoates: bioplastics with a green agenda. *Curr. Opin. Microbiol.* **13,** 321–6 (2010).

30. Suriyamongkol, P., Weselake, R., Narine, S., Moloney, M. & Shah, S. Biotechnological approaches for the production of polyhydroxyalkanoates in microorganisms and plants - a review. *Biotechnol. Adv.* **25,** 148–75 (2007).

31. Kasuya, K., Inoue, Y., Yamada, K. & Doi, Y. Kinetics of surface hydrolysis of poly[(R)-3-hydroxybutyrate] film by PHB depolymerase from Alcaligenes faecalis T1. *Polym. Degrad. Stab.* **48,** 167–174 (1995).

32. Mukai, K., Yamada, K. & Doi, Y. Kinetics and mechanism of heterogeneous hydrolysis of poly[(R)-3-hydroxybutyrate] film by PHA depolymerases. *Int. J. Biol. Macromol.* **15,** 361–366 (1993).

33. Labuza, T. P. *Shelf-life dating of foods.* (Food & Nutrition Press, Inc., 1982).

34. Anbukarasu, P., Sauvageau, D. & Elias, A. Tuning the properties of polyhydroxybutyrate films using acetic acid via solvent casting. *Sci. Rep.* **5,** 17884 (2015).

35. Koyama, N. & Doi, Y. Effects of Solid-State Structures on the Enzymatic Degradability of Bacterial Poly(hydroxyalkanoic acids). *Macromolecules* **30,** 826–

832 (1997).

36. Kasuya, K. ichi, Doi, Y. & Yao, T. Enzymatic degradation of poly[(R)-3-hydroxybutyrate] by Comamonas testosteroni ATSU of soil bacterium. *Polym. Degrad. Stab.* **45,** 379–386 (1994).

37. Hiraishi, T. *et al.* Degradation and adsorption characteristics of PHB depolymerase as revealed by kinetics of mutant enzymes with amino acid substitution in substrate-binding domain. *Biomacromolecules* **11,** 113–119 (2010).

38. Mukai, K., Yamada, K. & Doi, Y. Enzymatic degradation of poly(hydroxyalkanoates) by a marine bacterium. *Polym. Degrad. Stab.* **41,** 85–91 (1993).

7. Summary and Conclusions

The present work demonstrates that the enzymatic response of PHB can be controlled by using acetic acid solvent casting and suitable processing parameters. Additionally, PHB surface degradation can be characterized by using polymer surface patterned with diffraction gratings. The findings and the methods developed in this work were used to create an enzyme-responsive architecture which can be used in a platform technology for food quality assessment and bacterial sensing. More specific conclusions of the studies presented in each chapter follow.

The use of glacial acetic acid as a viable eco-friendly solvent for processing and controlling PHB properties has been demonstrated in Chapter 3 entitled: “Tuning the properties of polyhydroxybutyrate films using acetic acid via solvent casting”. The work was the first instance of acetic acid being demonstrated as a useful solvent to process PHB, for which chloroform was the only widely-used solvent until this work. Solvent casting temperature has been shown to play an important role in determining the physical properties of PHB, with variations observed in the optical, mechanical and thermal properties of PHB. These properties were compared with PHB films cast from chloroform, and the results showed that using acetic acid provides more flexibility in the conditions for PHB processing. In addition, the versatility of the acetic acid based solvent casting process has been demonstrated by preparing PHB films with a wide range of thicknesses (ranging from 50 μm to 10 nm) and different optical properties

(ranging from transparent to opaque), and by spray coating of PHB thin films on flexible substrates.

A method for sensitive characterization of the surface degradation of polymeric films was proposed and validated in Chapter 4 entitled “A Diffraction-Based Degradation Sensor for Polymer Thin Films.” The work demonstrated that the surface degradation behavior of polymers could be studied by patterning the test surface with diffraction gratings and by observing the diffraction patterns as the polymer surface degraded. The intensity of the diffracted beam was found to decrease concomitantly with the erosion of the polymer surface. A probabilistic model has been developed to determine semi-quantitatively the degradation behavior of the polymer surface and its relationship with the decrease in diffraction intensity. In the chapter, the effect of solvent casting temperature on the enzymatic degradation of PHB and dissolution stability of silk films were explored as a proof of concept. The method was further utilized to study the effect of dimensional constraint on the degradation behavior of PHB in Chapter 5 entitled “Enzymatic degradation of dimensionally constrained polyhydroxybutyrate films” (Chapter 5). The results showed that the thickness of the films have a substantial impact on the degradation of PHB, with thin films degrading more rapidly than their thicker counterparts. However, when the films were constrained down to the nanoscale, the degradation was found to cease. This behavior was attributed to the absence of crystalline structures necessary for the enzymatic attachment and degradation of PHB.

In Chapter 6 entitled “Time-temperature indicator based on enzymatic degradation of dye-loaded polyhydroxybutyrate.”, the temperature dependent degradation behavior of

a dye-loaded PHB film was utilized to fabricate and demonstrate a time-temperature indicator which can be used for quality assessment of food products. The degradation temperature was found to influence the dye-release rate, thus providing a simple visual indication of the integrated time and temperature history to which a food product has been exposed. The suitability of the proposed time-temperature indicator for application in food products, namely fresh meat and dairy, was assessed based on the apparent activation energy of the degradation process.

The findings in this thesis, in addition to forming an integral part of the platform technology for pathogen detection, can have application in a wide variety of fronts. For instance, the method to process PHB using acetic acid (Chapter 3) can be utilized to prepare biodegradable parts and sensing components (such as porous implants and micro-optical sensors) which are challenging or impossible to manufacture using traditional fabrication techniques. The diffraction-based degradation sensor described in Chapter 4 has potential to enable rapid, non-contact analysis of degradation and stability of several materials, including polymers and metals. The method also has the potential to be incorporated into a plate reader enabling high throughput analysis of samples. The method is of interest to industrial research labs during large-scale materials screening where a semi-quantitative estimate of degradation rate is sufficient in the initial stages. The results presented in Chapter 5 provides an insight into the fundamental degradation behavior of a polymer film constrained in the nanoscale. This chapter adds to the current literature and provides exciting future directions wherein the degradation of the polymer can be controlled by changing the dimensional constraint

applied on the material. Further, the nanoscale PHB films fabricated in this chapter can be used in biomolecule sensors and food quality sensors. Enzymatic TTI based on PHB thin film demonstrated in Chapter 6 has potential application in the meat and dairy supply chain for total quality assessment. The novel TTI architecture based on a dye-loaded polymer film could lead to more research on TTIs involving other polymer and enzyme systems.

Bibliography

A bibliography of all the works cited in this thesis is listed below. The references are sorted in alphabetical order by the author's last name.

Abd El-Rehim, H. A., Hegazy, E.-S. A., Ali, A. M., & Rabie, A. M. (2004). Synergistic effect of combining UV-sunlight-soil burial treatment on the biodegradation rate of LDPE/starch blends. *Journal of Photochemistry and Photobiology A: Chemistry*, *163*(3), 547–556. http://doi.org/10.1016/j.jphotochem.2004.02.003

Abe, H., Kikkawa, Y., Iwata, T., Aoki, H., Akehata, T., & Doi, Y. (2000). Microscopic visualization on crystalline morphologies of thin films for poly [(R) -3-hydroxybutyric acid] and its copolymer, *41*, 867–874.

Abe, H., Matsubara, I., Doi, Y., Hori, Y., & Yamaguchi, A. (1994). Physical Properties and Enzymic Degradability of Poly(3-hydroxybutyrate) Stereoisomers with Different Stereoregularities. *Macromolecules*, *27*(21), 6018–6025. http://doi.org/10.1021/ma00099a013

Abe, H., Matsubara, I., Doi, Y., & Matsubara, I. (1995). Physical Properties and Enzymatic Degradability of Polymer Blends of Bacterial Poly[(R)-3-hydroxybutyrate] and Poly[(R,S)-3-hydroxybutyrate] Stereoisomers. *Macromolecules*, *28*(4), 844–853. http://doi.org/10.1021/ma00108a007

Acar, H., Çınar, S., Thunga, M., Kessler, M. R., Hashemi, N., & Montazami, R. (2014a). Study of Physically Transient Insulating Materials as a Potential Platform for

Transient Electronics and Bioelectronics. *Advanced Functional Materials*, *24*(26), 4135–4143. http://doi.org/10.1002/adfm.201304186

Acar, H., Çınar, S., Thunga, M., Kessler, M. R., Hashemi, N., & Montazami, R. (2014b). Study of Physically Transient Insulating Materials as a Potential Platform for Transient Electronics and Bioelectronics. *Advanced Functional Materials*, *24*(26), 4135–4143. http://doi.org/10.1002/adfm.201304186

Aguilar, M. R., & San Román, J. (2014). Introduction to smart polymers and their applications. *Smart Polymers and Their Applications*, 1–11. http://doi.org/10.1533/9780857097026.1

Alexis, F. (2005). Factors affecting the degradation and drug-release mechanism of poly(lactic acid) and poly[(lactic acid)-co-(glycolic acid)]. *Polymer International*, *54*(1), 36–46. http://doi.org/10.1002/pi.1697

Anbukarasu, P., Martínez-Tobón, D. I., Sauvageau, D., & Elias, A. L. (2017). A diffraction-based degradation sensor for polymer thin films. *Polymer Degradation and Stability*. http://doi.org/10.1016/j.polymdegradstab.2017.05.020

Anbukarasu, P., Sauvageau, D., & Elias, A. (2015). Tuning the properties of polyhydroxybutyrate films using acetic acid via solvent casting. *Scientific Reports*, *5*, 17884. http://doi.org/10.1038/srep17884

Andrady, A. L. (1997). *Wavelength Sensitivity in Polymer Photodegradation*. *Advances in Polymer Science* (Vol. 128).

Angelo, K. M., Conrad, A. R., Saupe, A., Dragoo, H., West, N., Sorenson, A., Jackson, B. R. (2017). Multistate outbreak of Listeria monocytogenes infections linked to whole apples used in commercially produced, prepackaged caramel apples: United

States, 2014–2015. *Epidemiology and Infection*, *145*(5), 848–856. http://doi.org/10.1017/S0950268816003083

Anne, A., & Demaille, C. (2012). Kinetics of enzyme action on surface-attached substrates: a practical guide to progress curve analysis in any kinetic situation. *Langmuir : The ACS Journal of Surfaces and Colloids*, *28*(41), 14665–71. http://doi.org/10.1021/la3030827

Baekeland, L. H. (1909). Original papers: The synthesis, constitution, and uses of bakelite. *Industrial and Engineering Chemistry*, *1*(3), 149–161. http://doi.org/10.1021/ie50003a004

Baekeland, L. H. (1910). Bakelite, a condensation product of phenols and formaldehyde, and its uses. *Journal of the Franklin Institute*, *169*(1).

Baeumner, A. J. (2003). Biosensors for environmental pollutants and food contaminants. *Analytical and Bioanalytical Chemistry*, *377*(3), 434–445. http://doi.org/10.1007/s00216-003-2158-9

Barham, P. J., Barker, P., & Organ, S. J. (1992). Physical properties of poly(hydroxybutyrate) and copolymers of hydroxybutyrate and hydroxyvalerate. *FEMS Microbiology Letters*, *103*(2–4), 280–298. http://doi.org/10.1111/j.1574-6968.1992.tb05850.x

Barham, P. J., & Keller, A. (1986). The Relationship between Microstructure and Mode of Fracture in Polyhydroxybutyrate, *24*, 69–77.

Barnes, D. K. A., Galgani, F., Thompson, R. C., & Barlaz, M. (2009). Accumulation and fragmentation of plastic debris in global environments. *Philosophical Transactions of the Royal Society B: Biological Sciences*, *364*(1526), 1985–1998.

http://doi.org/10.1098/rstb.2008.0205

Bauer, H., & Owen, A. J. (1988). Some structural and mechanical properties of bacterially produced poly-β-hydroxybutyrate-co-β-hydroxyvalerate. *Colloid and Polymer Science*, *266*(3), 241–247. http://doi.org/10.1007/BF01452586

Bennett, T. P. (1966). *Modern topics in biochemistry; structure and function of biological molecules*. New York,: Macmillan. Retrieved from https://www.library.ualberta.ca/catalog/357268

Berggren, M., & Richter-Dahlfors, A. (2007). Organic bioelectronics. *Advanced Materials*, *19*(20), 3201–3213. http://doi.org/10.1002/adma.200700419

Berghem, L. E. R., & Pettersson, L. G. (1974). The Mechanism of Enzymatic Cellulose Degradation. Isolation and Some Properties of a beta-Glucosidase from Trichoderma viride. *European Journal of Biochemistry*, *46*(2), 295–305. http://doi.org/10.1111/j.1432-1033.1974.tb03621.x

Bermel, M. S. (2007, January). Polyvinyl alcohol films prepared by coating methods.

Bhatta, D., Christie, G., Blyth, J., & Lowe, C. R. (2008). Development of a holographic sensor for the detection of calcium dipicolinate-A sensitive biomarker for bacterial spores. *Sensors and Actuators, B: Chemical*, *134*(2), 356–359. http://doi.org/10.1016/j.snb.2008.06.021

Bhatta, D., Christie, G., Madrigal-González, B., Blyth, J., & Lowe, C. R. (2007). Holographic sensors for the detection of bacterial spores. *Biosensors and Bioelectronics*, *23*(4), 520–527. http://doi.org/10.1016/j.bios.2007.06.006

Bobelyn, E., Hertog, M. L. a T. M., & Nicolaï, B. M. (2006). Applicability of an enzymatic time temperature integrator as a quality indicator for mushrooms in the distribution

chain. *Postharvest Biology and Technology*, *42*(1), 104–114. http://doi.org/10.1016/j.postharvbio.2006.05.011

Bodenhamer, W. T. (2000, April). Method and apparatus for selective biological material detection.

Boisen, A., Dohn, S., Keller, S. S., Schmid, S., & Tenje, M. (2011). Cantilever-like micromechanical sensors. *Reports on Progress in Physics*, *74*(3), 36101. http://doi.org/10.1088/0034-4885/74/3/036101

Brizio, A. P. D. R., & Prentice, C. (2015). Development of Aa New Time Temperature Indicator for Enzymatic Validation of Pasteurization of Meat Products. *Journal of Food Science*, *80*(6), M1271–M1276. http://doi.org/10.1111/1750-3841.12889

Brodin, M., Vallejos, M., Opedal, M. T., Area, M. C., & Chinga-Carrasco, G. (2017). Lignocellulosics as sustainable resources for production of bioplastics – A review. *Journal of Cleaner Production*, *162*, 646–664. http://doi.org/10.1016/j.jclepro.2017.05.209

Bruckenstein, S., & Shay, M. (1985). Experimental aspects of use of the quartz crystal microbalance in solution. *Electrochimica Acta*, *30*(10), 1295–1300. http://doi.org/10.1016/0013-4686(85)85005-2

Bucci, D. Z., Tavares, L. B. B., & Sell, I. (2005). PHB packaging for the storage of food products. *Polymer Testing*, *24*(5), 564–571. http://doi.org/10.1016/j.polymertesting.2005.02.008

Buchanan, R. L., & Klawitter, L. A. (1991). Effect of temperature history on the growth of Listeria monocytogenes Scott A at refrigeration temperatures. *International Journal of Food Microbiology*, *12*(2–3), 235–245. http://doi.org/10.1016/0168-

1605(91)90074-Y

Capitán, M. J., Rueda, D. R., & Ezquerra, T. a. (2004). Inhibition of the crystallization in nanofilms of poly(3-hydroxybutyrate). *Macromolecules*, *37*(15), 5653–5659. http://doi.org/10.1021/ma049576p

Capone, C., Di Landro, L., Inzoli, F., Penco, M., & Sartore, L. (2007). Thermal and mechanical degradation during polymer extrusion processing. *Polymer Engineering and Science*, *47*(11). http://doi.org/10.1002/pen.20882

Chandrawati, R. (2016). Enzyme-responsive polymer hydrogels for therapeutic delivery. *Experimental Biology and Medicine*, *241*(9), 972–979. http://doi.org/10.1177/1535370216647186

Characterization of polyhydroxybutyrate-hydroxyvalerate (PHB-HV)/maize starch blend films. (2008). *Journal of Food Engineering*, *89*(4), 361–369. http://doi.org/10.1016/J.JFOODENG.2008.04.022

Charych, D., Cheng, Q., Reichert, A., Kuziemko, G., Stroh, M., Nagy, J. O., … Stevens, R. C. (1996). A “litmus test” for molecular recognition using artificial membranes. *Chemistry & Biology*, *3*(2), 113–120. http://doi.org/10.1016/S1074-5521(96)90287-2

Chen, G.-Q. (2009). A microbial polyhydroxyalkanoates (PHA) based bio- and materials industry. *Chemical Society Reviews*, *38*(8), 2434–46. http://doi.org/10.1039/b812677c

Chen, G.-Q., & Wu, Q. (2005). The application of polyhydroxyalkanoates as tissue engineering materials. *Biomaterials*, *26*(33), 6565–78. http://doi.org/10.1016/j.biomaterials.2005.04.036

Chen, Y., Geever, L. M., Killion, J. A., Lyons, J. G., Higginbotham, C. L., & Devine, D.

M. (2016). Review of Multifarious Applications of Poly (Lactic Acid). *Polymer - Plastics Technology and Engineering*, *55*(10), 1057–1075. http://doi.org/10.1080/03602559.2015.1132465

Christopher Robin Lowe, Roger Bradley Millington, J. B. and A. G. M. (1999). Hologram containing sensor.

Chu, C. C. (1982). The effect of pH on thein vitro degradation of poly(glycolide lactide) copolymer absorbable sutures. *Journal of Biomedical Materials Research*, *16*(2), 117–124. http://doi.org/10.1002/jbm.820160204

Cichy, B., Kwiecień, J., Piątkowska, M., Kuzdzał, E., Gibas, E., & Rymarz, G. (2010). Polyolefin oxo-degradation accelerators - A new trend to promote environmental protection. *Polish Journal of Chemical Technology*, *12*(4), 44–52. http://doi.org/10.2478/v10026-010-0049-3

Clarke, W. J. (1945). V. Properties of Different Polyethylenes. *Transactions of the American Institute of Electrical Engineers*, *64*(12), 919–922. http://doi.org/10.1109/T-AIEE.1945.5059065

Cobntbekt, J. & Marchessault, R. H. Physical properties of poly-β-hydroxybutyrate. IV. Conformational analysis and crystalline structure. *J. Mol. Biol.* **71,** 735–756 (1972).

Cole, M. A., Voelcker, N. H., Thissen, H., & Griesser, H. J. (2009). Stimuli-responsive interfaces and systems for the control of protein-surface and cell-surface interactions. *Biomaterials*, *30*(9), 1827–1850. http://doi.org/10.1016/j.biomaterials.2008.12.026

Crist, B. (2013). Structure of Polycrystalline Aggregates. In *Handbook of Polymer Crystallization* (pp. 73–124). Hoboken, NJ, USA: John Wiley & Sons, Inc.

http://doi.org/10.1002/9781118541838.ch3

Currie, A., Farber, J. M., Nadon, C., Sharma, D., Whitfield, Y., Gaulin, C., Sierpinska, U. (2015). Multi-Province Listeriosis Outbreak Linked to Contaminated Deli Meat Consumed Primarily in Institutional Settings, Canada, 2008. *Foodborne Pathogens and Disease*, *12*(8), 645–652. http://doi.org/10.1089/fpd.2015.1939

Cyras, V. P., Commisso, M. S., Mauri, A. N., & Vázquez, A. (2007). Biodegradable double-layer films based on biological resources: Polyhydroxybutyrate and cellulose. *Journal of Applied Polymer Science*, *106*(2), 749–756. http://doi.org/10.1002/app.26663

D'Souza, A. J. M., & Topp, E. M. (2004). Release from polymeric prodrugs: Linkages and their degradation. *Journal of Pharmaceutical Sciences*, *93*(8), 1962–1979. http://doi.org/10.1002/jps.20096

Dagdeviren, C., Hwang, S.-W., Su, Y., Kim, S., Cheng, H., Gur, O., … Rogers, J. A. (2013). Transient, biocompatible electronics and energy harvesters based on ZnO. *Small (Weinheim an Der Bergstrasse, Germany)*, *9*(20), 3398–404. http://doi.org/10.1002/smll.201300146

Dai, X., Zhang, J., Ren, Z., Li, H., Sun, X., & Yan, S. (2016). A grazing incident XRD study on the structure of poly(3-hydroxybutyrate) ultrathin films sandwiched between Si wafers and amorphous polymers. *Polym. Chem.*, *7*(22), 3705–3713. http://doi.org/10.1039/C6PY00613B

Daszczuk, A., Dessalegne, Y., Drenth, I., Hendriks, E., Jo, E., van Lente, T., … Veening, J.-W. (2014). *Bacillus subtilis* Biosensor Engineered To Assess Meat Spoilage. *ACS Synthetic Biology*, *3*(12), 999–1002.

http://doi.org/10.1021/sb5000252

Davidson, R. S. (1996). The photodegradation of some naturally occurring polymers. *Journal of Photochemistry and Photobiology B: Biology*, *33*(1), 3–25. http://doi.org/10.1016/1011-1344(95)07262-4

de Koning, G. J. M., & Lemstra, P. J. (1993). Crystallization phenomena in bacterial poly[(R)-3-hydroxybutyrate]: 2. Embrittlement and rejuvenation. *Polymer*, *34*(19), 4089–4094. http://doi.org/10.1016/0032-3861(93)90671-V

de Koning, G. J. M., Lemstra, P. J., Hill, D. J. T., Carswell, T. G., & O'Donnell, J. H. (1992). Ageing phenomena in bacterial poly[(R)-3-hydroxybutyrate]: 1. A study on the mobility in poly[(R)-3-hydroxybutyrate] powders by monitoring the radical decay with temperature after γ-radiolysis at 77 K. *Polymer*, *33*(15), 3295–3297. http://doi.org/10.1016/0032-3861(92)90250-Z

de la Rica, R., Aili, D., & Stevens, M. M. (2012). Enzyme-responsive nanoparticles for drug release and diagnostics. *Advanced Drug Delivery Reviews*, *64*(11), 967–978. http://doi.org/10.1016/j.addr.2012.01.002

Díez-Pascual, A. M., & Díez-Vicente, A. L. (2014). Poly(3-hydroxybutyrate)/ZnO Bionanocomposites with Improved Mechanical, Barrier and Antibacterial Properties. *International Journal of Molecular Sciences*, *15*(6), 10950–10973. http://doi.org/10.3390/ijms150610950

Doi, Y. (1995). Microbial synthesis, physical properties, and biodegradability of polyhydroxyalkanoates. *Macromolecular Symposia*, *98*(1), 585–599. http://doi.org/10.1017/CBO9781107415324.004

Dorgan, J. R., Braun, B., Wegner, J. R., & Knauss, D. M. (2006). Poly(lactic acids): A

Brief Review. In *Degradable Polymers and Materials Principles and Practice* (pp. 102–125). http://doi.org/10.1021/bk-2006-0939.ch007

Drumright, R. E., Gruber, P. R., & Henton, D. E. (2000). Polylactic acid technology. *Advanced Materials*, *12*(23), 1841–1846. http://doi.org/10.1002/1521-4095(200012)12:23<1841::AID-ADMA1841>3.0.CO;2-E

Eason, R. (2007). *Pulsed Laser Deposition of Thin Films: Applications-Led Growth of Functional Materials*. John Wiley & Sons. Retrieved from https://books.google.com/books?hl=en&lr=&id=0jIO3cwkiOIC&pgis=1

El-Hadi, A., Schnabel, R., Straube, E., Müller, G., & Henning, S. (2002). Correlation between degree of crystallinity, morphology, glass temperature, mechanical properties and biodegradation of poly (3-hydroxyalkanoate) PHAs and their blends. *Polymer Testing*, *21*(6), 665–674. http://doi.org/10.1016/S0142-9418(01)00142-8

Elias, A., Sauvageau, D., Storms, Z., Wang, C., Anbukarasu, P., & Martinez-Tobon, D. (2015). Bacteriophage-based biosensor for microbial detection. USPTO. Retrieved from https://patents.google.com/patent/US20160061830A1/en

Ellouze, M., & Augustin, J. C. (2010). Applicability of biological time temperature integrators as quality and safety indicators for meat products. *International Journal of Food Microbiology*, *138*(1–2), 119–129. http://doi.org/10.1016/j.ijfoodmicro.2009.12.012

Erceg, M., Kovačić, T., & Klarić, I. (2005). Thermal degradation of poly(3-hydroxybutyrate) plasticized with acetyl tributyl citrate. *Polymer Degradation and Stability*, *90*(2), 313–318. http://doi.org/10.1016/j.polymdegradstab.2005.04.048

Erythropel, H. C., Maric, M., Nicell, J. A., Leask, R. L., & Yargeau, V. (2014). Leaching

of the plasticizer di(2-ethylhexyl)phthalate (DEHP) from plastic containers and the question of human exposure. *Applied Microbiology and Biotechnology*, *98*(24), 9967–9981. http://doi.org/10.1007/s00253-014-6183-8

Eubeler, J. P., Bernhard, M., & Knepper, T. P. (2010). Environmental biodegradation of synthetic polymers II. Biodegradation of different polymer groups. *TrAC - Trends in Analytical Chemistry*, *29*(1), 84–100. http://doi.org/10.1016/j.trac.2009.09.005

Fasano, E., Bono-Blay, F., Cirillo, T., Montuori, P., & Lacorte, S. (2012). Migration of phthalates, alkylphenols, bisphenol A and di(2-ethylhexyl)adipate from food packaging. *Food Control*, *27*(1), 132–138. http://doi.org/10.1016/j.foodcont.2012.03.005

Forrest, J. A., & Dalnoki-Veress, K. (2001). The glass transition in thin polymer films. *Advances in Colloid and Interface Science*, *94*(1), 167–195. http://doi.org/10.1016/S0001-8686(01)00060-4

Frank, C. W., Rao, V., Despotopoulou, M. M., Pease, R. F. W., Hinsberg, W. D., Miller, R. D., & Rabolt, J. F. (1996). Structure in Thin and Ultrathin Spin-Cast Polymer Films. *Science*, *273*(5277), 912–915. http://doi.org/10.1126/science.273.5277.912

Fu, B., Taoukis, P. S., & Labuza, T. P. (1991). Predictive Microbiology for Monitoring Spoilage of Dairy Products with Time-Temperature Integrators. *Journal of Food Science*, *56*(5), 1209–1215. http://doi.org/10.1111/j.1365-2621.1991.tb04736.x

Galagan, Y., & Su, W. F. (2008). Fadable ink for time-temperature control of food freshness: Novel new time-temperature indicator. *Food Research International*, *41*(6), 653–657. http://doi.org/10.1016/j.foodres.2008.04.012

Galotto, M., & Ulloa, P. (2010). Development and Application of Time–temperature

Indicators Used on Food during the Cold Chain Logistics. *Packaging and Technology and Science*, *23*(May), 253–266. http://doi.org/10.1002/pts

Gazzano, M., Tomasi, G., & Scandola, M. (1997). X-ray investigation on melt-crystallized bacterial poly(3-hydroxybutyrate). *Macromolecular Chemistry and Physics*, *198*(1), 71–80. http://doi.org/10.1002/macp.1997.021980106

Gentile, P., Chiono, V., Carmagnola, I., & Hatton, P. V. (2014). An overview of poly(lactic-co-glycolic) acid (PLGA)-based biomaterials for bone tissue engineering. *International Journal of Molecular Sciences*, *15*(3), 3640–59. http://doi.org/10.3390/ijms15033640

Ghormade, V., Pathan, E. K., & Deshpande, M. V. (2017). Can fungi compete with marine sources for chitosan production? *International Journal of Biological Macromolecules*, *104*, 1415–1421. http://doi.org/10.1016/j.ijbiomac.2017.01.112

Gil, E. S., & Hudson, S. M. (2004). Stimuli-reponsive polymers and their bioconjugates. *Progress in Polymer Science (Oxford)*, *29*(12), 1173–1222. http://doi.org/10.1016/j.progpolymsci.2004.08.003

Giuliana, G., & Roberto, P. (2013). Effect of PLA grades and morphologies on hydrolytic degradation at composting temperature: Assessment of structural modification and kinetic parameters. *Polymer Degradation and Stability*, *98*(5), 1006–1014. http://doi.org/10.1016/J.POLYMDEGRADSTAB.2013.02.005

Goldsmith, R. M. (1994, April). Detection of contaminants in food.

Goldsmith, R. M., Goldsmith, C. H., & Woodaman, J. G. (2002, November). Dual bar code for food contamination detection.

Gonzalez-Aguilar, G. A., Ayala-Zavala, J. F., Ruiz-Cruz, S., Acedo-F??lix, E., & D??az-

Cinco, M. E. (2004). Effect of temperature and modified atmosphere packaging on overall quality of fresh-cut bell peppers. *LWT - Food Science and Technology*, *37*(8), 817–826. http://doi.org/10.1016/j.lwt.2004.03.007

Gopferich, A. (1996). Mechanism of Polymer Degradation and Erosion. *Biomaterials*, *17*(2), 103–114. http://doi.org/10.1016/0142-9612(96)85755-3

Griffin, G. J. L. (1973). Biodegradable Fillers In Thermoplastics. *Am Chem Soc Div Org Coatings Plast Chem Prepr*, *33*(2), 88–96.

Griffin, M., Casadio, R., & Bergamini, C. M. (2002). Transglutaminases: Nature's biological glues. *Biochemical Journal*, *368*(2). http://doi.org/10.1042/BJ20021234

Gunaratne, L. M. W. K., & Shanks, R. A. (2005). Multiple melting behaviour of poly(3-hydroxybutyrate-co-hydroxyvalerate) using step-scan DSC. *European Polymer Journal*, *41*(12), 2980–2988. http://doi.org/10.1016/j.eurpolymj.2005.06.015

Gunaratne, L. M. W. K., Shanks, R. a., & Amarasinghe, G. (2004). Thermal history effects on crystallisation and melting of poly(3-hydroxybutyrate). *Thermochimica Acta*, *423*(1–2), 127–135. http://doi.org/10.1016/j.tca.2004.05.003

Hancock, B. C., & Zografi, G. (1997). Characteristics and Significance of the Amorphous State in Pharmaceutical Systems. *Journal of Pharmaceutical Sciences*, *86*(1), 1–12. http://doi.org/10.1021/js9601896

Hariharan, A., Kumar, S. K., & Russell, T. P. (1990). A lattice model for the surface segregation of polymer chains due to molecular weight effects. *Macromolecules*, *23*(15), 3584–3592. http://doi.org/10.1021/ma00217a009

He, Y., Shuai, X., Kasuya, K. I., Doi, Y., & Inoue, Y. (2001). Enzymatic degradation of atactic poly(R,S-3-hydroxybutyrate) induced by amorphous polymers and the

enzymatic degradation temperature window of an amorphous polymer system. *Biomacromolecules*, *2*(3), 1045–1051. http://doi.org/10.1021/bm010087w

Hiraishi, T., Hirahara, Y., Doi, Y., Maeda, M., & Taguchi, S. (2006). Effects of mutations in the substrate-binding domain of poly[(R)-3-hydroxybutyrate] (PHB) depolymerase from Ralstonia pickettii T1 on PHB degradation. *Applied and Environmental Microbiology*, *72*(11), 7331–7338. http://doi.org/10.1128/AEM.01187-06

Hiraishi, T., Komiya, N., & Maeda, M. (2010). Y443F mutation in the substrate-binding domain of extracellular PHB depolymerase enhances its PHB adsorption and disruption abilities. *Polymer Degradation and Stability*, *95*(8), 1370–1374. http://doi.org/10.1016/j.polymdegradstab.2010.01.022

Hiraishi, T., Komiya, N., Matsumoto, N., Abe, H., Fujita, M., & Maeda, M. (2010). Degradation and adsorption characteristics of PHB depolymerase as revealed by kinetics of mutant enzymes with amino acid substitution in substrate-binding domain. *Biomacromolecules*, *11*(1), 113–119. http://doi.org/10.1021/bm900967a

Hoffman, A. S., Stayton, P. S., Shimoboji, T., Chen, G., Ding, Z., Chilkoti, A., … Nakamae, K. (1997). Conjugates of Stimuli-Responsive Polymers and Biomolecules: Random and Site-Specific Conjugates of Temperature-Sensitive Polymers and Proteins. *Macromolecular Symposia*, *118*, 553–563.

Hofmann, D., Entrialgo-Castaño, M., Kratz, K., & Lendlein, A. (2009). Knowledge-Based Approach towards Hydrolytic Degradation of Polymer-Based Biomaterials. *Advanced Materials*, *21*(32–33), 3237–3245. http://doi.org/10.1002/adma.200802213

Holmes, P. A. (1985). Applications of PHB - a microbially produced biodegradable thermoplastic. *Physics in Technology*, *16*(1), 32–36. http://doi.org/10.1088/0305-4624/16/1/305

Holum, J. R. (1987). *Elements of general and biological chemistry*. Wiley. Retrieved from https://books.google.ca/books/about/Elements_of_General_and_Biological_Chemi.html?id=gw41AAAAMAAJ&redir_esc=y

Hsiao, B. S., Zuo, F., Mao, Y., & Schick, C. (2013). Experimental Techniques. In E. Piorkowska & G. C. Rutledge (Eds.), *Handbook of Polymer Crystallization* (pp. 1–30). John Wiley & Sons, Inc.

Hu, J., Zhang, G., & Liu, S. (2012). Enzyme-responsive polymeric assemblies, nanoparticles and hydrogels. *Chemical Society Reviews*, *41*(18), 5933–5949. http://doi.org/10.1039/c2cs35103j

Hu, J., Zhang, G., & Liu, S. (2012). Enzyme-responsive polymeric assemblies, nanoparticles and hydrogels. *Chemical Society Reviews*, *41*(18), 5933. http://doi.org/10.1039/c2cs35103j

Hu, X., Shmelev, K., Sun, L., Gil, E.-S., Park, S.-H., Cebe, P., & Kaplan, D. L. (2011). Regulation of silk material structure by temperature-controlled water vapor annealing. *Biomacromolecules*, *12*(5), 1686–96. http://doi.org/10.1021/bm200062a

Hurrell, B. L., & Cameron, R. E. (1998). A wide-angle X-ray scattering study of the ageing of poly(hydroxybutyrate). *Journal of Materials Science*, *33*(7), 1709–1713. http://doi.org/10.1023/A:1004364112658

Hutmacher, D. W. (2000). Scaffolds in tissue engineering bone and cartilage.

Biomaterials, *21*(24), 2529–2543.

Iordanskii, A. L., Zaikov, G. E., & Berlin, A. A. (2015). Diffusion kinetics of hydrolysis of biodegradable polymers. Weight loss and control of the release of low molecular weight substances. *Polymer Science - Series D*, *8*(3), 211–218. http://doi.org/10.1134/S1995421215030053

Ikejima, I., Inoue, Y. Crystallization behavior and environmental biodegradability of the blend films of poly(3-hydroxybutyric acid) with chitin and chitosan. (2000). *Carbohydrate Polymers*, *41*(4), 351–356. http://doi.org/10.1016/S0144-8617(99)00105-8

Irimia-Vladu, M., Troshin, P. A., Reisinger, M., Shmygleva, L., Kanbur, Y., Schwabegger, G., … Bauer, S. (2010). Biocompatible and Biodegradable Materials for Organic Field-Effect Transistors. *Advanced Functional Materials*, *20*(23), 4069–4076. http://doi.org/10.1002/adfm.201001031

Islam, M. R., Gao, Y., Li, X., & Serpe, M. J. (2014). Responsive polymers for biosensing and protein delivery. *Journal of Materials Chemistry B*, *2*(17), 2444–2451. http://doi.org/10.1039/c3tb21657h

Islam, M. R., Lu, Z., Li, X., Sarker, A. K., Hu, L., Choi, P., … Serpe, M. J. (2013). Responsive polymers for analytical applications: A review. *Analytica Chimica Acta*, *789*, 17–32. http://doi.org/10.1016/j.aca.2013.05.009

Iwata, T., Abe, H., & Kikkawa, Y. (2010). *Enzymatic Degradation*. *Poly(Lactic Acid): Synthesis, Structures, Properties, Processing, and Applications*. http://doi.org/10.1002/9780470649848.ch22

Iwata, T., Doi, Y., Kasuya, K., & Inoue, Y. (1997). Visualization of Enzymatic

Degradation of Poly[(R)-3-hydroxybutyrate] Single Crystals by an Extracellular PHB Depolymerase,Ä†. *Macromolecules*, *30*(4), 833–839. http://doi.org/10.1021/ma961352m

Iwata, T., Doi, Y., Tanaka, T., Akehata, T., Shiromo, M., & Teramachi, S. (1997a). Enzymatic Degradation and Adsorption on Poly[(R)-3-hydroxybutyrate] Single Crystals with Two Types of Extracellular PHB Depolymerases from Comamonas acidovorans YM1609 and Alcaligenes faecalis T1. *Macromolecules*, *30*(18), 5290–5296. http://doi.org/10.1021/ma970491g

Iwata, T., Doi, Y., Tanaka, T., Akehata, T., Shiromo, M., & Teramachi, S. (1997b). Enzymatic Degradation and Adsorption on Poly[(R)-3-hydroxybutyrate] Single Crystals with Two Types of Extracellular PHB Depolymerases from Comamonas acidovorans YM1609 and Alcaligenes faecalis T1. *Macromolecules*, *30*(97), 5290–5296. http://doi.org/10.1021/ma970491g

Jacquel, N., Lo, C.-W., Wu, H.-S., Wei, Y.-H., & Wang, S. S. (2007). Solubility of polyhydroxyalkanoates by experiment and thermodynamic correlations. *AIChE Journal*, *53*(10), 2704–2714. http://doi.org/10.1002/aic.11274

Jambeck, J. R., Geyer, R., Wilcox, C., Siegler, T. R., Perryman, M., Andrady, A., … Law, K. L. (2015). Marine pollution. Plastic waste inputs from land into the ocean. *Science (New York, N.Y.)*, *347*(6223), 768–71. http://doi.org/10.1126/science.1260352

Janigová, I., Lacík, I., & Chodák, I. (2002). Thermal degradation of plasticized poly(3-hydroxybutyrate) investigated by DSC. *Polymer Degradation and Stability*, *77*(1), 35–41. http://doi.org/10.1016/S0141-3910(02)00077-0

Jendrossek, D., & Handrick, R. (2002). *Microbial degradation of polyhydroxyalkanoates*. *Annual Review of Microbiology* (Vol. 56). http://doi.org/10.1146/annurev.micro.56.012302.160838

Jendrossek, D., & Handrick, R. (2002). Microbial Degradation of Polyhydroxyalkanoates*. *Annual Review of Microbiology*, *56*(1), 403–432. http://doi.org/10.1146/annurev.micro.56.012302.160838

Jeon, H.-Y., Jung, S.-H., Jung, Y. M., Kim, Y.-M., Ghandehari, H., & Ha, K.-S. (2016). Array-Based High-Throughput Analysis of Silk-Elastinlike Protein Polymer Degradation and C-Peptide Release by Proteases. *Analytical Chemistry*, *88*(10), 5398–5405. http://doi.org/10.1021/acs.analchem.6b00739

Jeong, B., Bae, Y. H., Lee, D. S., & Kim, S. W. (1997). Biodegradable block copolymers as injectable drug-delivery systems. *Nature*, *388*(6645), 860–862. http://doi.org/10.1038/42218

John A. Rogers, Dae Hyeong Kim, Joshua D. Moss, David J. Callins, Brian Litt, J. V. (2012, June 21). High-Speed, High-Resolution Electrophysiology In-Vivo Using Conformal Electronics. United States: US Patent. Retrieved from https://www-google-com.login.ezproxy.library.ualberta.ca/patents/US20120157804

Kabilan, S., Marshall, A. J., Sartain, F. K., Lee, M. C., Hussain, A., Yang, X., … Lowe, C. R. (2005). Holographic glucose sensors. *Biosensors and Bioelectronics*, *20*(8 SPEC. ISS.), 1602–1610. http://doi.org/10.1016/j.bios.2004.07.005

Kai, D., & Loh, X. J. (2014). Polyhydroxyalkanoates: Chemical Modifications Toward Biomedical Applications. *ACS Sustainable Chemistry & Engineering*, *2*(2), 106–119. http://doi.org/10.1021/sc400340p

Kaltenbrunner, M., Sekitani, T., Reeder, J., Yokota, T., Kuribara, K., Tokuhara, T., … Someya, T. (2013). An ultra-lightweight design for imperceptible plastic electronics. *Nature*, *499*(7459), 458–63. http://doi.org/10.1038/nature12314

Kang, S.-K., Murphy, R. K. J., Hwang, S.-W., Lee, S. M., Harburg, D. V., Krueger, N. A., … Rogers, J. A. (2016). Bioresorbable silicon electronic sensors for the brain. *Nature*, *530*(7588), 71–76. http://doi.org/10.1038/nature16492

Karlsson, S., & Albertsson, A. (1998). Biodegradable polymers and environmental interaction. *Polymer Engineering & Science*, *38*(8), 1251–1253. http://doi.org/10.1002/pen.10294

Kasuya, K. ichi, Doi, Y., & Yao, T. (1994). Enzymatic degradation of poly[(R)-3-hydroxybutyrate] by Comamonas testosteroni ATSU of soil bacterium. *Polymer Degradation and Stability*, *45*(3), 379–386. http://doi.org/10.1016/0141-3910(94)90208-9

Kasuya, K., Inoue, Y., Yamada, K., & Doi, Y. (1995). Kinetics of surface hydrolysis of poly[(R)-3-hydroxybutyrate] film by PHB depolymerase from Alcaligenes faecalis T1. *Polymer Degradation and Stability*, *48*(1), 167–174. http://doi.org/10.1016/0141-3910(95)00026-I

Kecskemeti, G., Smausz, T., Kresz, N., Tóth, Z., Hopp, B., Chrisey, D., & Berkesi, O. (2006). Pulsed laser deposition of polyhydroxybutyrate biodegradable polymer thin films using ArF excimer laser. *Applied Surface Science*, *253*(3), 1185–1189. http://doi.org/10.1016/j.apsusc.2006.01.084

Keshavarz, T., & Roy, I. (2010). Polyhydroxyalkanoates: bioplastics with a green agenda. *Current Opinion in Microbiology*, *13*(3), 321–6.

http://doi.org/10.1016/j.mib.2010.02.006

Khasanah, Reddy, K. R., Ogawa, S., Sato, H., Takahashi, I., & Ozaki, Y. (2016a). Evolution of Intermediate and Highly Ordered Crystalline States under Spatial Confinement in Poly(3-hydroxybutyrate) Ultrathin Films.

Khasanah, Reddy, K. R., Ogawa, S., Sato, H., Takahashi, I., & Ozaki, Y. (2016b). Evolution of Intermediate and Highly Ordered Crystalline States under Spatial Confinement in Poly(3-hydroxybutyrate) Ultrathin Films. *Macromolecules*, acs.macromol.6b00431. http://doi.org/10.1021/acs.macromol.6b00431

Khasanah, Reddy, K. R., Ogawa, S., Sato, H., Takahashi, I., & Ozaki, Y. (2016c). Evolution of Intermediate and Highly Ordered Crystalline States under Spatial Confinement in Poly(3-hydroxybutyrate) Ultrathin Films. *Macromolecules*, acs.macromol.6b00431. http://doi.org/10.1021/acs.macromol.6b00431

Khorasani, M. T., Mirmohammadi, S. A., & Irani, S. (2011). Polyhydroxybutyrate (PHB) Scaffolds as a Model for Nerve Tissue Engineering Application: Fabrication and In Vitro Assay. *International Journal of Polymeric Materials*, *60*(8), 562–575. http://doi.org/10.1080/00914037.2010.531809

Kim, D.-H., Lu, N., Ma, R., Kim, Y.-S., Kim, R.-H., Wang, S., … Rogers, J. A. (2011). Epidermal electronics. *Science (New York, N.Y.)*, *333*(6044), 838–43. http://doi.org/10.1126/science.1206157

Kim, D.-H., Viventi, J., Amsden, J. J., Xiao, J., Vigeland, L., Kim, Y.-S., … Rogers, J. A. (2010). Dissolvable films of silk fibroin for ultrathin conformal bio-integrated electronics. *Nature Materials*, *9*(6), 511–7. http://doi.org/10.1038/nmat2745

Kim, J. U., Ghafoor, K., Ahn, J., Shin, S., Lee, S. H., Shahbaz, H. M., … Park, J. (2016).

Kinetic modeling and characterization of a diffusion-based time-temperature indicator (TTI) for monitoring microbial quality of non-pasteurized angelica juice. *LWT - Food Science and Technology*, *67*, 143–150. http://doi.org/10.1016/j.lwt.2015.11.034

Kim Meera. (2005). Antimicrobial Activity of PHB/Chitosan Films and Quality of White Bread Packaged with the Films. *Korean Journal of Human Ecology*, *14*(2), 321–330.

Knoll, W., & Advincula, R. C. (2011). *Functional Polymer Films*. *Functional Polymer Films* (Vol. 1–2). Weinheim: Wiley-VCH. http://doi.org/10.1002/9783527638482

Kossack, W., Seidlitz, A., Thurn-Albrecht, T., & Kremer, F. (2016). Interface and Confinement Induced Order and Orientation in Thin Films of Poly(ϵ-caprolactone).

Koyama, N., & Doi, Y. (1995). Morphology and biodegradability of a binary blend of poly((R)-3-hydroxybutyric acid) and poly((R,S)-lactic acid). *Canadian Journal of Microbiology*, *41*(13), 316–322. http://doi.org/10.1139/m95-203

Koyama, N., & Doi, Y. (1997). Effects of Solid-State Structures on the Enzymatic Degradability of Bacterial Poly(hydroxyalkanoic acids). *Macromolecules*, *30*(4), 826–832. http://doi.org/10.1021/ma961195r

Kumagai, Y., Kanesawa, Y., & Doi, Y. (1992a). Enzymatic degradation of microbial poly(3-hydroxybutyrate) films. *Die Makromolekulare Chemie*, *193*(1), 53–57. http://doi.org/10.1002/macp.1992.021930105

Kumagai, Y., Kanesawa, Y., & Doi, Y. (1992b). Enzymatic degradation of microbial poly(3-hydroxybutyrate) films. *Die Makromolekulare Chemie*, *193*(1), 53–57. http://doi.org/10.1002/macp.1992.021930105

Labet, M., & Thielemans, W. (2009). Synthesis of polycaprolactone: A review. *Chemical Society Reviews*, *38*(12), 3484–3504. http://doi.org/10.1039/b820162p

Labuza, T. P. (1982). *Shelf-life dating of foods.* Food & Nutrition Press, Inc. Retrieved from http://www.cabdirect.org/abstracts/19820482746.html

Lai, S.-M., Don, T.-M., & Huang, Y.-C. (2006). Preparation and properties of biodegradable thermoplastic starch/poly(hydroxy butyrate) blends. *Journal of Applied Polymer Science*, *100*(3), 2371–2379. http://doi.org/10.1002/app.23085

Lakshmanan, R. S., Guntupalli, R., Hu, J., Petrenko, V. A., Barbaree, J. M., & Chin, B. A. (2007). Detection of Salmonella typhimurium in fat free milk using a phage immobilized magnetoelastic sensor. *Sensors and Actuators B: Chemical*, *126*(2), 544–550. http://doi.org/10.1016/j.snb.2007.04.003

Lander, T., & Bodenhamer, W. T. (2005, March). Biological material detecting articles of manufacture.

Landuzzi, A., & Ghosh, J. (2003). Improving Functionality of Polyolefin Films Through the Use of Additives. *Journal of Plastic Film & Sheeting*, *19*(1). http://doi.org/10.1177/8756087903040175

Larsson, R. P. (1974). Time-temperature integrating indicator. US.

Law, J. W.-F., Ab Mutalib, N.-S., Chan, K.-G., & Lee, L.-H. (2015). Rapid methods for the detection of foodborne bacterial pathogens: principles, applications, advantages and limitations. *Frontiers in Microbiology*, *5*, 770. http://doi.org/10.3389/fmicb.2014.00770

Le Berre, C., Serp, P., Kalck, P., & Torrence, G. P. (2000). Acetic Acid. In *Ullmann's Encyclopedia of Industrial Chemistry*. Wiley-VCH Verlag GmbH & Co. KGaA.

Le Brasseur, G. (1975). Degradable polyethylenes for agricultural use. *INFORM. CHIM.*, *No. 149*, 231–235.

Lee, S. G., Choi, S.-S., Park, W. H., & Cho, D. (2003). Characterization of surface modified flax fibers and their biocomposites with PHB. *Macromolecular Symposia*, *197*(1), 089–100. http://doi.org/10.1002/masy.200350709

Lee, S. H., Kim, I. Y., & Song, W. S. (2014). Biodegradation of polylactic acid (PLA) fibers using different enzymes. *Macromolecular Research*, *22*(6), 657–663. http://doi.org/10.1007/s13233-014-2107-9

Lee, S. H., & Yeo, S. Y. (2016). Improvement of hydrophilicity of polylactic acid (PLA) fabrics by means of a proteolytic enzyme from Bacillus licheniformis. *Fibers and Polymers*, *17*(8), 1154–1161. http://doi.org/10.1007/s12221-016-5923-z

Lee, S. Y. (1996a). Bacterial polyhydroxyalkanoates. *Biotechnology and Bioengineering*, *49*(1), 1–14. http://doi.org/10.1002/(SICI)1097-0290(19960105)49:1<1::AID-BIT1>3.0.CO;2-P

Lee, S. Y. (1996b). Plastic bacteria? Progress and prospects for polyhydroxyalkanoate production in bacteria. *Trends in Biotechnology*, *14*(11), 431–438. http://doi.org/10.1016/0167-7799(96)10061-5

Lendlein, A., & Langer, R. (2002). Biodegradable, elastic shape-memory polymers for potential biomedical applications. *Science*, *296*(5573), 1673–1676. http://doi.org/10.1126/science.1066102

Leu, S.-Y., & Zhu, J. Y. (2013). Substrate-Related Factors Affecting Enzymatic Saccharification of Lignocelluloses: Our Recent Understanding. *BioEnergy Research*, *6*(2), 405–415. http://doi.org/10.1007/s12155-012-9276-1

Li, J., Li, X., Ni, X., Wang, X., Li, H., & Leong, K. W. (2006). Self-assembled supramolecular hydrogels formed by biodegradable PEO–PHB–PEO triblock copolymers and α-cyclodextrin for controlled drug delivery. *Biomaterials*, *27*(22), 4132–4140. http://doi.org/10.1016/j.biomaterials.2006.03.025

Li, M., Tang, H. X., & Roukes, M. L. (2007). Ultra-sensitive NEMS-based cantilevers for sensing, scanned probe and very high-frequency applications. *Nature Nanotechnology*, *2*(2), 114–20. http://doi.org/10.1038/nnano.2006.208

Lianou, A., & Sofos, J. N. (2007). A Review of the Incidence and Transmission of Listeria monocytogenes in Ready-to-Eat Products in Retail and Food Service Environments. *Journal of Food Protection*, *70*(9), 2172–2198. http://doi.org/10.4315/0362-028X-70.9.2172

Limbo, S., Torri, L., Sinelli, N., Franzetti, L., & Casiraghi, E. (2010). Evaluation and predictive modeling of shelf life of minced beef stored in high-oxygen modified atmosphere packaging at different temperatures. *Meat Science*, *84*(1), 129–136. http://doi.org/10.1016/j.meatsci.2009.08.035

Lin, Z.-T., Gu, J., Li, C.-H., Lee, T. R., Xie, L., Chen, S., … Wu, T. (2017). A Nanoparticle-Decorated Biomolecule-Responsive Polymer Enables Robust Signaling Cascade for Biosensing. *Advanced Materials*, *29*(31). http://doi.org/10.1002/adma.201702090

Liu, X., Gao, C., Sangwan, P., Yu, L., & Tong, Z. (2014). Accelerating the degradation of polyolefins through additives and blending. *Journal of Applied Polymer Science*, *131*(18), 9001–9015. http://doi.org/10.1002/app.40750

Liu, Y. X., & Chen, E. Q. (2010a). Polymer crystallization of ultrathin films on solid

substrates. *Coordination Chemistry Reviews*, *254*(9–10), 1011–1037. http://doi.org/10.1016/j.ccr.2010.02.017

Liu, Y. X., & Chen, E. Q. (2010b). Polymer crystallization of ultrathin films on solid substrates. *Coordination Chemistry Reviews*. http://doi.org/10.1016/j.ccr.2010.02.017

Loewen, E. G., & Popov, E. (1997). *Diffraction Gratings and Applications*. New York: CRC Press. Retrieved from https://books.google.com/books?id=llMBiFGO4pMC&pgis=1

Loh, X. J., Goh, S. H., & Li, J. (2007). Hydrolytic degradation and protein release studies of thermogelling polyurethane copolymers consisting of poly[(R)-3-hydroxybutyrate], poly(ethylene glycol), and poly(propylene glycol). *Biomaterials*, *28*(28), 4113–4123. http://doi.org/10.1016/j.biomaterials.2007.05.016

Loh, X. J., Zhang, Z.-X., Wu, Y.-L., Lee, T. S., & Li, J. (2009). Synthesis of Novel Biodegradable Thermoresponsive Triblock Copolymers Based on Poly[(R)-3-hydroxybutyrate] and Poly(N-isopropylacrylamide) and Their Formation of Thermoresponsive Micelles. *Macromolecules*, *42*(1), 194–202. http://doi.org/10.1021/ma8019865

Lynd, L. R., Weimer, P. J., van Zyl, W. H., & Pretorius, I. S. (2002). Microbial cellulose utilization: fundamentals and biotechnology. *Microbiology and Molecular Biology Reviews : MMBR*, *66*(3), 506–77, table of contents. http://doi.org/10.1128/MMBR.66.3.506-577.2002

Ma, C. D., Adamiak, L., Miller, D. S., Wang, X., Gianneschi, N. C., & Abbott, N. L. (2015). Liquid Crystal Interfaces Programmed with Enzyme-Responsive Polymers

and Surfactants. *Small*, *11*(43), 5747–5751. http://doi.org/10.1002/smll.201502137

Madhavan Nampoothiri, K., Nair, N. R., & John, R. P. (2010). An overview of the recent developments in polylactide (PLA) research. *Bioresource Technology*, *101*(22), 8493–8501. http://doi.org/10.1016/j.biortech.2010.05.092

Madison, L. L., & Huisman, G. W. (1999). Metabolic engineering of poly(3-hydroxyalkanoates): From DNA to plastic. *Microbiology and Molecular Biology Reviews*, *63*(1), 21–53.

Madras, G. (2005). *Enzymatic degradation of polymers*. *Biodegradable Polymers for Industrial Applications*. http://doi.org/10.1533/9781845690762.3.411

Manning, L., Wallace, C., & Soon, J. (2016). Foodborne Disease Outbreaks in Complex Manufacturing Establishments. In *Foodborne Diseases* (pp. 287–312). CRC Press. http://doi.org/10.1201/b19463-14

Marchessault, R. H., Bluhm, T. L., Deslandes, Y., Hamer, G. K., Orts, W. J., Sundararajan, P. R., … Holden, D. A. (1988). Poly(β-hydroxyalkanoates): Biorefinery polymers in search of applications. *Makromolekulare Chemie. Macromolecular Symposia*, *19*(1), 235–254. http://doi.org/10.1002/masy.19880190120

Marshall, A. J., Kabilan, S., Blyth, J., & Lowe, C. R. (2006). Analyte-responsive holograms for (bio)chemical analysis. *Journal of Physics: Condensed Matter*, *18*(18), S619–S626. http://doi.org/10.1088/0953-8984/18/18/S08

Marx, K. A. (2003). Quartz crystal microbalance: a useful tool for studying thin polymer films and complex biomolecular systems at the solution-surface interface. *Biomacromolecules*, *4*(5), 1099–120. http://doi.org/10.1021/bm020116i

Matthew Cole, Pennie Lindeque, Claudia Halsband, T. S. G. (2011). Microplastics as contaminants in the marine environment: A review. *Marine Pollution Bulletin*, *62*(12), 2588–2597. http://doi.org/10.1016/J.MARPOLBUL.2011.09.025

Maurizi, M. R. (1992). Proteases and protein degradation inEscherichia coli. *Experientia*, *48*(2), 178–201. http://doi.org/10.1007/BF01923511

Mayer, J. M., Kaplan, D. L., Stote, R. E., Dixon, K. L., Shupe, A. E., Allen, A. L., & McCassie, J. E. (1996). *Biodegradation of Polymer Films in Marine and Soil Environments*. *ACS Symposium Series* (Vol. 627).

Mayes, A. G., Blyth, J., Millington, R. B., & Lowe, C. R. (2002). Metal Ion-Sensitive Holographic Sensors. *Analytical Chemistry*, *74*(15), 3649–3657. http://doi.org/10.1021/ac020131d

Mead, P. S., Dunne, E. F., Graves, L., Wiedmann, M., Patrick, M., Hunter, S., Swaminathan, B. (2006). Nationwide outbreak of listeriosis due to contaminated meat. *Epidemiology and Infection*, *134*(4), 744. http://doi.org/10.1017/S0950268805005376

Menczel, J. D., & Prime, R. B. (2014). *Thermal Analysis of Polymers: Fundamentals and Applications*. John Wiley & Sons.

Mendes, P. M. (2008). Stimuli-responsive surfaces for bio-applications. *Chemical Society Reviews*, *37*(11), 2512–2529. http://doi.org/10.1039/b714635n

Mester, Z., & Sturgeon, R. E. (2003). *Sample Preparation for Trace Element Analysis*. Elsevier.

Michlmayr, H., & Kneifel, W. (2014). β-Glucosidase activities of lactic acid bacteria: Mechanisms, impact on fermented food and human health. *FEMS Microbiology*

Letters, *352*(1), 1–10. http://doi.org/10.1111/1574-6968.12348

Middleton, J. C., & Tipton, A. J. (2000). Synthetic biodegradable polymers as orthopedic devices. *Biomaterials*, *21*(23), 2335–2346. http://doi.org/10.1016/S0142-9612(00)00101-0

Middleton, J. C., & Tipton, A. J. (2000). Synthetic biodegradable polymers as orthopedic devices. *Biomaterials*, *21*(23), 2335–2346. http://doi.org/10.1016/S0142-9612(00)00101-0

Millan, M. D., Locklin, J., Fulghum, T., Baba, A., & Advincula, R. C. (2005). Polymer thin film photodegradation and photochemical crosslinking: FT-IR imaging, evanescent waveguide spectroscopy, and QCM investigations. *Polymer*, *46*(15), 5556–5568. http://doi.org/10.1016/j.polymer.2005.05.050

Miller, N. D., & Williams, D. F. (1987). On the biodegradation of poly-β-hydroxybutyrate (PHB) homopolymer and poly-β-hydroxybutyrate-hydroxyvalerate copolymers. *Biomaterials*, *8*(2), 129–137. http://doi.org/10.1016/0142-9612(87)90102-5

Mizuno, W., Maeda, Y., Kozima, K., Takamichi, T., Miyabe, K., & Takeuchi, S. (2001). Degradation behavior of injection molded biodegradable polymers in soil, aqueous environments, and an activated sludge. *Kobunshi Ronbunshu*, *58*(2), 59–65.

Mochizuki, M., Mukai, K., Yamada, K., Ichise, N., Murase, S., & Iwaya, Y. (1997). Structural Effects upon Enzymatic Hydrolysis of Poly(butylene succinate-co-ethylene succinate)s. *Macromolecules*, *30*(24), 7403–7407. http://doi.org/10.1021/ma970036k

Mohnen, D. (2008). Pectin structure and biosynthesis. *Current Opinion in Plant Biology*, *11*(3), 266–277. http://doi.org/10.1016/j.pbi.2008.03.006

Moreira, J. C., & Demarquette, N. R. (2001). Influence of temperature, molecular weight, and molecular weight dispersity on the surface tension of PS, PP, and PE. I. Experimental. *Journal of Applied Polymer Science*, *82*(8), 1907–1920. http://doi.org/10.1002/app.2036

Mrozik, A., Hupert-Kocurek, K., Nowak, B., & Łabuzek, S. (2008). Microbial lipases and their significance in the protection of the environment. *Postepy Mikrobiologii*, *47*(1), 43–50.

Muir, D. D. (1996). The shelf-life of dairy products: 1. Factors influencing raw milk and fresh products. *International Journal of Dairy Technology*, *49*(1), 24–32. http://doi.org/10.1111/j.1471-0307.1996.tb02616.x

Mukai, K., Yamada, K., & Doi, Y. (1993a). Enzymatic degradation of poly(hydroxyalkanoates) by a marine bacterium. *Polymer Degradation and Stability*, *41*(1), 85–91. http://doi.org/10.1016/0141-3910(93)90066-R

Mukai, K., Yamada, K., & Doi, Y. (1993b). Kinetics and mechanism of heterogeneous hydrolysis of poly[(R)-3-hydroxybutyrate] film by PHA depolymerases. *International Journal of Biological Macromolecules*, *15*(6), 361–366. http://doi.org/10.1016/0141-8130(93)90054-P

Mukai, K., Yamada, K., & Doi, Y. (1993). Kinetics and mechanism of heterogeneous hydrolysis of poly[(R)-3-hydroxybutyrate] film by PHA depolymerases. *International Journal of Biological Macromolecules*, *15*(6), 361–366. http://doi.org/10.1016/0141-8130(93)90054-P

Mukai, K., Yamada, K., & Doi, Y. (1993c). Kinetics and mechanism of heterogeneous hydrolysis of poly[(R)-3-hydroxybutyrate] film by PHA depolymerases. *International*

Journal of Biological Macromolecules, *15*(6), 361–366. http://doi.org/10.1016/0141-8130(93)90054-P

Müller, A. J., Arnal, M. L., & Lorenzo, A. T. (2013). Crystallization in Nano-Confined Polymeric Systems. In *Handbook of Polymer Crystallization* (pp. 347–378). Hoboken, NJ, USA: John Wiley & Sons, Inc. http://doi.org/10.1002/9781118541838.ch12

Muñoz, K. A., Krebs-Smith, S. M., Ballard-Barbash, R., & Cleveland, L. E. (1997). Food intakes of US children and adolescents compared with recommendations. *Pediatrics*, *100*(3), 323–329. http://doi.org/10.1542/peds.100.3.323

Nalli, S., Cooper, D. G., & Nicell, J. a. (2006). Metabolites from the biodegradation of di-ester plasticizers by Rhodococcus rhodochrous. *The Science of the Total Environment*, *366*(1), 286–94. http://doi.org/10.1016/j.scitotenv.2005.06.020

Napolitano, S.; Wübbenhorst, N. (2007). Deviation from bulk behaviour in the cold crystallization kinetics of ultrathin films of poly(3-hydroxybutyrate). *Journal of Physics: Condensed Matter*, *19*(20), 205121. http://doi.org/10.1088/0953-8984/19/20/205121

Napolitano, S., & Wübbenhorst, M. (2006). Slowing Down of the Crystallization Kinetics in Ultrathin Polymer Films: A Size or an Interface Effect? *Macromolecules*, *39*(18), 5967–5970. http://doi.org/10.1021/ma061304u

Nduko, J. M., Sun, J., & Taguchi, S. (2015). *Biosynthesis, Properties, and Biodegradation of Lactate-Based Polymers*. *ACS Symposium Series* (Vol. 1192). http://doi.org/10.1021/bk-2015-1192.ch008

Norris, J. O. W., Norman, S. A., & Tribble, M. J. (1990). Mechanical degradation of

polymer coated glass optical fibers under γ irradiation. In *Proceedings of SPIE - The International Society for Optical Engineering* (Vol. 1314).

Nychas, G. J. E., Skandamis, P. N., Tassou, C. C., & Koutsoumanis, K. P. (2008). Meat spoilage during distribution. *Meat Science*, *78*(1–2), 77–89. http://doi.org/10.1016/j.meatsci.2007.06.020

O'Shea, D. (2004). Scalar Diffraction Theory. In *Diffractive optics: design, fabrication, and test* (Vol. 1, pp. 17–35). Bellingham: SPIE. http://doi.org/10.1007/978-3-540-74296-8_10

O'Sullivan, A. C. (1997). Cellulose: the structure slowly unravels. *Cellulose*, *4*(3), 173–207. http://doi.org/10.1023/A:1018431705579

Odile Dechy-Cabaret, Blanca Martin-Vaca, A., & Bourissou*, D. (2004). Controlled Ring-Opening Polymerization of Lactide and Glycolide. *Chem. Rev.*, *104*(12), 6147–6176. http://doi.org/10.1021/CR040002S

Orts, W. J., Nobes, G. A. R., Kawada, J., Nguyen, S., Yu, G., & Ravenelle, F. (2008). Poly(hydroxyalkanoates): Biorefinery polymers with a whole range of applications. The work of Robert H. Marchessault. *Canadian Journal of Chemistry*, *86*(6), 628–640. http://doi.org/10.1139/v08-050

Orts, W., & Nobes, G. (2008). Poly (hydroxyalkanoates): biorefinery polymers with a whole range of applications. The work of Robert H. Marchessault. *Canadian Journal …*, *86*(6), 628–640. http://doi.org/10.1139/v08-050

Pacquit, A., Frisby, J., Diamond, D., Lau, K. T., Farrell, A., Quilty, B., & Diamond, D. (2007). Development of a smart packaging for the monitoring of fish spoilage. *Food Chemistry*, *102*(2), 466–470. http://doi.org/10.1016/j.foodchem.2006.05.052

Painter, P. C., & Coleman, M. M. (2009). *Essentials of polymer science and engineering*. DEStech Publications, Inc. Retrieved from https://books.google.ca/books/about/Essentials_of_Polymer_Science_and_Engine.html?id=CL7O_hH0aw4C&redir_esc=y

Pandey, A., Nigam, P., Soccol, C. R., Soccol, V. T., Singh, D., & Mohan, R. (2000). Advances in microbial amylases. *Biotechnology and Applied Biochemistry*, *31*(2), 135–152.

Panyam, J., & Labhasetwar, V. (2003). Biodegradable nanoparticles for drug and gene delivery to cells and tissue. *Advanced Drug Delivery Reviews*, *55*(3), 329–347. http://doi.org/10.1016/S0169-409X(02)00228-4

Paull, R. E. (1999). Effect of temperature and relative humidity on fresh commodity quality. *Postharvest Biology and Technology*, *15*(3), 263–277. http://doi.org/10.1016/S0925-5214(98)00090-8

Philip, S., Keshavarz, T., & Roy, I. (2007). Polyhydroxyalkanoates: biodegradable polymers with a range of applications. *Journal of Chemical Technology & Biotechnology*, *82*(3), 233–247. http://doi.org/10.1002/jctb.1667

Pitt, C. G., Hendren, R. W., Schindler, A., & Woodward, S. C. (1984). The enzymatic surface erosion of aliphatic polyesters. *Journal of Controlled Release*, *1*(1), 3–14. http://doi.org/10.1016/0168-3659(84)90016-6

Potts, J. E., Clendinning, R. A., & Ackart, W. B. (1973). *The effect of chemical structure on the biodegradability of plastics*. *The plastics inst. Conference on the degradability of polymers and plastics*.

Prat, D., Hayler, J., & Wells, A. (2014). A Survey of Solvent Selection Guides. *Green*

Chemistry. http://doi.org/10.1039/C4GC01149J

Puligundla, P., Jung, J., & Ko, S. (2012). Carbon dioxide sensors for intelligent food packaging applications. *Food Control*, *25*(1), 328–333. http://doi.org/10.1016/j.foodcont.2011.10.043

Qiu, Y., & Park, K. (2001). Environment-sensitive hydrogels for drug delivery. *Advanced Drug Delivery Reviews*, *53*(3), 321–339. http://doi.org/10.1016/S0169-409X(01)00203-4

Raheem, D. (2016). Outbreaks of listeriosis associated with deli meats and cheese: an overview. *AIMS Microbiology*, *2*(3), 230–250. http://doi.org/10.3934/microbiol.2016.3.230

Ramstad, D.E., Volz, F. E. (1950). Did it thaw? Gel will tell. *Food Industries*, *22*(12), 182–184.

Randolph M. Beaudry, Arthur C. Cameron, Ahmad Shirazi, and D. L. D.-L. (1992). Modified-atmosphere packaging of blueberry fruit: effect of temperature on package O2 and CO2. *Journal of the American Society for Horticultural Science*, *117*(3), 436–441. Retrieved from http://journal.ashspublications.org/content/117/3/436.short

Reis, P., Holmberg, K., Watzke, H., Leser, M. E., & Miller, R. (2009). Lipases at interfaces: A review. *Advances in Colloid and Interface Science*, *147–148*, 237–250. http://doi.org/10.1016/J.CIS.2008.06.001

Rinaudo, M. (2006). Chitin and chitosan: Properties and applications. *Progress in Polymer Science (Oxford)*, *31*(7), 603–632. http://doi.org/10.1016/j.progpolymsci.2006.06.001

Rizzarelli, P., & Carroccio, S. (2014). Modern mass spectrometry in the characterization

and degradation of biodegradable polymers. *Analytica Chimica Acta*, *808*, 18–43. http://doi.org/10.1016/j.aca.2013.11.001

Robertson, G. L. (1998). *Food Packaging: Principles and Practice*. CRC Press.

Rochman, C. M., Browne, M. A., Halpern, B. S., Hentschel, B. T., Hoh, E., Karapanagioti, H. K., … Thompson, R. C. (2013). Policy: Classify plastic waste as hazardous. *Nature*, *494*(7436), 169–171. http://doi.org/10.1038/494169a

Rockwood, D. N., Preda, R. C., Yücel, T., Wang, X., Lovett, M. L., & Kaplan, D. L. (2011). Materials fabrication from Bombyx mori silk fibroin. *Nature Protocols*, *6*(10), 1612–1631. http://doi.org/10.1038/nprot.2011.379

Rodrigues, F. (1971a). Prospects for biodegradable plastics. *Chemische Technik*, 409–415.

Rodrigues, F. (1971b). Prospects for biodegradable plastics. *Modern Plastics*, *48*(9), 92–94.

Rogers, J. A., Someya, T., & Huang, Y. (2010). Materials and mechanics for stretchable electronics. *Science (New York, N.Y.)*, *327*(5973), 1603–7. http://doi.org/10.1126/science.1182383

Roy, D., Cambre, J. N., & Sumerlin, B. S. (2010). Future perspectives and recent advances in stimuli-responsive materials. *Progress in Polymer Science (Oxford)*, *35*(1–2), 278–301. http://doi.org/10.1016/j.progpolymsci.2009.10.008

Said, S. S., El-Halfawy, O. M., El-Gowelli, H. M., Aloufy, A. K., Boraei, N. A., & El-Khordagui, L. K. (2012). Bioburden-responsive antimicrobial PLGA ultrafine fibers for wound healing. *European Journal of Pharmaceutics and Biopharmaceutics*, *80*(1). http://doi.org/10.1016/j.ejpb.2011.08.007

Samal, S. K., Dash, M., Dubruel, P., & Van Vlierberghe, S. (2014). *Smart polymer hydrogels: properties, synthesis and applications*. *Smart Polymers and their Applications*. Woodhead Publishing Limited. http://doi.org/10.1533/9780857097026.1.237

Sánchez-Jiménez, P. E., Pérez-Maqueda, L. A., Perejón, A., & Criado, J. M. (2010). A new model for the kinetic analysis of thermal degradation of polymers driven by random scission. *Polymer Degradation and Stability*, *95*(5), 733–739. http://doi.org/10.1016/j.polymdegradstab.2010.02.017

Sanjay Kumar Sharma, Ackmez Mudhoo, J. H. C. (2011). Biodegradation of Poly 3-hydroxyalakanoates. In *A Handbook of Applied Biopolymer Technology: Synthesis, Degradation and Applications* (p. 322). Royal Society of Chemistry. Retrieved from https://books.google.ca/books?id=nc9qzbqC06sC&pg=PA322&lpg=PA322&dq=enzymatic+degradation+binding+domain&source=bl&ots=86NmPSiT2K&sig=fibhO40pcg6gQ_94ast1IWCF7Wc&hl=en&sa=X&ved=0ahUKEwituZy3lMLTAhUBDmMKHXx9DgoQ6AEIQzAE#v=onepage&q=enzymatic%2520degradatio

Sauer, B. B., & Dee, G. T. (1991). Molecular weight and temperature dependence of polymer surface tension: comparison of experiment with theory. *Macromolecules*, *24*(8), 2124–2126. http://doi.org/10.1021/ma00008a070

Sauer, B. B., Kampert, W. G., Neal Blanchard, E., Threefoot, S. a., & Hsiao, B. S. (2000). Temperature modulated DSC studies of melting and recrystallization in polymers exhibiting multiple endotherms. *Polymer*, *41*(3), 1099–1108. http://doi.org/10.1016/S0032-3861(99)00258-X

Sauvageau, D., Cooper, D. G., & Nicell, J. A. (2009). Relative rates and mechanisms of

biodegradation of diester plasticizers mediated by Rhodococcus rhodochrous. *The Canadian Journal of Chemical Engineering*, *87*(3), 499–506. http://doi.org/10.1002/cjce.20170

Savenkova, L., Gercberga, Z., Nikolaeva, V., Dzene, a, Bibers, I., & Kalnin, M. (2000). Mechanical properties and biodegradation characteristics of PHB-based films. *Process Biochemistry*, *35*(6), 573–579. http://doi.org/10.1016/S0032-9592(99)00107-7

Scallan, E., Hoekstra, R. M., Angulo, F. J., Tauxe, R. V., Widdowson, M.-A., Roy, S. L., … Griffin, P. M. (2011). Foodborne Illness Acquired in the United States—Major Pathogens. *Emerging Infectious Diseases*, *17*(1), 7–15. http://doi.org/10.3201/eid1701.P11101

Schiffer, D., Tegl, G., Heinzle, A., Sigl, E., Metcalf, D., Bowler, P., … Guebitz, G. M. (2015). Enzyme-responsive polymers for microbial infection detection. *Expert Review of Molecular Diagnostics*, *15*(9), 1125–1131. http://doi.org/10.1586/14737159.2015.1061935

Schiffer, D., Verient, V., Luschnig, D., Blokhuis-Arkes, M. H. E., Palen, J. V. D., Gamerith, C., … Guebitz, G. M. (2015). Lysozyme-responsive polymer systems for detection of infection. *Engineering in Life Sciences*, *15*(4). http://doi.org/10.1002/elsc.201400145

Schmaljohann, D. (2006). Thermo- and pH-responsive polymers in drug delivery. *Advanced Drug Delivery Reviews*, *58*(15), 1655–1670. http://doi.org/10.1016/j.addr.2006.09.020

Schmaljohann, D. (2006). Thermo- and pH-responsive polymers in drug delivery.

Advanced Drug Delivery Reviews, *58*(15), 1655–1670. http://doi.org/10.1016/j.addr.2006.09.020

Schofield, D. A., Molineux, I. J., & Westwater, C. (2011). “Bioluminescent” Reporter Phage for the Detection of Category A Bacterial Pathogens. *Journal of Visualized Experiments : JoVE*, (53). http://doi.org/10.3791/2740

Schultz, J. M. (1984). Microstructural aspects of failure in semicrystalline polymers. *Polymer Engineering & Science*, *24*(10), 770–785. http://doi.org/10.1002/pen.760241007

Seoane, I. T., Manfredi, L. B., & Cyras, V. P. (2015). Properties and Processing Relationship of Polyhydroxybutyrate and Cellulose Biocomposites. *Procedia Materials Science*, *8*, 807–813. http://doi.org/10.1016/j.mspro.2015.04.139

Shackleton, J. W. (1945). II. General Characteristics of Polyethylene. *Transactions of the American Institute of Electrical Engineers*, *64*(12), 912–916. http://doi.org/10.1109/T-AIEE.1945.5059062

Siemann, U. (2005). Solvent cast technology – a versatile tool for thin film production, (June), 1–14. http://doi.org/10.1007/b107336

Sinelli, N., Limbo, S., Torri, L., Di Egidio, V., & Casiraghi, E. (2010). Evaluation of freshness decay of minced beef stored in high-oxygen modified atmosphere packaged at different temperatures using NIR and MIR spectroscopy. *Meat Science*, *86*(3), 748–752. http://doi.org/10.1016/j.meatsci.2010.06.016

Singh, A., Poshtiban, S., & Evoy, S. (2013). Recent Advances in Bacteriophage Based Biosensors for Food-Borne Pathogen Detection. *Sensors*, *13*(2), 1763–1786. http://doi.org/10.3390/s130201763

Siracusa, V., Rocculi, P., Romani, S., & Rosa, M. D. (2008). Biodegradable polymers for food packaging: a review. *Trends in Food Science & Technology*, *19*(12), 634–643. http://doi.org/10.1016/j.tifs.2008.07.003

Smolander, M., Alakomi, H. L., Ritvanen, T., Vainionpää, J., & Ahvenainen, R. (2004). Monitoring of the quality of modified atmosphere packaged broiler chicken cuts stored in different temperature conditions. A. Time-temperature indicators as quality-indicating tools. *Food Control*, *15*(3), 217–229. http://doi.org/10.1016/S0956-7135(03)00061-6

Smolander, M., Hurme, E., Latva-Kala, K., Luoma, T., Alakomi, H.-L., & Ahvenainen, R. (2002). Myoglobin-based indicators for the evaluation of freshness of unmarinated broiler cuts. *Innovative Food Science & Emerging Technologies*, *3*(3), 279–288. http://doi.org/10.1016/S1466-8564(02)00043-7

Smyth, A. B., Song, J., & Cameron, A. C. (1998). Modified Atmosphere Packaged Cut Iceberg Lettuce : Effect of Temperature and O 2 Partial Pressure on Respiration and Quality. *Journal of Agricultural and Food Chemistry*, *46*(May 1997), 4556–4562. http://doi.org/10.1021/jf980208s

Sperling, L. H. (2005). *Introduction to Physical Polymer Science: Fourth Edition*. *Introduction to Physical Polymer Science: Fourth Edition*. CRC Press. http://doi.org/10.1002/0471757128

Spyros, A., Kimmich, R., Briese, B. H., & Jendrossek, D. (1997). 1H NMR Imaging Study of Enzymatic Degradation in Poly(3-hydroxybutyrate) and Poly(3-hydroxybutyrate-co-3-hydroxyvalerate). Evidence for Preferential Degradation of the Amorphous Phase by PHB Depolymerase B from Pseudomonas lemoignei.

Macromolecules, *30*(26), 8218–8225. http://doi.org/10.1021/ma971193m

Stafford, C. M., Harrison, C., Beers, K. L., Karim, A., Amis, E. J., VanLandingham, M. R., … Simonyi, E. E. (2004). A buckling-based metrology for measuring the elastic moduli of polymeric thin films. *Nature Materials*, *3*(8), 545–550. http://doi.org/10.1038/nmat1175

Steinbüchel, A., & Valentin, H. E. (1995). Diversity of bacterial polyhydroxyalkanoic acids. *FEMS Microbiology Letters*, *128*(3), 219–228. http://doi.org/10.1016/0378-1097(95)00125-O

Stuart, M. A. C., Huck, W. T. S., Genzer, J., Müller, M., Ober, C., Stamm, M., … Minko, S. (2010). Emerging applications of stimuli-responsive polymer materials. *Nature Materials*, *9*(2), 101–113. http://doi.org/10.1038/nmat2614

Sun, X., Gao, N., Li, Q., Zhang, J., Yang, X., Ren, Z., & Yan, S. (2016). Crystal Morphology of Poly(3-hydroxybutyrate) on Amorphous Poly(vinylphenol) Substrate.

Sundarrajan, S., Surianarayanan, M., & Srinivasan, K. S. V. (2005). Synthesis and characterization of saturated and unsaturated polysulfide polymers and their thermal degradation processes investigated by flash pyrolysis-gas chromatography/mass spectrometry. *Journal of Polymer Science Part A: Polymer Chemistry*, *43*(3), 638–649. http://doi.org/10.1002/pola.20535

Suriyamongkol, P., Weselake, R., Narine, S., Moloney, M., & Shah, S. (2007). Biotechnological approaches for the production of polyhydroxyalkanoates in microorganisms and plants - a review. *Biotechnology Advances*, *25*(2), 148–75. http://doi.org/10.1016/j.biotechadv.2006.11.007

Takeda, R., & Shiraishi, H. (1992, October). Process for producing cellulose triacetate

film.

Tao, H., Brenckle, M. a, Yang, M., Zhang, J., Liu, M., Siebert, S. M., … Omenetto, F. G. (2012). Silk-based conformal, adhesive, edible food sensors. *Advanced Materials (Deerfield Beach, Fla.)*, *24*(8), 1067–72. http://doi.org/10.1002/adma.201103814

Taoukis, P. S, L. T. P. (2003). Time-Temperature Indicators (TTIs). In *Novel Food Packaging Techniques* (pp. 104–125).

Tardiff, R. G. (1977). Health Effects of Organics: Risk and Hazard Assessment of Ingested Chloroform. *Journal (American Water Works Association)*, *69*(12), 658–661.

Terada, M., & Marchessault, R. H. (1999). Determination of solubility parameters for poly(3-hydroxyalkanoates). *International Journal of Biological Macromolecules*, *25*(1–3), 207–215. http://doi.org/10.1016/S0141-8130(99)00036-7

Terefe, N. S., Buckow, R., & Versteeg, C. (2014). Quality-Related Enzymes in Fruit and Vegetable Products: Effects of Novel Food Processing Technologies, Part 1: High-Pressure Processing. *Critical Reviews in Food Science and Nutrition*, *54*(1), 24–63. http://doi.org/10.1080/10408398.2011.566946

Tharanathan, R. N., & Kittur, F. S. (2003). Chitin - The Undisputed Biomolecule of Great Potential. *Critical Reviews in Food Science and Nutrition*, *43*(1), 61–87. http://doi.org/10.1080/10408690390826455

Tokiwa, Y., Calabia, B. P., Ugwu, C. U., & Aiba, S. (2009). Biodegradability of Plastics. *International Journal of Molecular Sciences*, *10*(9), 3722–3742. http://doi.org/10.3390/ijms10093722

Tokiwa, Y., & Ugwu, C. U. (2007). Biotechnological production of (R)-3-hydroxybutyric

acid monomer. *Journal of Biotechnology*, *132*(3), 264–272. http://doi.org/10.1016/j.jbiotec.2007.03.015

Tomasi, G., & Scandola, M. (1997). X-Ray investigation on melt-crystallized bacterial, *0*, 71–80.

Tsuji, H., & Ikada, Y. (1997). Blends of crystalline and amorphous poly(lactide). III. Hydrolysis of solution-cast blend films. *Journal of Applied Polymer Science*, *63*(7), 855–863. http://doi.org/10.1002/(SICI)1097-4628(19970214)63:7<855::AID-APP5>3.0.CO;2-P

Tung, L. J., & Buckser, S. (1958). The Effects of Molecular Weight on the Crystallinity of Polyethylene. *The Journal of Physical Chemistry*, *62*(12), 1530–1534. http://doi.org/10.1021/j150570a015

Tyler, B., Gullotti, D., Mangraviti, A., Utsuki, T., & Brem, H. (2016). Polylactic acid (PLA) controlled delivery carriers for biomedical applications. *Advanced Drug Delivery Reviews*, *107*, 163–175. http://doi.org/10.1016/j.addr.2016.06.018

Ulijn, R. V, Bibi, N., Jayawarna, V., Thornton, P. D., Todd, S. J., Mart, R. J., Gough, J. E. (2007). Bioresponsive hydrogels. *Materials Today*, *10*, 40–48. http://doi.org/10.1016/S1369-7021(07)70049-4

Vaikousi, H., Biliaderis, C. G., & Koutsoumanis, K. P. (2009). Applicability of a microbial Time Temperature Indicator (TTI) for monitoring spoilage of modified atmosphere packed minced meat. *International Journal of Food Microbiology*, *133*(3), 272–278. http://doi.org/10.1016/j.ijfoodmicro.2009.05.030

Van De Witte, P., Dijkstra, P. J., Van Den Berg, J. W. A., & Feijen, J. (1996). Phase separation processes in polymer solutions in relation to membrane formation.

ELSEVIER Journal of Membrane Science, *117*, 1–31.

Vert, M. (2005). Aliphatic polyesters: Great degradable polymers that cannot do everything. *Biomacromolecules*, *6*(2), 538–546. http://doi.org/10.1021/bm0494702

Vert, M., Li, S. M., Spenlehauer, G., & Guerin, P. (1992). Bioresorbability and biocompatibility of aliphatic polyesters. *Journal of Materials Science: Materials in Medicine*, *3*(6), 432–446. http://doi.org/10.1007/BF00701240

Wagner, M., Scherer, C., Alvarez-Muñoz, D., Brennholt, N., Bourrain, X., Buchinger, S., … Reifferscheid, G. (2014). Microplastics in freshwater ecosystems: what we know and what we need to know. *Environmental Sciences Europe*, *26*(1), 12. http://doi.org/10.1186/s12302-014-0012-7

Wang, F. C.-Y. (1999). Polymer analysis by pyrolysis gas chromatography. *Journal of Chromatography A*, *843*(1–2), 413–423. http://doi.org/10.1016/S0021-9673(98)01051-6

Wang, L., Zhu, W., Wang, X., Chen, X., Chen, G.-Q., & Xu, K. (2008). Processability modifications of poly(3-hydroxybutyrate) by plasticizing, blending, and stabilizing. *Journal of Applied Polymer Science*, *107*(1), 166–173. http://doi.org/10.1002/app.27004

Wang, M., Braun, H., Meyer, E., & Zhu, J. (n.d.). Morphogenesis and Chain Behaviors Related to Crystallization in Ultrathin Polymer Films ∗, 1–11.

Wang, X., Liu, X., & Wang, X. (2014). Hydrogel diffraction grating as sensor: A tool for studying volume phase transition of thermo-responsive hydrogel. *Sensors and Actuators B: Chemical*, *204*, 611–616. http://doi.org/10.1016/j.snb.2014.08.013

Wang, Y., Han, X., Pan, J., & Sinka, C. (2010). An entropy spring model for the Young's

modulus change of biodegradable polymers during biodegradation. *Journal of the Mechanical Behavior of Biomedical Materials*, *3*(1), 14–21. http://doi.org/10.1016/j.jmbbm.2009.02.003

Wanihsuksombat, C., Hongtrakul, V., & Suppakul, P. (2010). Development and characterization of a prototype of a lactic acid-based time-temperature indicator for monitoring food product quality. *Journal of Food Engineering*, *100*(3), 427–434. http://doi.org/10.1016/j.jfoodeng.2010.04.027

R.M.Hodge, Graham H.Edward, George P.Simon, Water absorption and states of water in semicrystalline poly(vinyl alcohol) films. (1996). *Polymer*, *37*(8), 1371–1376. http://doi.org/10.1016/0032-3861(96)81134-7

Weisel, C. P., & Jo, W. K. (1996). Ingestion, inhalation, and dermal exposures to chloroform and trichloroethene from tap water. *Environmental Health Perspectives*, *104*(1), 48.

Whitaker, J. R. (1991). Enzymes: monitors of food stability and quality. *Trends in Food Science and Technology*, *2*(C), 94–97. http://doi.org/10.1016/0924-2244(91)90636-W

Williams, P. M. (1995). Degradation of a Thin Polymer Film Studied by Simultaneous in situ Atomic Force Microscopy and Surface Plasmon Resonance Analysis. *Drug Delivery*.

Worne, H. (1971). Modify plastics for degradability. *Plastics Technol*, *17*(7), 23–28.

Wu, D., Hou, S., Chen, J., Sun, Y., Ye, X., Liu, D., … Wang, Y. (2015). Development and characterization of an enzymatic time-temperature indicator (TTI) based on Aspergillus niger lipase. *LWT - Food Science and Technology*, *60*(2), 1100–1104.

http://doi.org/10.1016/j.lwt.2014.10.011

Wu, D., Wang, Y., Chen, J., Ye, X., Wu, Q., Liu, D., & Ding, T. (2013). Preliminary study on time-temperature indicator (TTI) system based on urease. *Food Control*, *34*(1), 230–234. http://doi.org/10.1016/j.foodcont.2013.04.041

Xia, Y., Kim, E., Zhao, X.-M., Rogers, J. A., Prentiss, M., & Whitesides, G. M. (1996). Complex Optical Surfaces Formed by Replica Molding Against Elastomeric Masters. *Science*, *273*(5273), 347–349. http://doi.org/10.1126/science.273.5273.347

Xia, Y., & Whitesides, G. M. (1998). Soft Lithography. *Annual Review of Materials Science*, *28*(1), 153–184. http://doi.org/10.1146/annurev.matsci.28.1.153

Y. Wang, S. Ge, M. Rafailovich, J. Sokolov, Y. Zou, H. Ade, … Maron, G. (2004). Crystallization in the Thin and Ultrathin Films of Poly(ethylene−vinyl acetate) and Linear Low-Density Polyethylene. Macromolecules, 37 (9), pp 3319–3327.

Yada, R. Y. (2015). Improving and tailoring enzymes for food quality and functionality. http://doi.org/10.1016/C2013-0-16520-8

Yalpani, M. (1993, March). Functionalized poly(hydroxyalkanoates) and method of manufacturing same. US5191016A.

Yalpani, M., Marchessault, R. H., Morin, F. G., & Monasterios, C. J. (1991). Synthesis of poly(3-hydroxyalkanoate) (PHA) conjugates: PHA-carbohydrate and PHA-synthetic polymer conjugates. *Macromolecules*, *24*(22), 6046–6049. http://doi.org/10.1021/ma00022a024

Yan, S., Huawei, C., Limin, Z., Fazheng, R., Luda, Z., & Hengtao, Z. (2008). Development and characterization of a new amylase type time-temperature

indicator. *Food Control*, *19*(3), 315–319. http://doi.org/10.1016/j.foodcont.2007.04.012

Yang, C. Z., Yaniger, S. I., Jordan, V. C., Klein, D. J., & Bittner, G. D. (2011). Most Plastic Products Release Estrogenic Chemicals : A Potential Health Problem that Can Be Solved, *119*(7), 989–996. http://doi.org/10.1289/ehp.1003220

Yoshie, N., Oike, Y., Kasuya, K., Doi, Y., & Inoue, Y. (2002a). Change of Surface Structure of Poly(3-hydroxybutyrate) Film upon Enzymatic Hydrolysis by PHB Depolymerase. *Biomacromolecules*, *3*(6), 1320–1326. http://doi.org/10.1021/bm020077a

Yoshie, N., Oike, Y., Kasuya, K., Doi, Y., & Inoue, Y. (2002b). Change of Surface Structure of Poly (3-hydroxybutyrate) Film upon Enzymatic Hydrolysis by PHB Depolymerase. *Biomacromolecules*, *3*(3), 1320–1326.

Yu, J., Plackett, D., & Chen, L. X. L. (2005). Kinetics and mechanism of the monomeric products from abiotic hydrolysis of poly[(R)-3-hydroxybutyrate] under acidic and alkaline conditions. *Polymer Degradation and Stability*, *89*(2), 289–299. http://doi.org/10.1016/j.polymdegradstab.2004.12.026

Yu, J., Plackett, D., & Chen, L. X. L. (2005). Kinetics and mechanism of the monomeric products from abiotic hydrolysis of poly [(R) -3-hydroxybutyrate] under acidic and alkaline conditions, *89*. http://doi.org/10.1016/j.polymdegradstab.2004.12.026

Zappe, H. (2010). Diffractive micro-optics. In *Fundamentals of Micro-Optics* (pp. 265–310). Cambridge University Press. Retrieved from https://books.google.com/books?id=0gwksRktpCQC&pgis=1

Zelikin, A. N. (2010). Drug Releasing Polymer Thin Films new Era of Surface-Mediated

Drug Delivery. *ACS Nano*, *4*(5), 2494–2509.

Zelzer, M., Todd, S. J., Hirst, A. R., McDonald, T. O., & Ulijn, R. V. (2013). Enzyme responsive materials: design strategies and future developments. *Biomater. Sci.*, *1*(1), 11–39. http://doi.org/10.1039/C2BM00041E

Zelzer, M., & Ulijn, R. V. (2014a). *Enzyme-responsive polymers: properties, synthesis and applications*. *Smart Polymers and their Applications*. Woodhead Publishing Limited. http://doi.org/10.1533/9780857097026.1.166

Zelzer, M., & Ulijn, R. V. (2014b). *Enzyme-responsive polymers: Properties, synthesis and applications*. *Smart Polymers and their Applications*. http://doi.org/10.1533/9780857097026.1.166

Zen, A., Marina, S., Neher, D., Grenzer, J., Grigorian, S., Pietsch, U., … Wegner, G. (2006). Effect of Molecular Weight on the Structure and Crystallinity of Poly(3-hexylthiophene). *Macromolecules*, *39*(6), 2162–2171. http://doi.org/10.1021/MA0521349

Zhang, M., & Thomas, N. L. (2011). Blending polylactic acid with polyhydroxybutyrate: The effect on thermal, mechanical, and biodegradation properties. *Advances in Polymer Technology*, *30*(2), 67–79. http://doi.org/10.1002/adv.20235

Zhou, J., & Sheiko, S. S. (2016). Reversible shape-shifting in polymeric materials. *Journal of Polymer Science, Part B: Polymer Physics*, *1*(c), 1365–1380. http://doi.org/10.1002/polb.24014

Zinn, M., Witholt, B., & Egli, T. (2001). Occurrence, synthesis and medical application of bacterial polyhydroxyalkanoate. *Advanced Drug Delivery Reviews*, *53*(1), 5–21. http://doi.org/10.1016/S0169-409X(01)00218-6

Zinn, M., Witholt, B., & Egli, T. (2001). Occurrence , synthesis and medical application of bacterial polyhydroxyalkanoate, *53*, 5–21.

Zuchowska, D., Steller, R., & Meissner, W. (1998). Structure and properties of degradable polyolefin - Starch blends. *Polymer Degradation and Stability*, *60*(2–3), 173–187.